The Ascidian Pyloric Gland: Aspects of its Form and Function in *Clavelina huntsmani* Van Name,1931, *Corella inflata* Huntsman,1912 and *Styela gibbsii*(Stimpson,1864)

by

Richard Frederick Gowan

B.Sc., Mount Allison University, 1982
B.Ed., Mount Allison University, 1983

A THESIS SUBMITTED IN PARTIAL FULFILLMENT

OF THE REQUIREMENTS FOR THE DEGREE OF

MASTER OF SCIENCE

in the Department

of

Biology

We accept this thesis as conforming
to the required standard

[redacted]
(G. O. Mackie)

[redacted]
(A. R. Fontaine)

[redacted]
(T. J. Trust)

[redacted]
(J. S. Ryland)

ABSTRACT

Supervisor: Dr. George O. Mackie

The ascidian pyloric gland is an enigmatic organ for which a number of functions have been suggested including excretion, osmoregulation, digestion and glycogen storage. This study used light and electron microscopy to study pyloric gland structure, autoradiography to examine ^{14}C-1-glucose uptake along the gastrointestinal tract, and light and electron microscopy to examine starvation response.

1.) The pyloric gland has a variable number of ducts leaving the stomach which branch into smaller tubules. The tubules cover all or most of the gastrointestinal tract and near the mid-intestinal epithelium they terminate as large dilated pyloric ampullae.

2.) The pyloric gland consists of a single-layered epithelium arranged around a central lumen. Within the pyloric cells, particularly the pyloric ampullae, a cytonuclear cycle occurs which results in the release of glycogen-rich PAS positive material into the gland lumen.

3.) In the solitary ascidians which were studied, starvation results in a marked decrease in the number of pyloric cells releasing contents into the pyloric lumen, as

well as a drastic decrease in the amount of PAS positive glycogen-rich material within the pyloric cells.

4.) With starvation, many of the pyloric cells of Styela gibbsii release their contents into the surrounding haemocoel following degeneration of the basal lamina of connective tissue which surrounds the gland.

5.) In Clavelina huntsmani the release of PAS positive material by the pyloric cells is maintained up to the point of starvation-induced zooid regression.

6.) Results concerning the uptake of ^{14}C-l-glucose by Corella inflata indicate that the stomach and mid-intestinal epithelium have absorptive functions. The post-intestinal epithelium is non-absorptive and glucose diffuses into the haemocoel through the branchial basket and the esophagus.

7.) ^{14}C-l-glucose accumulates within the mid-intestinal pyloric ampullae of C. inflata but not within pyloric tubules. The amount of labelled glucose within ampullae of C. inflata (Phlebobranchia) is greater than that noted for an Aplousobranch and less than that seen in Stolidobranchs (Gaill, 1981).

I suggest that after prolonged starvation in S. gibbsii, the basal disintegration of the pyloric cells is a means of releasing nutrients from the pyloric ampullae into

the surrounding haemocoel. Since this basal disintegration is associated with a cessation of the pyloric cytonuclear cycle and the absence of PAS positive staining, the nutrient released into the haemocoel is most likely glucose derived from the glycogen found within the cells of fed animals.

Basal disintegration of pyloric cells is not seen in C. inflata following starvation due to its short 6 month life-span which would not normally necessitate a means for maintenance during low nutrient periods (e.g. the winter). However, the release of glycogen via the cytonuclear cycle is shut down to maximize survival.

In C. huntsmani the overwintering strategy involves regression of the zooids and storage of nutrients within the stolonic system. As a result, the pyloric cell basal disintegration is not seen and the cytonuclear cycle is maintained until nutrients become scarce enough to trigger zooid regression.

The glycogen-rich PAS positive material, released by the pyloric cytonuclear cycle into the pyloric lumen, is probably released via the main pyloric ducts into the stomach. If this material is required for digestion of the food cord, its absence during starvation (in solitary ascidians) is of little consequence since very little food is present in the stomach.

Examiners: [redacted]

(G. O. Mackie)

[redacted]

(A. R. Fontaine)

[redacted]

(T. J. Trust)

[redacted]

(J. S. Ryland)

[redacted]

Table of Contents

List of Tables

List of Figures

ACKNOWLEDGMENTS

I gratefully acknowledge all who assisted me in the course of this study: Dr. George Mackie for his support throughout this work; Jack Dietrich and Dr. Chaman Singla for their E.M. expertise and advice; Dr. Tome Gore for his assistance with photography; Dr. Robert Burke and Dr. Maureen De Burgh for advice concerning autoradiography; Ralph Scheurle and Gordon Davies for their assistance with apparatus and Dr. George Mackie, Dr. A.R. Fontaine, Dr. T. J. Trust and Dr. J. S. Ryland for critically reviewing this thesis.

This work was supported by National Science and Engineering Research Council grant no. 346862 to Dr. George Mackie.

INTRODUCTION

Chapter 1. General Introduction

Previous studies examining the form and function of the pyloric gland in ascidians have resulted in excretory, osmoregulatory, digestive and glycogen storage functions being suggested for the organ (Table 1; Fouque, 1954; Millar, 1949; Gaill, 1973; Goodbody, 1974).

It is generally believed that the pyloric gland in ascidians may be homologous to the vertebrate liver (Table 1; Ermak, 1977) and as such should possess functional and structural characteristics which reflect this relationship. With this in mind, this study examines ultrastructure, glucose uptake and glycogen storage within the pyloric gland of three local ascidians.

The following introduction outlines relevant information to date concerning the cellular constituents of the gastrointestinal tract. Following this the structure and characteristic cytonuclear cycle of the ascidian pyloric gland is introduced. The final subject introduced includes observations to date relating to the possible role(s) of the pyloric gland as an invertebrate homolog of the vertebrate liver. Specific objectives of this study are presented at the end of the introduction section.

Table 1. Summary of research to date concerning gastrointestinal and pyloric gland structure and function in ascidians.

Ascidians	Authors
Branchial Basket Absorption	
Clavelina, Phallusia, Ciona, Styela	Fiala-Medioni & Pequignat, 1980
Esophagus	
Ciona, Styela	Roule,1884;Yonge,1925;Das 1944;Millar,1953;Thomas, 1970a;Croxall,1971;Brevis & Thorndyke,1977,1978;Ermak, 1981;Gaill,1981; Zhuravlijova,1985
Stomach	
Botrylloides,Ciona Botryllus,Styela Microcosmus,Pyura	Yonge,1925;Berrill,1929; Millar,1953;Fouque,1954,1959; vanWeel,1940;Das,1944;Morton, 1960;DeGail & Levi,1964;Relini-Orsi,1968,1969;Thomas,1970a, b;Koch & Marsch,1972;Burighel, 1973;Burighel & Milanesi,1973, 1975a,1975b;Ermak,1975,1981; Fritsch,1976;Fritsch & Sprang, 1977;Thorndyke,1977;Thorndyke & Brevis,1978;Pestarino,1982
Intestine	
Botryllus,Ciona	Das,1944;Fouque,1949,1954; Chambost & Thomassin-Steck, 1972;Thomas,1970a;Burighel & Milanesi,1977;Ermak,1981
Pyloric Gland	
Amaroucium,Dendrodoa, Cystodites,Halocynthia, Didemnum,Diazona,Styela Lissoclinum,Ascidia,Molgula, Diplosoma,Botryllus,Ciona, Microcosmus,Clavelina, Polyclinum,Aplidium,Pyura	Chandelon,1875;Isert,1903; Colton,1910;Azema,1937;Millar, 1949;Fouque,1954;Godeaux,1954; Biava,1963;Coimbra,1967;Brown & Davies,1971;Gaill,1973,1974,1976, 1977,1980,1981;Goodbody,1974; Ermak,1977;Mirre & Thouveny,1977

Chapter 2. The Alimentary Tract and its Cellular Contituents

A. Filtering, Digestion and Excretion

In ascidians, the gastrointestinal tract typically consists of a branchial sac, esophagus, stomach, mid-intestine, post-intestine, and anus (fig. 1).

Mucus is secreted by the endostyle which runs antero-posteriorly along the ventral side of the branchial sac. As the mucous net moves across the branchial sac it filters particles from seawater which is flowing through the branchial basket. The mucous net is collected along the dorsal surface of the branchial basket and is drawn into the esophagus which lies at or near the bottom of the branchial basket.

The branchial basket is a food-collecting and respiratory apparatus and as such does not have a role in digestion and absorption. Absorption and digestion take place in the stomach and intestine, although there is some evidence to suggest that the branchial basket of some ascidians is capable of absorbing amino acids and glucose dissolved in seawater (Fiala-Medioni & Pequignat, 1980).

Ingested material travels the length of the digestive tract and feces are eliminated, via the anus, into the

Figure 1. Diagram of overall body plan of Corella inflata illustrating structures typically found in most ascidians. Water enters the animal through the branchial siphon (B), filters through the mucous net on the branchial basket (BB), enters the atrium (AT) and exits the animal via the atrial siphon (A). The mucous net is secreted by the endostyle (EN) and travels across the branchial basket. The mucus collects at the dorsal lamina (D) and is drawn into the esophagus (E). The food cord moves through the stomach (S), mid-intestine (MI) and post-intestine (PI). Feces are removed through the anus (AN) and eventually exit the animal via contraction of the atrial chamber. The gonads, located within the gut loop, have been removed. M = mantle; T = trabecula; TU = tunic; * = haemocoel between the mantle epidermis and the atrial epithelium within which the viscera, blood cells and connective tissue are located.

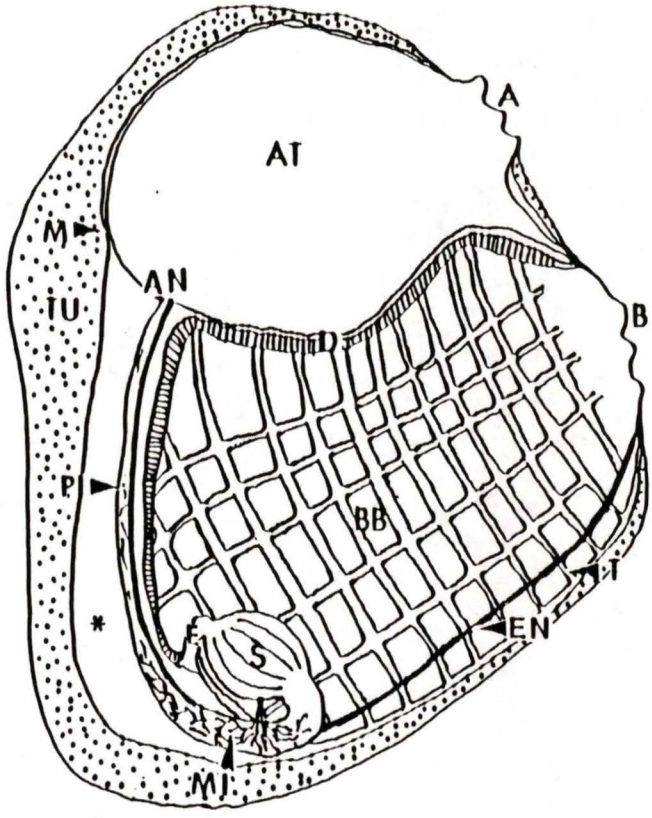
A
AT
M
AN
TU
B
P
BB
T
EN
S
MJ

atrial chamber. Feces are eventually discharged from the animal via contraction of the atrial chamber (squirting).

B. Esophagus

The esophagus lies at or near the bottom of the branchial basket, connecting the branchial sac to the stomach (fig. 1). The esophagus consists of a single type of mucous-secreting ciliated cell (Table 1). Mucus is produced as granules which discharge by rupture of the apical plasma membrane (Thomas, 1970a). The wall of the esophagus functions mainly in the transport of the food cord (Yonge, 1925) although dissolved glucose will diffuse through the esophagus and into the haemocoel (Fiala-Medioni & Pequignat, 1980; Gaill, 1981).

C. Stomach

The stomach is the main site of digestion and to some extent absorption (Yonge, 1925; van Weel, 1940; Morton, 1960; Burighel, 1973). The ascidian gastric epithelium is characterised by 5 types of cells; ciliated mucus-secreting, endocrine, vacuolated, protein-secreting and undifferentiated cells (DeGail and Levi, 1964; Relini-Orsi, 1968, 1969; Thomas, 1970a, b; Burighel and Milanesi, 1972, 1975a; Thorndyke, 1977).

Ciliated mucus-secreting cells are found on the crests of the stomach ridges. These cells secrete an acid mucopolysaccharide similar to that released by the esophageal cells (Thomas, 1970a; Burighel and Milanesi, 1975a).

Endocrine cells which are characterized by the presence of numerous electron-dense granules, particularly at the base of the cell, are found scattered throughout the mucous cap cells (Thorndyke, 1977).

Vacuolated cells are found lining the sides of the stomach ridges. Vacuolated cells contain prominent golgi complexes at the base of supranuclear vacuoles. These cells are also recognized by a variety of vesicles or multivesicular bodies in the apical cytoplasm (Thorndyke, 1977).

The function of the vacuolated cells remains unclear. Some investigators suggest that the cells are secretory (Degail & Levi, 1964; Relini-Orsi, 1968; Thomas, 1970b) while others suggest that the vacuolated cells of the ascidian stomach function primarily in absorption (Yonge, 1925; Berrill, 1929; van Weel, 1940; Morton, 1960; Burighel & Milanesi, 1973; Thorndyke, 1977). Thorndyke (1977) notes the presence of large numbers of apical microvilli and an active population of heterophagosomes which is in keeping

with features of vertebrate absorptive cells (Toner, 1968; Parsons & Boyd, 1972).

Protein secreting `zymogenic´ cells are found along the sides of stomach ridges (Degail & Levi, 1964; Thomas, 1970b; Burighel, 1973; Burighel & Milanesi, 1973; Thorndyke, 1977). Thorndyke (1977) notes that these cells have a number of features similar to protein secreting cells of vertebrates such as highly developed rough endoplasmic reticulum, numerous apical secretory granules and a well-developed supranuclear golgi system (Jamieson and Palade, 1966; Palade, 1966). Thorndyke suggests that the secretory product of the zymogen cells is probably an enzyme, as enzymes have been well-documented in the ascidian stomach (Yonge, 1925; Berrill, 1929; van Weel, 1940; Fouque, 1959; Koch and Marsch, 1972).

Undifferentiated cells are found in the crypts between stomach ridges (Millar, 1953; Fouque, 1954; Burighel and Milanesi, 1970; Thomas, 1970b; Thorndyke, 1977). It has been suggested that these cells are probably the source of both vacuolated and protein secreting cells since they possess an active nucleus and clusters of free ribosomes which are both characteristics of embryonic cells (Stephens & Bils, 1967). Ermak (1981) confirmed this hypothesis by examining cell proliferation patterns in ascidian stomach using autoradiography and tritiated thymidine.

D. Intestine

The cellular constituents of the intestinal portion of the alimentary tract differ depending on the region in question (mid-intestine or post-intestine).

Ciliated mucous-secreting cells are found in the proximal intestine. These cells have low cilia and microvilli, granules or masses of mucus in the apical cytoplasm and supranuclear golgi complexes. The cilia are arranged in rows, usually to the side of the cell. Ciliated mucus-secreting cells are also found in the proximal intestine and they produce carbohydrated protein complexes unlike the esophagus and stomach where acid mucopolysaccharides predominate (Burighel and Milanesi, 1977).

Vacuolated cells, similar to those found in the gastric epithelium, are also found in the proximal intestine. The vacuolated cells constitute the majority of the cells in the region of the proximal intestine which is covered by an extensive network of pyloric gland ampullae. These vacuolated cells often show marked degenerative changes including cell vacuolation, involution of cell organelles, chromatin denaturation and extraction of the nuclear and cytoplasmic matrix (Burighel and Milanesi, 1977).

Burighel and Milanesi (1977) also present evidence for cells which resemble the endocrine cells found in the stomach in that they possess strongly electron-opaque granules. These cells are found scattered within the mucous cells and are quite rare.

Vacuolated cells are also found in the distal portion of the intestine and are similar in morphology to cells found in the rectum These cells have a giant supranuclear vacuole occupying most of the cell volume. In general, the rectal cells are low, ciliated cells with histochemical reactions similar to esophageal cells (Burighel and Milanesi, 1977).

Chapter 3. The Pyloric Gland - Form and Function

A. Pyloric Gland Structure

The main collecting duct of the ascidian pyloric gland extends from the distal portion of the stomach. Typically a single duct leads from the stomach and branches and ramifies over the intestine to varying degrees depending on the species in question (fig. 1).

The terminal portions of some of the ducts end in dilations called ampullae (Fouque, 1954). The ampullae are dilated to varying extents depending upon the species and the particular area of the gland in question. The ampullae

are invariably more numerous and dilated around the mid-intestine and form what Fouque (1954) refers to as the zone of contiguous ampullae. Some ducts branch into small tubules which are found all along the gastrointestinal tract. All areas of the gland are composed of a single layered epithelium which contains microvilli and cilia (Goodbody, 1974).

B. Glycogen Storage in the Pyloric Gland

Refringent concretions have been noted within the lumen of the pyloric gland, particularly in the area surrounding the post-intestine (Chandelon, 1875; Isert, 1903; Millar, 1949, 1953; Fouque, 1954).

Ermak (1977) feels that the concretions may be glycogen due to the refractive qualities of the molecule (Eakin & Kuda, 1972). Ermak specifically refers to the concretions noted in Ciona intestinalis by Millar (1953) as identical, with respect to size and shape, to those he found in Styela clava. Digestion of these large deposits by alpha amylase (Biava, 1963; Coimbra, 1967; Ermak, 1977) but not of other periodic acid-schiff positive sites in the intestinal wall indicates that the particles may be glycogen. Ermak also notes that the glycogen particles are not in the typical alpha rosette form but are arranged in compound units.

In general, the glycogen deposits in the pyloric gland of aplousobranchs are much smaller than those observed in the stolidobranchs (Gaill, 1980). Ermak (1977) notes that since the nutritional state of an animal directly affects the storage of glycogen by the tissues a difference in glycogen storage might reflect differing nutritional states at the time of fixation. Alternatively, different species of ascidians may store differing amounts of glycogen within the pyloric gland relative to storage within other body tissues. Regionalized concentration of glycogen in the gastrointestinal tract of invertebrates is common (e.g. echinoderm intestine, Doezema & Philips, 1970; gastropod digestive gland, Chatterjee & Ghose, 1974; crustacean hepatopancreas, Vonk, 1960)

C. The Pyloric Gland and the Cytonuclear Cycle

Throughout the entire pyloric gland there is a cytonuclear cycle involving the epithelium. The end result of the cycle is drastic holocrine secretion of the cellular contents of the pyloric cell into the lumen of the pyloric duct (Table 1).

Gaill (1980) describes four phases of cellular breakdown within the pyloric gland of Dendrodoa grossularia. In phase one the cell nucleus and apical microvilli are intact. The phase one cell also contains a large number of

ribosomes and apical mitochondria as well as beta rosettes of glycogen which are usually located near the base of the cell. Through the next three phases the cell progressively degenerates. Apical microvilli become club-shaped and eventually disintegrate. Glycogen masses within the cell become vacuolated and eventually occupy the entire remainder of the cell as well as the lumen of the gland. The nucleus increases in volume as a dark reticulated network forms in the nucleoplasm. The nucleus is completely degenerated by the fourth phase.

In the course of the cell cycle described for the pyloric gland of Microcosmus sulcatus and Styela plicata (Goodbody, 1974) the events differ in some respects from those described for D. grossularia by Gaill. However the final fate of the pyloric cell is total release of almost all of the cellular contents in each of the species for which this phenomenon has been described (Table 1).

In M. sulcatus and S. plicata the cytoplasm becomes strongly basophile and vacuolated, which is similar to the vacuolization noted for the glycogen deposits in D. grossularia. However, in M. sulcatus and S. plicata, the nucleus contracts instead of expanding. The nucleus expels chromatin, which forms a ring around the degenerating nucleus, and refringent concretions are formed within the cytoplasm and eventually end up in the lumen of the gland.

The basal membrane of connective tissue and occasionally a cytoplasmic network are all that remain of the cell following degeneration.

In all three species for which this phenomenon has been described the cytonuclear cycle does not occur synchronously throughout all the cells of the lining epithelium and one cell can be intact while breakdown is taking place in an adjacent cell (Gaill, 1973). The cycle has been found to be most evident in that portion of the gland next to the mid-intestine. In the more distal parts of the pyloric gland, such as around the esophagus and the post-intestine, the cycle is less evident (Gaill, 1973, 1980).

Fouque (1954) describes a modification of the mid-intestine in which the cells have characteristics similar in many respects to the intact cells of the pyloric ampullae and are more basophile and flatter than cells in other areas of the intestine. Fouque also describes `parapyloric cells´ near the mid-intestine which are believed to have their origin from ampullary cells. Fouque noted that the parapyloric cells are absent in Botryllus and Diplosoma but in the later `haemolymph´ cells are noted surrounding the pyloric vesicle.

D. The Role of the Pyloric Gland

It has been suggested that the pyloric gland is an excretory organ based on its ability to process dyes as well as ultrastructural characteristics such as the infolding of the basal plasmalemma which is a characteristic of excretory cells (Colton, 1910; Azema, 1937; Fouque, 1954; Gaill, 1973; Mirre & Thouveny, 1977). It has also been suggested that the pyloric gland functions in a digestive (Fouque, 1954) or an hepatic capacity (Ermak, 1977). All of these proposed roles for the pyloric gland would necessitate significant glycogen concentrations either for storage or in order to fuel energy requiring activities (Gaill, 1980).

Experiments concerning the uptake and storage of various dyes (Fouque, 1954; Godeaux, 1954; Brown & Davies, 1971) have been presented as supporting the role of an excretory organ. However, these types of experiments are of questionable merit in this regard when one considers that the storage or excretion of dyes could be a functional characteristic of either an hepatic or an excretory organ.

In Styela, Ermak (1977) suggests that the infoldings of the basal plasmalemma of pyloric cells, which were noted by Gaill, are actually infoldings of the lateral plasma membrane and this is a condition which exists in all transporting epithelia including the atrial epithelium. The

mitochondria, which are in intimate association with basal infoldings of the cell in renal epithelia, are actually in closer contact with glycogen deposits in the case of the pyloric cells (Ermak, 1977). Gaill (1980) suggests that the only way of distinguishing between the hepatic and the excretory roles would be to demonstrate the direct passage through the pyloric gland of substances absorbed by the digestive tract, a property which she feels the excretory system should not possess.

Gaill (1981) examines the movement of labelled glucose along the gastrointestinal tract of Dendrodoa grossularia and Sidnyum argus in order to determine which of the proposed roles is the most valid. A comparative study using a Stolidobranch (D. grossularia) and an Aplousobranch (S. argus) was done in order to see if differences in glycogen storage, and hence pyloric gland function, could be correlated with the species being examined.

Gaill (1981) found that the movement of labelled glucose along the digestive tract is comparable in the two species. Glucose absorption is found in all parts of the digestive tract of D. grossularia except for the esophagus. In less than 3 days D. grossularia accumulates labelled glucose within the pyloric ampullae suggesting that the pyloric gland, in this species at least, has more ability to store glucidic compounds than other body tissues. The

pyloric gland of Molgula occulta reacts similarly although the pyloric gland of the aplousobranch studied, namely S. argus, never accumulates labelled products regardless of the substance given as food.

The aggregation of silver grains observed in the pyloric gland of D. grossularia after 3 days serves to indicate the inclusion of the radioactive product in a polymerized macromolecule such as glycogen, particularly since the glucose was labelled at the first carbon atom. The endothelium, which is a tissue known to contain glycogen, is also distinctly labelled. Also, the heterogenous labelling in tubules as the homogenous labelling in ampullae reflect the respective distribution of the cellular stages rich in glycogen (Gaill, 1981).

As a result of these observations Gaill interprets the accumulation of labelled products by the pyloric gland as an incorporation of glucose into glycogen. The absence of any evidence for the accumulation of intestinally-absorbed labelled glucose within the pyloric gland of S. argus, which contains only a small amount of glycogen, is presented as confirming this interpretation. Gaill (1981) suggests an hepatic role of the pyloric gland in the stolidobranchs and implies a non-hepatic role for the pyloric gland in aplousobranchs.

Chapter 4. Study Objectives

This study includes an examination of the different structural components of the pyloric gland in *Corella inflata*, *Styela gibbsii* and *Clavelina huntsmani*. The relationship between the occurrence of the different gastrointestinal cell types and the presence or absence of overlying pyloric ampullae and tubules is examined.

The degree of glycogen storage within different regions of the pyloric gland, relative to other body tissues such as the gastrointestinal tract, is determined using different staining, microscopic and experimental procedures. Glycogen is identified in thick sections using periodic acid-schiff (PAS; Leeson & Leeson, 1970) staining and periodic acid-thiosemicarbazide-silver proteinate (PA-TSC-SP; Thiery, 1967) staining is used to stain for glycogen at the ultrastructural level. The rate of loss of glycogen, due to nutrient deprivation, is examined in mature specimens of all three species in order to determine if the degree of glycogen storage within the pyloric gland is species specific and/or nutrient dependent. The rate and degree of glycogen loss from the different tissues in which it occurs is examined in order to determine if the ascidian pyloric gland, or some other tissue, is the primary site of glycogen storage.

This study includes an autoradiographic examination of the ability of a local phlebobranch ascidian, namely Corella inflata, to absorb ^{14}C-l-glucose into the intestinal wall. The degree to which this labelled glucose is subsequently stored within the pyloric gland is examined in order to determine if a glycogen storage role exists within the phlebobranch pyloric gland.

The cellular ultrastructure of the pyloric gland within C. inflata, S. gibbsii and C. huntsmani is also examined in order to determine if a cytonuclear cycle is present within the pyloric glands of each of these 3 species. The nature and distribution of the cell cycle within the different morphological components of the gland is also examined.

MATERIALS AND METHODS

The species examined in this study include representatives from each of the three orders of ascidians. These species are:

Order: Aplousobranchia
Family: Polycitoridae
Clavelina huntsmani Van Name,1931

Order: Phlebobranchia
Family: Corellidae
Corella inflata Huntsman,1912

Order: Stolidobranchia
Family: Styelidae
Styela gibbsii(Stimpson,1864)

Chapter 5. Uptake of ^{14}C-1-Glucose by *C. inflata*

A. Experimental Protocol for Autoradiography

Corella inflata were collected in September, 1984 and maintained in running seawater. Following a one week acclimation period, during which the animals were fed 1 drop of Marine Invertebrate Diet(Hawaiian Marine Imports) per four litres of seawater every other day, twelve animals were placed in ^{14}C-1-glucose(5.0 μCi/ml of seawater) for 90 min. Following the labelled glucose pulse the animals were returned to unlabelled seawater for various post-incubation periods.

Animals were removed randomly from the aquarium at post-incubation periods of 2 hours, 12 hours, 36 hours, 3

and 5 days. During the time spent in post-incubation the animals were fed Marine Invertebrate Diet (Hawaiian Imports) at the dosage mentioned above. Internal body tissues (esophagus, stomach, mid-gut and post-gut) were dissected and fixed for 2 hours in 5% glutaraldehyde in 0.1 M sodium cacodylate buffer and 0.14 M sodium chloride (C.L. Singla, University of Victoria, pers comm). A control, not exposed to labelled glucose, was also fixed. Tissues were rinsed with water, dehydrated through ethanol, and embedded in Epon.

Thick sections (1.0 μm) were cut using glass knives and a Reichert OMU2 ultramicrotome. The sections were heat-fixed onto gelatin-coated (subbed) slides (Humason, 1967) in order to minimize stress artefacts due to lateral displacements of the emulsion on drying. The slides were then coated with undiluted Kodak NTB3 Nuclear track emulsion (Lot-LSB2-18-4-Cat#165-4433) following a procedure derived from the general guidelines presented by Rogers(1979). Non-labelled sections of each tissue type within the control animal were also coated with emulsion as a control for positive chemography (silver grains not resulting from ^{14}C beta emmissions).

The emulsion was placed in an oven at 34 ^{o}C for one hour (Burke, pers comm) prior to being poured into a 250 ml graduated cylinder (cut off at the 50 ml mark) at 43 ^{o}C.

Fourty-five minutes were allowed for bubbles to rise to the surface. All dipping was carried out under the prescribed Wratten No2 safelight (Rogers, 1979). Slides were dipped in the emulsion, checked for bubbles, and placed on a cold plexiglass plate over dry ice.

The cold plate helps the emulsion to gel fast as well as ensuring that the initial rate of drying is fairly slow (Rogers, 1979). Previous studies have demonstrated that lower background grain densities are produced by very slow drying (Richardson, 1963; Tsuk,et. al., 1964; Ullberg, 1954).

Dipped slides were dried and placed in black plastic slide boxes, together with dried silica gel, and stored in a refrigerator at 4 ^{o}C for 10 days prior to processing. Several emulsion-coated slides for each tissue were exposed to light prior to incubation in order to control for negative chemography (tissue preventing the production of the latent image). The 10 day exposure period was determined empirically by developing slides every other day until the optimal exposure period was reached.

Slides were developed in Eastman-Kodak Dektol developer diluted 1:2 with distilled water for 2 min at 17 ^{o}C. This was followed by a rinse in distilled water and fixation in a 30 % aqeous solution of sodium thiosulphate for 8 min.

Following fixation the slides were rinsed with water and allowed to air-dry. All tissue sections were stained with 0.25 % toluidine blue in 0.5 % aqueous sodium borate (R. Burke, University of Victoria, pers comm).

Photomicrographs of tissue sections were taken with a Vickers Automatic Camera on a Zeiss Universal R microscope using Kodak Technical Pan 35 mm film. Grain counts were made using 13 X 19.5 cm photomicrographs (final magnification = 1,000 X) of the emulsion-coated tissues and a transparent acetate grid of 100 equal squares (1 square = $25\ \mu m^2$ on the photomicrograph). Twenty grids were counted for all tissues and non-labelled background areas at each of the incubation times. Grain counts were corrected by subtracting the mean background grain count (N = 20) for a control area (presumed to contain no significant radioactivity) from each grain count obtained for the corresponding labelled tissue. In this way the final grain counts reflect the proportion of radioactivity present in the ^{14}C-1-glucose exposed tissues (Rogers, 1979).

B. Statistical Analysis of Grain Counts

One-way ANOV's are used in order to determine; 1.if labelled glucose uptake at a particular incubation time, as reflected by mean silver grain density,is the same in seven different tissues (esophagus, stomach, mid-intestinal

epithelium, post-intestinal epithelium, mid-intestinal pyloric ampullae, post-intestinal pyloric tubules and vitellogenic oocytes) and 2. if a particular tissue accumulates labelled glucose equally over each of five different incubation periods (2 hours, 12 hours, 36 hours, 3 days and 5 days).

Because each of the incubation times and the tissues examined were not randomly selected but specifically chosen, the analysis involved 12 different Model I or fixed-effects model ANOV's (7 different tissues and 5 different incubation times). Since the animals were removed from the aquarium at random the single factor ANOV's represent a completely randomized experimental design.

The single factor ANOV's for which the null hypothesis (all mean grain counts are equal) was rejected were subjected to the Newman-Keuls multiple range test, in order to determine between which population means differences exist.

Chapter 6. Nutrient Depletion Experimental Protocol

C. inflata, C. huntsmani and S. gibbsi were collected at McKenzie Bight, Saanich Inlet in August, 1985 at 4 m depth and within a 3 m radius of each other. Animals were either maintained in nutrient depleted seawater at University of Victoria or fixed immediately as follows: The

gastrointestinal tract of C. inflata was removed from the tunic and placed in fixative. The tract was flushed with fixative prior to being dissected into smaller pieces and placed in fresh fixative. The stomach and intestinal tract of C. huntsmani was flushed with fixative prior to the entire zooid being removed from the tunic, dissected into smaller pieces, and placed in fresh fixative. The fixation and dissection procedure for S. gibbsii followed that outlined for C. inflata.

Fixation of all tissue was in Torrence's fixative (Torrence and Cloney, 1981) for 5 hours on ice followed by several rinses in Torrence's buffer rinse and dehydration in ice-cold ethanol. All tissue was brought to room temperature in the first change of absolute ethanol. Tissue was embedded in Epon and sectioned with a Reichert OMU2 ultramicrotome using glass knives.

Animals to be starved were placed in an aquarium of nutrient depleted seawater. Nutrients were removed from the water entering the tank via a glass wool filtering tube. The volume of the tank (16 l) and the rate of seawater movement through the glass wool filter apparatus (5 ml/min) was such that the seawater in the tank turned over completely approximately every 2 days. This was determined in pilot studies to be necessary for maximum survival times.

C. inflata were fixed after 10, 18 and 27 days of nutrient deprivation. S. gibbsii were fixed after 18 and 27 days in filtered seawater and C. huntsmani were fixed after 10 days starvation since all of the C. huntsmani zooids had regressed by the end of 14 days of starvation.

Chapter 7. Histological and Histochemical Methods

A. Periodic Acid-Schiff(PAS) Staining of Glycogen in Thick Sections

Epon sections (1.0 μm) of each tissue were stained using a PAS staining procedure for epon-embedded tissues for light microscopy (Leeson and Leeson, 1970). The PAS staining method stains aldehyde groups produced by periodic acid (HIO_4) oxidation of free unsubstituted hydroxyl groups on adjacent carbon atoms, such as those found in glycogen. The PAS and related methods give positive results with glycogen, glycoproteins, mucoproteins and some mucosubstances (Pearse, 1968).

In addition to the basic staining procedure, as outlined by Leeson and Leeson, four additional control procedures were included to aid in the interpretation of the staining reaction (Lewis and Knight, 1977). The specific control procedures used in the PAS staining protocol were:

1. To control for the possibility that the staining results from aldehyde, carboxyl or other reducing groups which may be pre-existing in the tissue, or introduced by glutaraldehyde fixation, one slide of sections was treated with the Schiff's aldehyde detecting reagent (Lillie, 1954) without first receiving periodic acid oxidation.

2. One slide was placed in a saturated solution of Dimedone (5,5-dimethyl-1,3-cyclohexanedione; Sigma Chemical Co.) in 5 % aqeous acetic acid for 18 hours at 60 °C, prior to HIO_4 oxidation, in order to block pre-existing or introduced aldehyde groups (Bulmer, 1959; Pickett-Heaps, 1967). Subsequent treatment with periodic acid does not uncouple the link between the Dimedone and the aldehyde (Chayen et. al., 1973; Lewis and Knight, 1977).

3. To ensure that the Schiff's reagent was detecting aldehyde groups introduced by the periodic acid oxidation one slide was blocked with Dimedone after the periodic acid treatment and prior to the addition of the Schiff's reagent.

4. As a control for the action of the periodic acid, one slide was placed in 1 % hydrogen peroxide (a non-specific oxidant) which is known to result in no polysaccharide staining when substituted for periodic acid in the PAS staining procedure (Rybicka, 1979, 1981).

After PAS staining the slides are air-dried and mounted with Histoclad synthetic mounting medium (Clay Adams). Photomicrographs of thick sections were taken with a Vickers automatic camera on a Zeiss Universal R microscope (phase contrast illumination) using Kodak Technical Pan 35 mm film.

B. Periodic Acid-Thiosemicarbazide-Silver Proteinate(PA-TSC-SP) Staining of Glycogen in Thin Sections.

Thin sections (silver-gold) from each of the tissue areas studied were mounted on gold grids (200 mesh). Several grids of thin sections were treated with 0.5 % alpha-amylase in phosphate buffer for 3 h at 37 ^{o}C in order to remove glycogen (Lewis and Knight, 1977). Some grids were coated with Formvar in order to maintain the integrity of the section under the electron beam following the alpha amylase extraction of glycogen.

Bound osmium in tissue is known to inhibit the removal of glycogen by the amylase enzyme as well as resulting in non-specific deposition of silver (Lewis and Knight, 1977). As a result osmium fixation was not used in this study since amylase extraction of glycogen is an essential control and silver is required as the electron-opaque aldehyde tag.

The staining procedure used to verify the presence of glycogen in thin sections was the periodic acid-thiosemicarbazide-silver proteinate (PA-TSC-SP) procedure

(Lewis and Knight, 1977). Hanker et. al. (1964) introduced thiosemicarbazide (TSC) for the ultrastructural demonstration of macromolecules in thin sections. Like Schiff's reagent, TSC binds to the 1,2 dialdehyde groups generated by the periodic acid oxidation of carbohydrates and subsequently reduces osmium tetroxide to electron-dense osmium black.

The specificity of this staining procedure is similar to the PAS staining procedure used in light microscopy (Hanker, et. al., 1964; Seligman, et.al., 1965). Thiery (1967) intoduced a variation of this procedure using a solution of silver proteinate (SP) rather than osmium tetroxide vapour as the counter-stain. SP, which was already being used as a non-selective stain in electron microscopy by Movat (1961), increases the convenience of the method by eliminating the need for osmium tetroxide vapour.

Vye and Fischman (1971) found that SP reveals a definite glycogen unit substructure while osmium tetroxide not only fails to accentuate glycogen substructure but actually obscures it. The detailed PA-TSC-SP staining procedure used in this study, including the necessary controls, is outlined in Lewis and Knight (1977).

Two additional controls are required in the thin section staining procedure due to the aldehyde detecting

mechanism. Since reducing agents including catecholamines, free sulfhydryl groups and possibly disulphide linkages may reduce silver ions to metallic silver, one set of controls received reduction and alkylation with benzyl mercaptan and iodoacetate respectively, after periodic acid oxidation, in order to mask these groups (Swiff, 1969).

Since silver ions as well as metallic silver can result in electron density one set of controls involved washing overnight in a 10% aqeous solution of sodium thiosulphate, following the regular PA-TSC-SP treatment, in order to remove silver ions which may be attached to the tissue by chelation.

RESULTS

Chapter 8. Pyloric Gland Morphology

A. C. inflata

The pyloric gland of C. inflata is composed of a network of collecting ducts, tubules and ampullae. The main collecting ducts exit from the stomach lining and cross the mesenchymal space to the mid-intestinal epithelium (figs. 2,3). The number of main pyloric gland collecting ducts joining the stomach is variable. In one animal 4 points of duct entry were observed (figs. 4-8) and in another 5 points of duct entry were noted.

Upon reaching the mid-intestine the ducts branch repeatedly to form a network over the mid-intestinal epithelium (figs. 2,9-12).

Around the midgut the pyloric gland consists of branching pyloric tubules and pyloric ampullae. The pyloric ampullae, which lie next to the mid-intestinal epithelium, are dilated to varying extents. Pyloric ducts connect the ampullae to larger ducts which eventually lead to the main pyloric gland collecting ducts.

The pyloric gland in C. inflata extends distally along the alimentary canal to the postgut. Around the postgut the pyloric gland is comprised of pyloric tubules which do not

Figure 2. Diagram of isolated gut loop of *C. inflata* illustrating the arrangement of the pyloric structures. Several main pyloric gland collecting ducts (PG) exit from the stomach (S) and form a network of pyloric ampullae (PA) over the mid-intestinal epithelium (MI). The main ducts also give rise to the pyloric tubules (PT) which surround the post-intestine and mid-intestine. A = anus

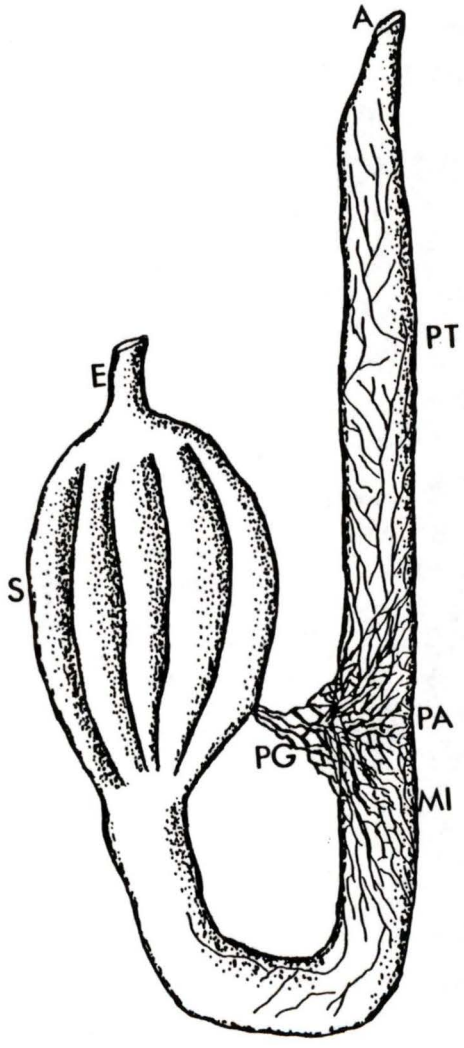
A
PT
E
S
PA
PG
MI

Figure 3. Gut loop of C. inflata isolated from the tunic. Most of the connective tissue, testicular follicles and spermduct have been removed in order to reveal the main collecting ducts of the pyloric gland. The pyloric ducts leave the stomach and can be seen crossing to the intestine were they form a branching network (light photomicrograph; scale = 1 mm).

Figures 4-8. Serial paraffin sections of C. inflata at the point of junction between the stomach and the main pyloric gland collecting ducts (PAS staining; phase contrast light photomicrographs; scale = 50 μm).

Figure 4. Six separate pyloric ducts, labelled 1 through 6, are seen outside the stomach epithelium.

Figure 5. Ducts 1 and 2 can be seen entering the stomach epithelium.

Figure 6. Ducts 1 and 2 can be seen within the stomach epithelium. Ducts 3 and 4 are beginning to merge into a single duct as are ducts 5 and 6.

Figure 7. Ducts 1 and 2 can still be seen within the stomach epithelium. Ducts 3 and 4 have joined into a common duct as have ducts 5 and 6.

Figure 8. Pyloric ducts 1 and 2 can still be seen within the stomach lining and pyloric ducts 3-4 and 5-6 can be seen merging with the stomach epithelium.

C: connective tissue
E: esophagus
I: intestine
PG: pyloric gland collecting duct
ST: stomach epithelium
T: testicular follicle

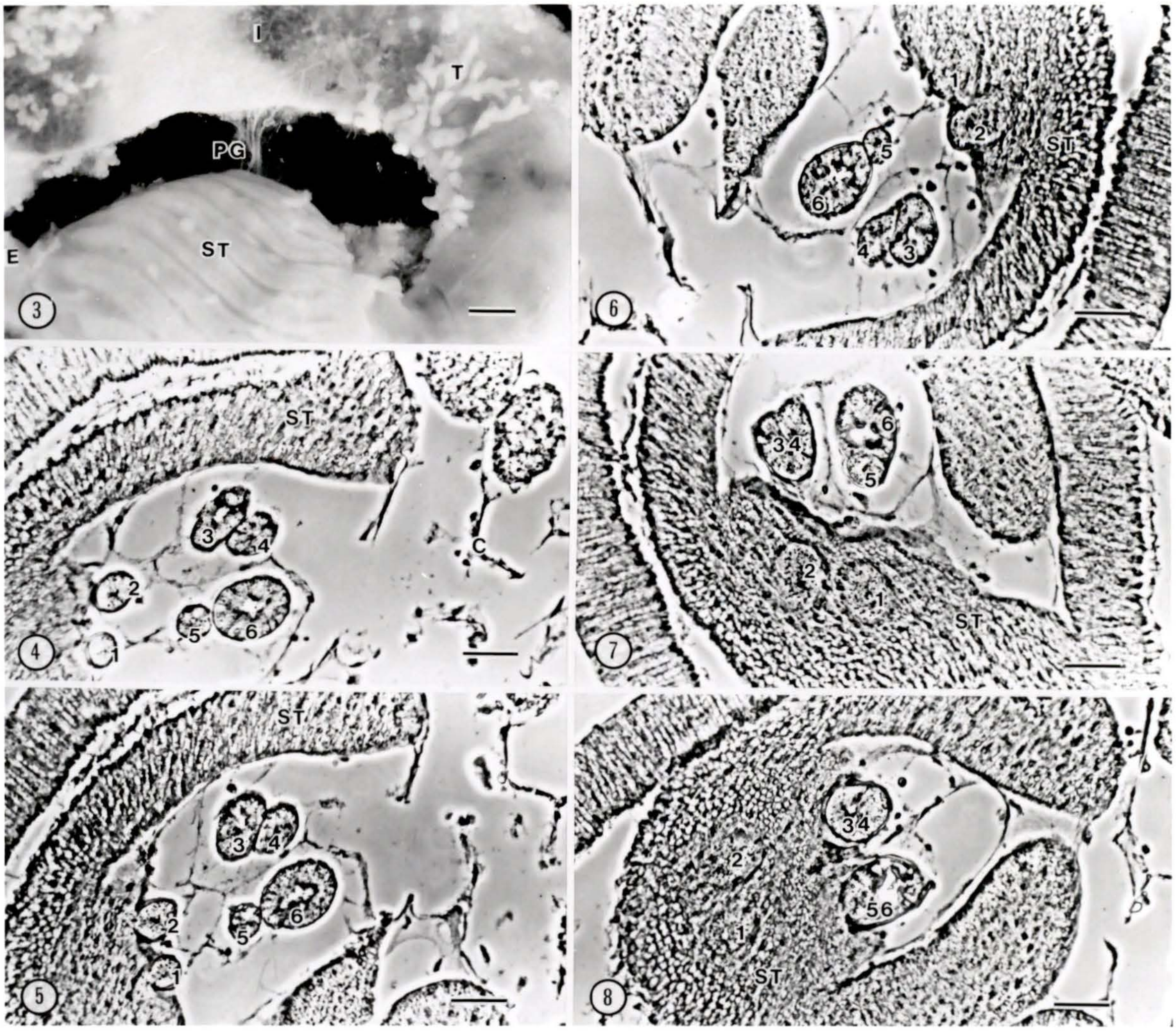
I
T
PG
E
ST
3
1
2
ST
5
6
4
3
6
ST
3
4
C
2
5
6
4
1
3
4
6
5
2
1
ST
7
ST
3
4
2
6
5
1
5
34
2
56
1
ST
8

Figures 9-12. Scanning electron photomicrographs (SEM's) of the mid-intestinal area of C. inflata.

Figure 9. Note the thick basal membrane of connective tissue beneath the intestinal cells (scale = 40 μm).

Figure 10. An anastomosing network of pyloric tubules, embedded in connective tissue, surrounds the intestine (scale = 100 μm).

Figure 11. The branching pyloric gland tubule is normally embedded in thick connective tissue. Blood cells can also be seen within the connective tissue (scale = 10 μm).

Figure 12. This photomicrograph shows the point of connection between a small pyloric tubule (removed) and a larger pyloric gland collecting duct. Note the single cell layer arrangement of the pyloric gland cells (scale = 5 μm).

BC:blood cell
C: connective tissue
I: intestine
PG: pyloric gland collecting duct
PT: pyloric tubule

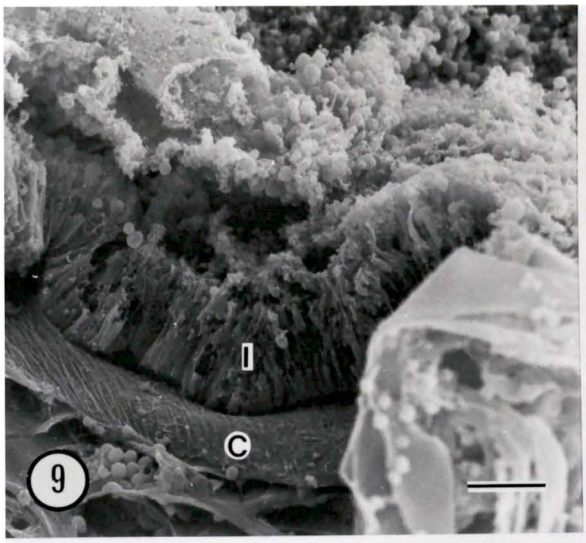
I
C
9

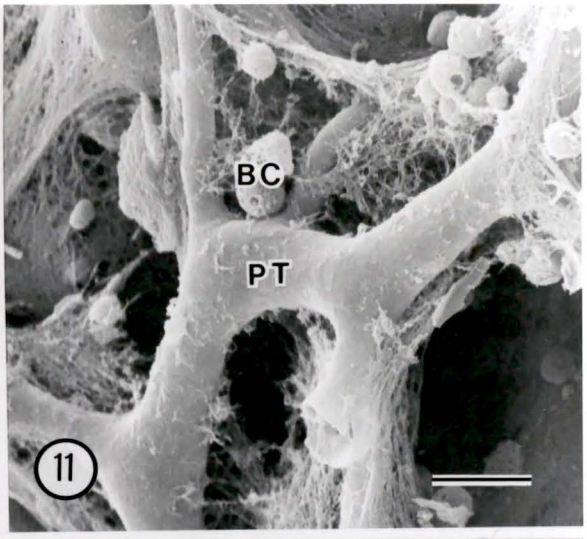
BC
PT
11

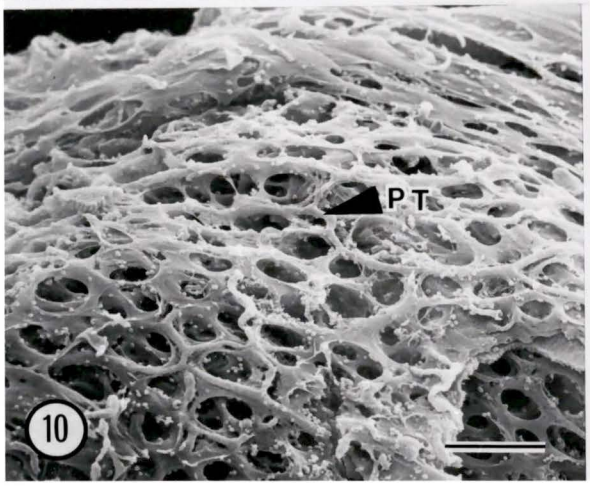
PT
10

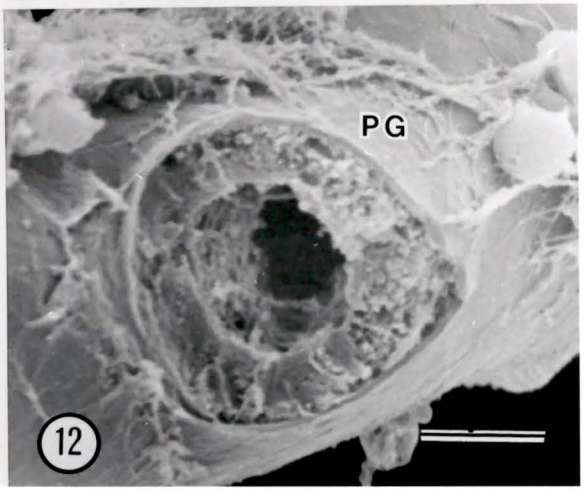
PG
12

end in dilations and are rarely in contact with the post-intestinal epithelium. In C. inflata pyloric gland tubules and ampullae are not located around the proximal intestine, stomach or esophagus (fig. 2).

B. S. gibbsii

Unlike C. inflata, in S. gibbsii a single pyloric gland main collecting duct leads from the stomach. The duct branches repeatedly and forms a network of branching ducts and tubules over the mid-intestinal epithelium. Pyloric ampullae and tubules are found between the folds of the stomach and in the area between the stomach epithelium and the overlying peridigestive endothelium. The peridigestive endothelium is continous with the atrial epithelium.

In the mid-intestinal area, pyloric gland ampullae are more dilated and numerous than in C. inflata. Pyloric gland ampullae are also present along a greater proportion of the alimentary canal relative to C. inflata.

C. C. huntsmani

The pyloric gland of C. huntsmani is also composed of pyloric ampullae and pyloric tubules. The large dilated pyloric ampullae are less numerous and limited to a smaller portion of the mid-intestinal epithelium relative to C. inflata and S. gibbssi.

Pyloric tubules extend up the ascending intestinal limb approximately half the distance between the area of contiguous pyloric ampullae and the anus. Pyloric tubules are not found in the more distal areas of the ascending limb of the intestine. Pyloric tubules are also not located around the descending limb of the intestine, the stomach and the esophagus.

Chapter 9. Glycogen Storage and Depletion

A. PAS Controls

PAS staining of tissue sections yields information concerning the storage of glycogen and its depletion from tissues in which it is usually found. PAS positive reactivity is seen as dense red/black refractive areas within the tissue (fig. 13).

If a non-specific oxidant (1% hydrogen peroxide) is used in the staining procedure instead of periodic acid the staining of glycogen is no longer apparent (fig. 14).

Using Dimedone to block the reducing groups introduced by the periodic acid, as well as those pre-existing in the tissue, ensures that PAS positivity which is seen within the tissues is due to the specific action of periodic acid on hydroxyl groups of the glycogen molecule (figs. 15,16).

Figures 13-17. Tissue sections of C. inflata following PAS staining for glycogen, illustrating the appropriate controls (phase contrast light photomicrographs).

Figure 13. PAS positive reaction sites are seen as black refractive areas within the mid-intestinal cells and the cells of the pyloric ampullae following PAS staining (scale = 20 μm).

Figure 14. In this hydrogen peroxide control, PAS positive sites are no longer evident (scale = 20 μm).

Figure 15. This section was blocked with Dimedone prior to periodic acid oxidation in order to mask aldehyde groups. Note the PAS positive reaction sites within the pyloric ampullae (scale = 30 μm).

Figure 16. This section was blocked by Dimedone after the periodic acid treatment in order to ensure that the Schiff's reagent detects aldehyde groups introduced by the periodic acid oxidation. Note the absence of any PAS positive sites (scale = 30 μm).

Figure 17. This section was treated with the Schiff's aldehyde detecting reagent without periodic acid oxidation in order to control for reducing groups which may be pre-existing in the tissue. Note the absence of any PAS positive sites (scale = 20 μm).

A: pyloric ampulla
BC: blood cell
C: connective tissue
I: intestine
IL: intestinal lumen
T: testicular follicle
O: oocyte


O
C
BC
IL
A
13

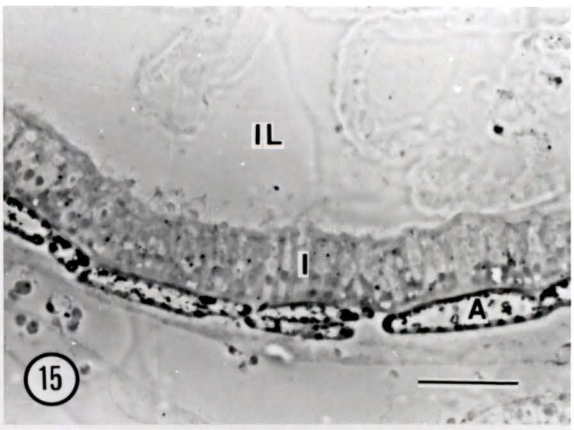
IL
I
A
15

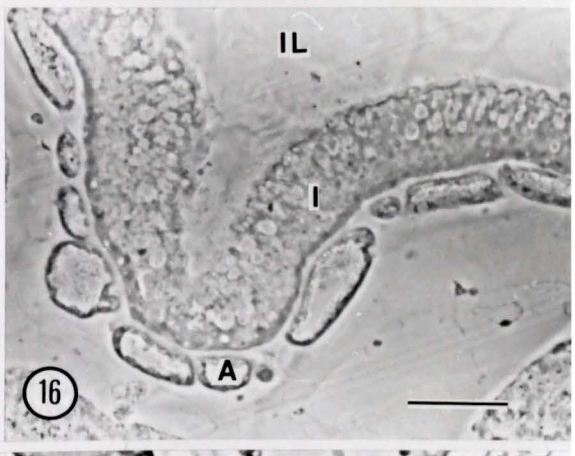
IL
I
A
16

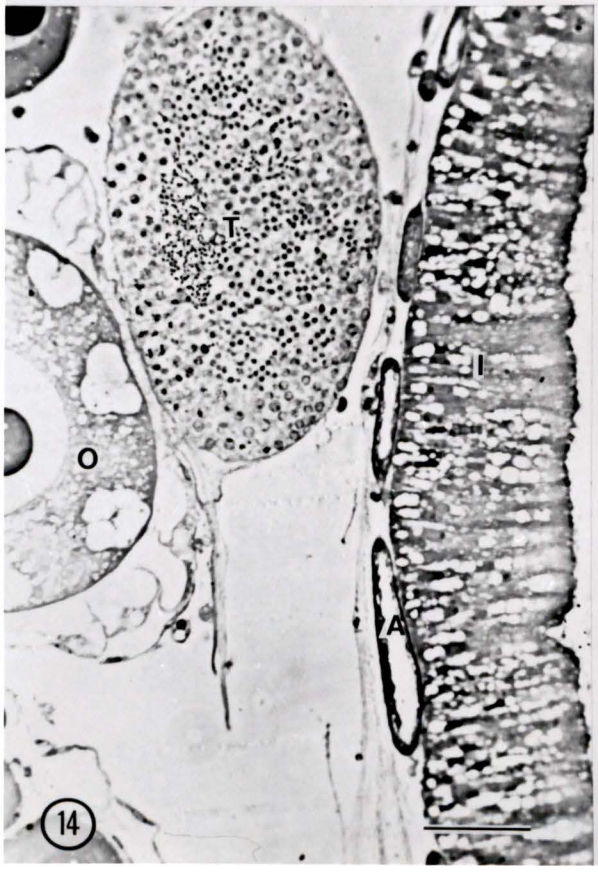
T
O
I
A
14


A
I
O
T
17

Staining tissue sections with the Schiff's aldehyde detecting reagent, without first recieving periodic acid oxidation, was used as a control for pre-existing reducing groups within the tissue (fig. 17).

B. C. inflata Control

Glycogen is found in a number of tissues in C. inflata. Glycogen is found along the sides of the stomach ridges and in the area of undifferentiated cells between the ridges (figs. 18,19,20).

PAS positive reactivity is also noted within the cells of the main pyloric gland collecting ducts (fig. 20), the mid-intestinal epithelium (fig. 21), mid-intestinal pyloric gland ampullae (fig. 21), post-intestinal pyloric gland tubules and ampullae (fig. 22) and the atrial epithelium (fig. 23). PAS positive reaction sites were also noted within the vitellogenic oocytes but were not apparent in the branchial basket, the esophagus or the post-intestinal epithelium.

C. C. inflata starved 10 days

Following 10 days of nutrient depletion, the location of glycogen within tissues of C. inflata differs from that found in non-starved animals. PAS positive reaction sites are still not evident within the branchial basket nor within

Figures 18-23. Tissue sections of C. inflata following PAS staining (phase contrast light photomicrographs; scale = 30 μm).

Figure 18. PAS positive reaction sites are evident within cells located on the sides of the stomach ridge but are absent in the ciliated mucous cells on the crest of the ridge.

Figure 19. PAS positive staining is evident in cells on the sides of the stomach ridge and within undifferentiated cells located in the trough of the ridge.

Figure 20. Note the positive staining reaction within the stomach cells and the cells of the main pyloric gland collecting duct.

Figure 21. PAS positive reaction sites are evident within the cells of the mid-intestinal epithelium as well as within the pyloric gland ampullae. The testicular follicles are not PAS positive.

Figure 22. Note the PAS positive sites within the pyloric ampullae but not within the cells of the post-intestinal epithelium or esophagus.

Figure 23. PAS positive sites are evident within the atrial epithelium but not within the esophagus.

A: pyloric ampulla
AE: atrial epithelium
BC: blood cell
C: connective tissue
CM: ciliated mucous cell
E: esophagus
IL: intestinal lumen
MI: mid-intestinal epithelium
PI: post-intestinal epithelium
PG: pyloric gland collecting duct
SI: side of stomach ridge
ST: stomach epithelium
T: testicular follicle
U: undifferentiated cell

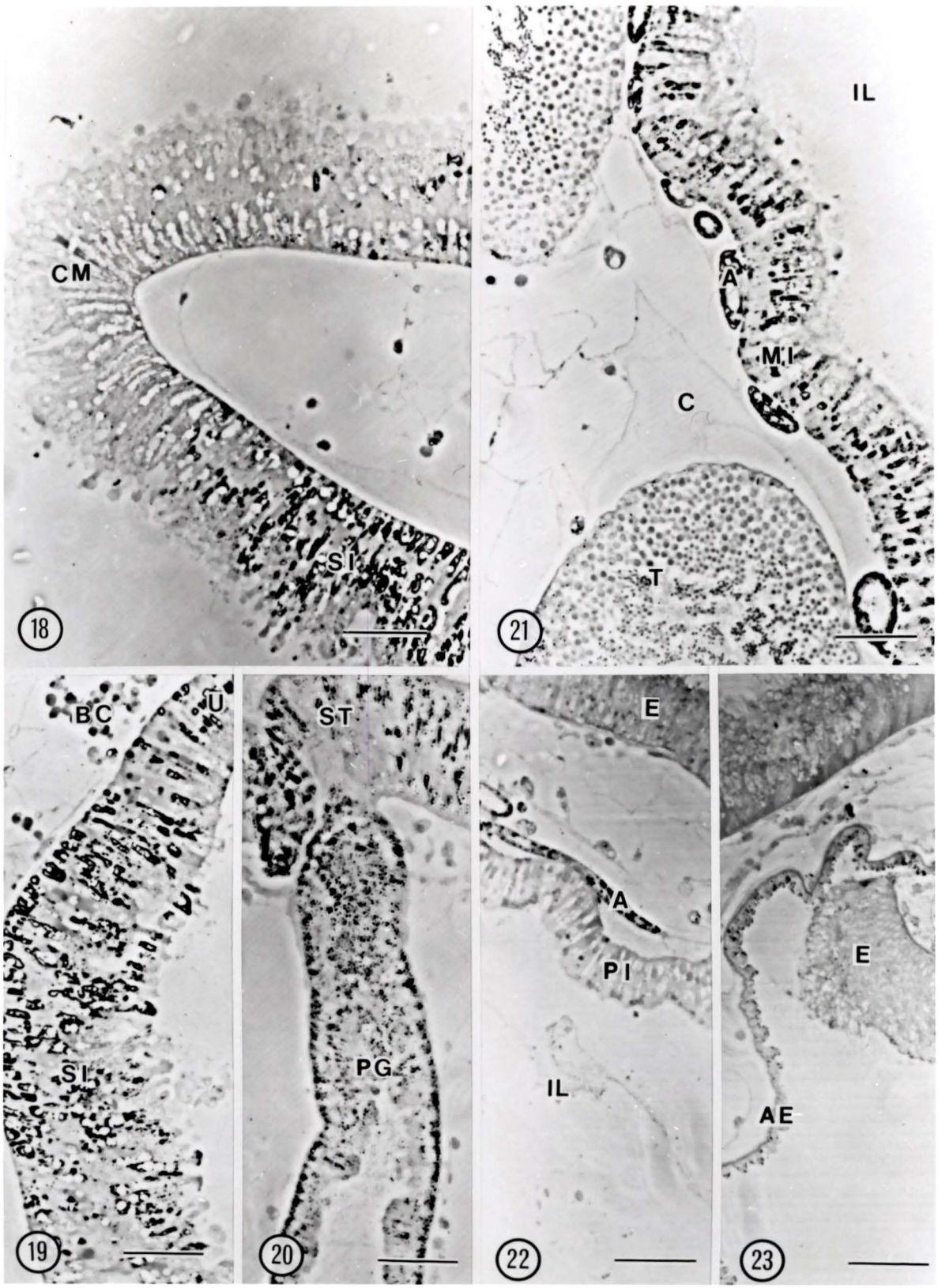
CM
SI
18
IL
A
M.I
C
T
21
BC
U
SI
19
ST
PG
20
E
A
PI
IL
22
E
AE
23

the esophagus and are less intense within the cells of the atrial epithelium, relative to non-starved animals (fig. 24).

The crests of the stomach ridges are still not PAS positive and the PAS reaction on the sides and the troughs of the stomach ridges, which was apparent in non-starved animals, is absent after 10 days of nutrient deprivation (fig. 25).

Glycogen is still apparent within the main pyloric gland collecting ducts (fig. 26) but the extent of the PAS reaction is barely noticeable.

PAS positivity is not visible within the mid-intestinal or post-intestinal epithelia (figs. 27,28,29). The pyloric gland ampullae and tubules, which surround the post-intestinal epithelium, and the ampullae which underlie missing mid-intestinal epithelium all fail to show PAS positivity (figs. 27,28). However, the pyloric gland ampullae which underlie intact mid-intestinal epithelium are intensely PAS positive (fig. 29).

D. C. inflata Starved 18 Days

After 18 days of starvation, the atrial epithelium of C. inflata still shows some PAS positivity (fig. 30). The

Figures 24-29. PAS stained tissue sections of C. inflata which has been starved for 10 days (phase contrast light photomicrographs; scale = 30 μm).

Figure 24. Point of connection between the atrial epithelium and the esophagus. PAS positive sites are evident within the atrial epithelial cells.

Figure 25. PAS positive sites are no longer evident on the sides and bottom of the stomach ridge. The stomach crest still does not show signs of PAS reactivity.

Figure 26. PAS positive sites are evident in the main pyloric gland collecting duct but the extent of the reaction is much less than that noted for comparable tissue in a non-starved C. inflata.

Figure 27. This area of dense pyloric gland ampullae shows no evidence of PAS positive sites within the ampullae which underlie missing mid-intestinal epithelium. All remaining pyloric gland ampullae, which underlie intact mid-intestinal epithelium, are PAS positive.

Figure 28. PAS positive staining within the pyloric ampullae, pyloric tubules and post-intestinal epithelium is negligible relative to comparable tissue in non-starved C. inflata.

Figure 29. Heavy PAS positive staining is seen within the pyloric ampullae while staining not evident within the mid-intestinal epithelium.

A: pyloric ampulla
AE: atrial epithelium
C: connective tissue
CM: ciliated mucous cell
E: esophagus
IL: intestinal lumen
MI: mid-intestinal epithelium
PI: post-intestinal epithelium
PG: pyloric gland collecting duct
PT: pyloric tubule
SC: stigmatic cilia
SI: side of stomach ridge
ST: stomach epithelium

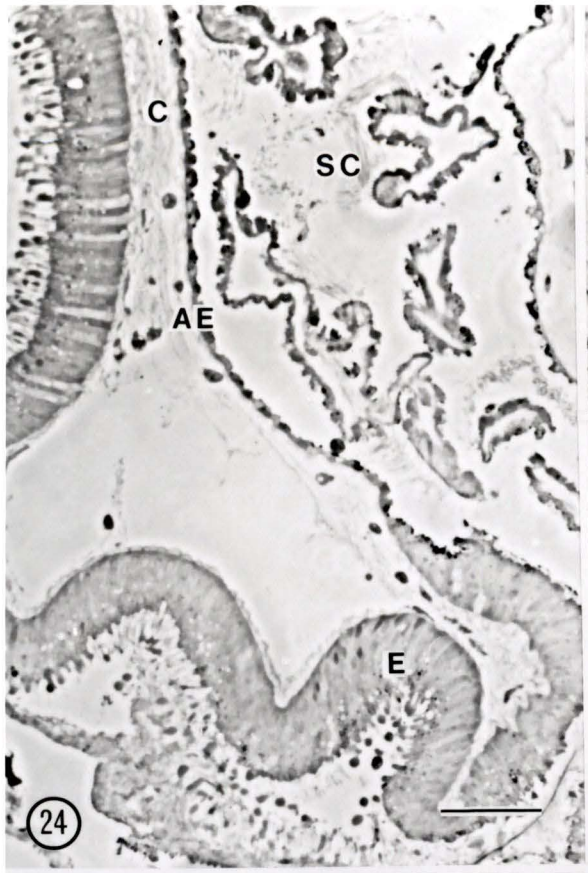
C
SC
AE
E
24

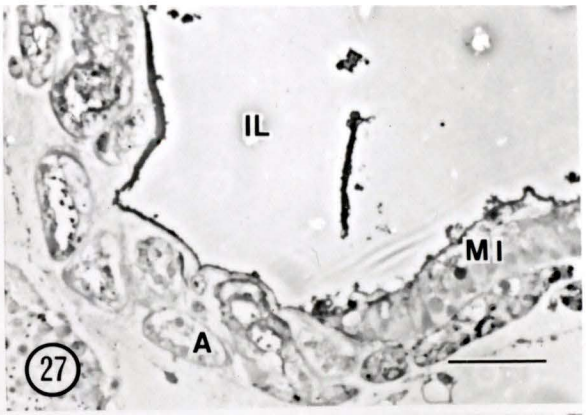
IL
MI
A
27

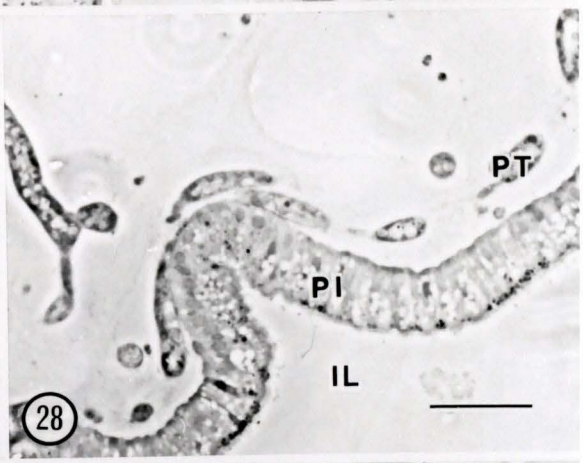
PT
PI
IL
28

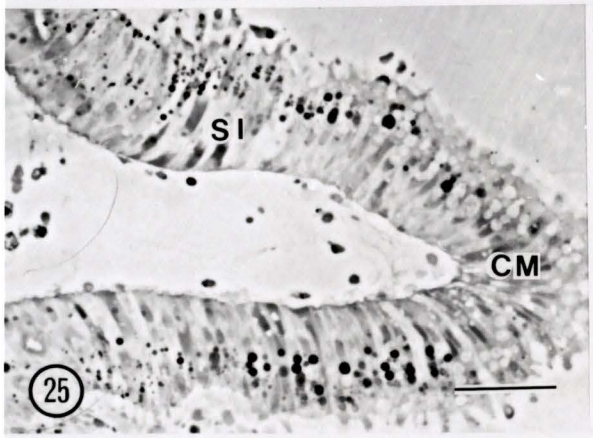
SI
CM
25

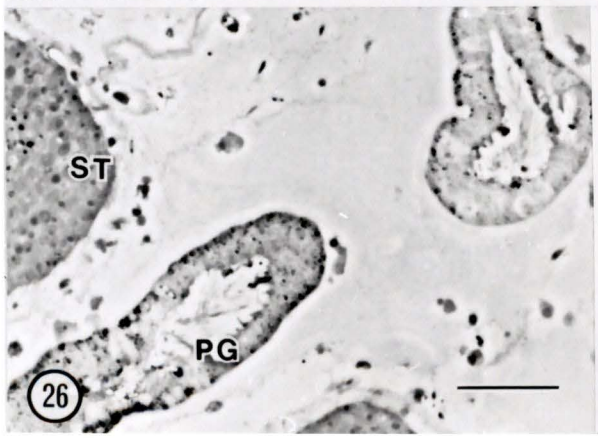
ST
PG
26


IL
A
MI
29

Figures 30-35. PAS stained tissue sections of C. inflata which has been starved for 18 days (phase contrast light photomicrographs).

Figure 30. Limited PAS positive staining is evident within the atrial epithelial cells. PAS positive sites are not apparent within the esophageal cells (scale = 20 μm).

Figure 31. Note the absence of PAS positive staining sites within any of the stomach cells (scale = 20 μm).

Figure 32. PAS positive sites are no longer evident within any of the main pyloric gland collecting ducts (scale = 20 μm).

Figure 33. PAS positive reaction sites are not present within the mid-intestinal epithelial cells and the cells of the pyloric ampullae and pyloric tubules (scale = 30 μm).

Figure 34. PAS positive reaction sites are not evident within the cells of the post-intestinal epithelium nor within the pyloric gland ampullae and tubules (scale = 30 μm).

Figure 35. PAS positive sites are seen within the vitellogenic oocytes and to a lesser extent within the early vitellogenic oocytes (scale = 20 μm).

A: pyloric ampulla
AE: atrial epithelium
C: connective tissue
CM: ciliated mucous cell
E: esophagus
EV: early vitellogenic oocyte

IL: intestinal lumen
MI: mid-intestinal epithelium
PI: post-intestinal epithelium
PG: pyloric gland collecting duct
PT: pyloric tubule
SI: side of stomach ridge
ST: stomach epithelium
VO: vitellogenic oocyte

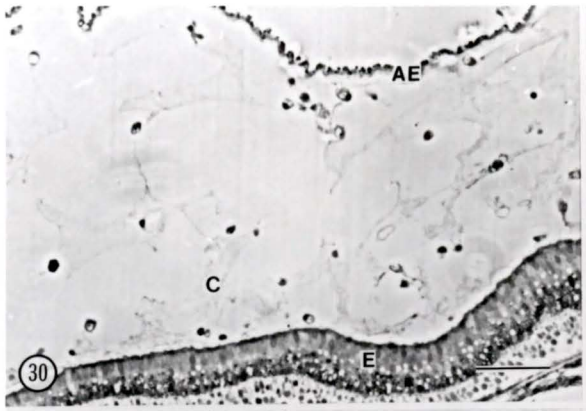
AE
C
E
30

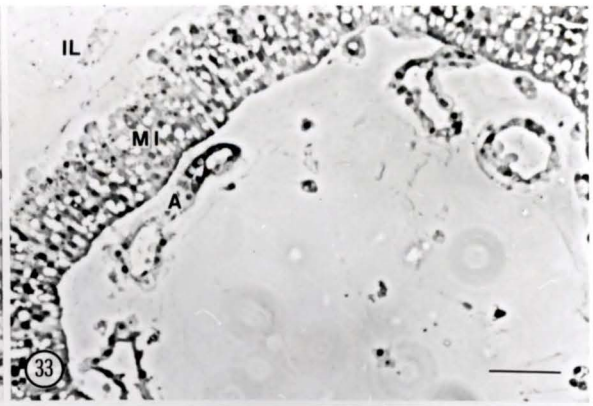
IL
MI
A
33


SI
CM
C
31


IL
PI
PT
34


ST
C
PG
32


EV
VO
35

esophagus and the stomach do not have PAS positive sites. (figs. 30,31).

PAS positive sites are not apparent within the main pyloric gland collecting ducts, mid-intestinal epithelium, mid-intestinal pyloric ampullae, post-intestinal epithelium and post-intestinal pyloric tubules following 18 days of starvation (figs. 32-34). Vitellogenic oocytes still demonstrate PAS positivity (fig. 35).

E. C. inflata Starved 27 Days

Following 27 days of nutrient depletion few, if any, PAS positive sites are seen within any of the tissues of C. inflata except for vitellogenic oocytes which are still PAS positive (figs. 36-40).

F. S. gibbsii Control

All areas of the pyloric gland of S. gibbsii are intensely PAS positive (figs. 41-44). The stomach cells and the pyloric ampullae and tubules, which are located between the folds of the stomach, are all PAS positive (fig. 41).

The pyloric ampullae and the pyloric tubules surrounding the mid-intestinal epithelium are also PAS positive (figs. 42, 43). The atrial epithelium is PAS positive although the germinal mid-intestinal epithelial cells do not show any PAS positivity (figs. 42,43).

Figures 36-40. PAS stained tissue sections of C. inflata which has been starved for 27 days (phase contrast light photomicrographs).

Figure 36. PAS positive sites are not evident within any of the stomach cells (scale = 30 μm).

Figure 37. PAS positive sites are not evident within the esophageal cells (scale = 30 μm).

Figure 38. PAS positive sites are not evident within the mid-intestinal epithelial cells nor within the cells of the pyloric ampullae (scale = 30 μm).

Figure 39. Note the absence of PAS positive sites within the pyloric gland collecting duct cells and within the lumen of the collecting duct (scale = 20 μm).

Figure 40. PAS positive sites are not evident in the post-intestine, pyloric tubules and atrial epithelium (scale = 30 μm).

A: pyloric ampulla
AE: atrial epithelium
BC: blood cell
C: connective tissue
CM: ciliated mucous cell
E: esophagus
IL: intestinal lumen
LU: lumen of pyloric gland collecting duct
MI: mid-intestinal epithelium
PI: post-intestinal epithelium
PG: pyloric gland collecting duct
PT: pyloric tubule
SI: side of stomach ridge


CM
SI
C
BC
36

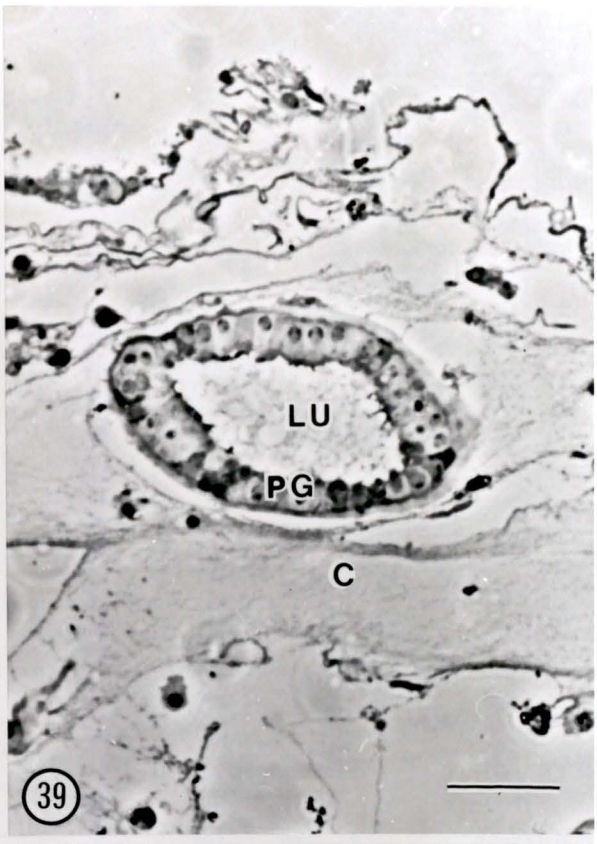
LU
PG
C
39


E
37

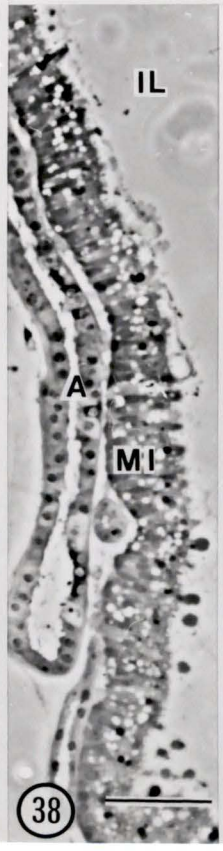
IL
A
MI
38

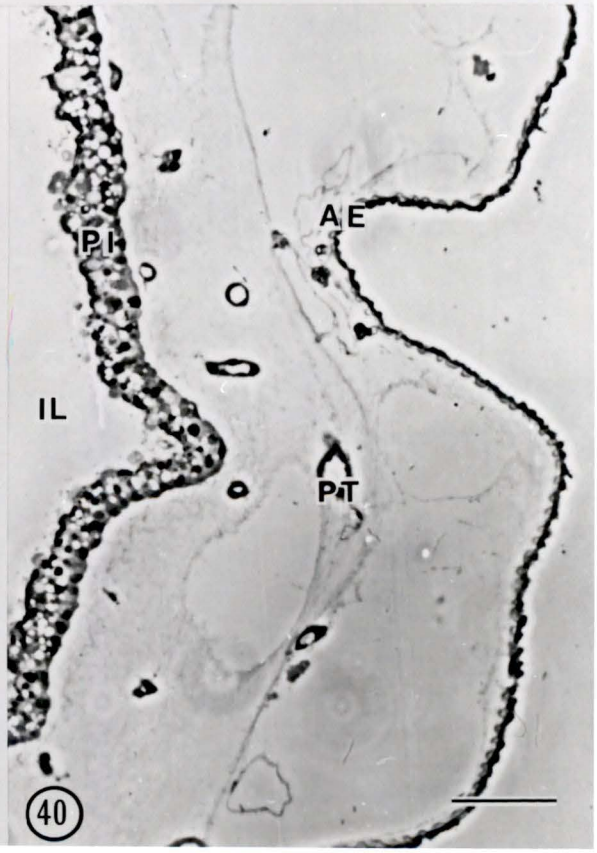
PI
AE
IL
PaT
40

Figures 41-44. Tissue sections of S. gibbsii following PAS staining (phase contrast light photomicrographs; scale = 30 μm).

Figure 41. Intense PAS positivity is seen within the pyloric ampullae and to a lesser extent within the stomach epithelial cells.

Figure 42. Intense PAS staining is seen within the pyloric ampullae which underlie the absorptive mid-intestinal cells. Pyloric ampullae are not located beneath the germinal mid-intestinal cells which also fail to show PAS positive staining.

Figure 43. Intense PAS reactivity is seen within the pyloric ampullae and pyloric tubules which underlie the absorptive mid-intestinal epithelial cells. PAS reactivity can also be seen within the atrial epithelium.

Figure 44. Intense PAS staining is seen within the pyloric tubules, pyloric ampullae and post-intestinal epithelium. The cells of the atrial epithelium are also PAS positive.

A: pyloric ampulla
AE: atrial epithelium
AI: absorptive intestinal cell
GI: germinal intestinal cell
IL: intestinal lumen
MI: mid-intestinal epithelium
PI: post-intestinal epithelium
PT: pyloric tubule
S: stomach


AE
A
S
S
41


AE
A
PT
MI
43


A
AI
IL
PT
AE
GI
42

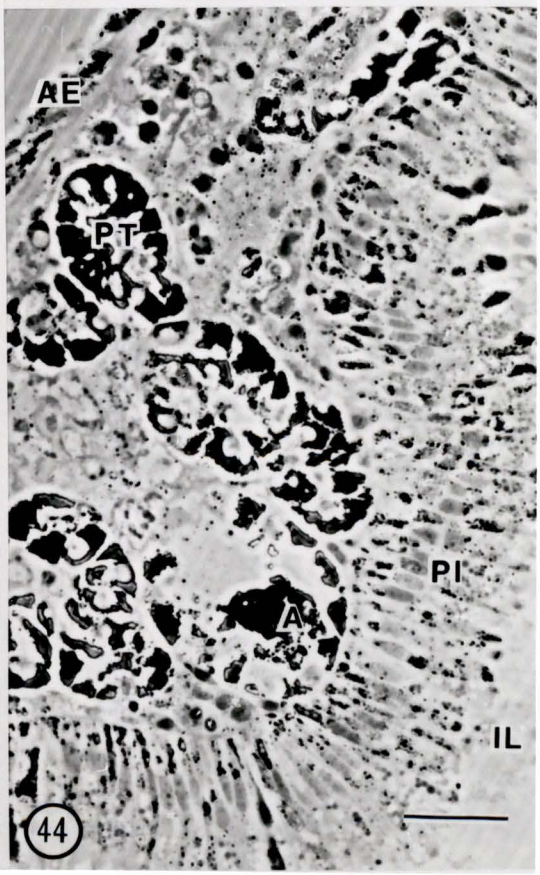
AE
PT
PI
A
IL
44

Absorptive mid-intestinal cells, mid-intestinal pyloric tubules and ampullae, post-intestinal cells and post-intestinal pyloric ampullae and tubules all demonstrate PAS positivity (figs. 43,44).

G. S. gibbsii Starved 18 Days

All tissues of S. gibbsii, which have been starved for 18 days, fail to show the intense PAS positivity noted in the pyloric tissues, stomach and intestinal epithelia of non-starved animals (figs. 45-48).

H. S. gibbsii Starved 27 Days

In S. gibbsii which have been starved for 27 days, PAS reactivity is similar to that noted in tissues of animals starved for 18 days. That is, all tissues fail to show the intense PAS reactivity noted in the tissues of non-starved animals (figs. 49-52).

I. C. huntsmani

Similar to C. inflata and S. gibbsii, PAS positive sites were not found within the esophagus of C. huntsmani (fig. 53).

However, PAS positive reaction sites were found in the cells of the ascending intestine and within the pyloric

Figures 45-48. PAS stained tissue sections of S. gibbsii which has been starved for 18 days (phase contrast light photomicrographs).

Figure 45. PAS positive sites are not apparent within any of the cells of the stomach (scale = 30 μm).

Figure 46. PAS reactivity is completely absent in pyloric ampullae associated with the stomach. PAS reactivity is also not apparent in the undifferentiated stomach cells, vacuolated stomach cells and the atrial epithelium (scale = 20 μm).

Figure 47. PAS reactivity is no longer evident within the pyloric ampullae and the pyloric tubules which underlie the mid-intestinal epithelium (scale = 20 μm).

Figure 48. PAS reactivity is not apparent within the pyloric tubules, pyloric ampullae, post-intestinal epithelium and the atrial epithelium (scale = 30 μm).

A: pyloric ampulla
AE: atrial epithlium
CM: ciliated mucous cell
IL: intestinal lumen
MI: mid-intestinal epithelium
PI: post-intestinal epithelium
PT: pyloric tubule
SI: side of stomach ridge
U: undifferentiated stomach cell
V: vacuolated stomach cell


CM
SI
45

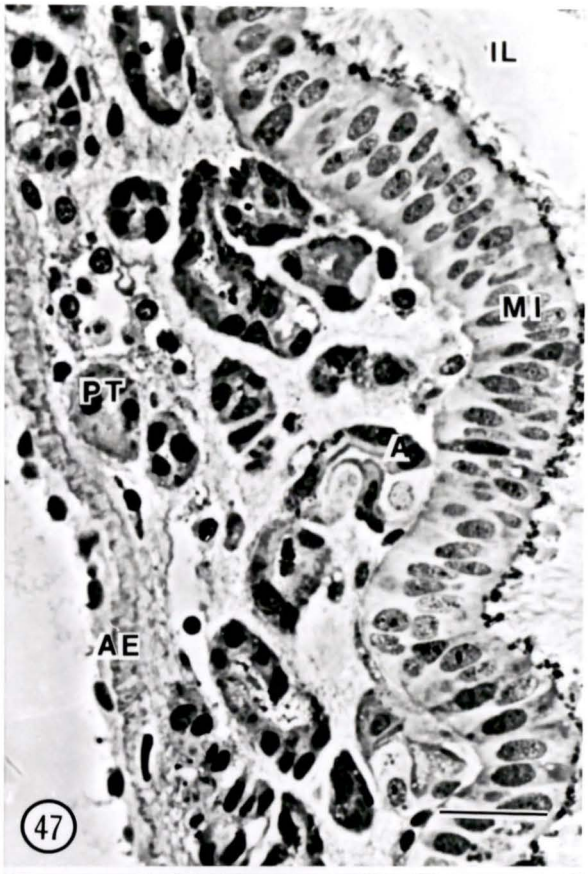
IL
MI
PT
A
AE
47

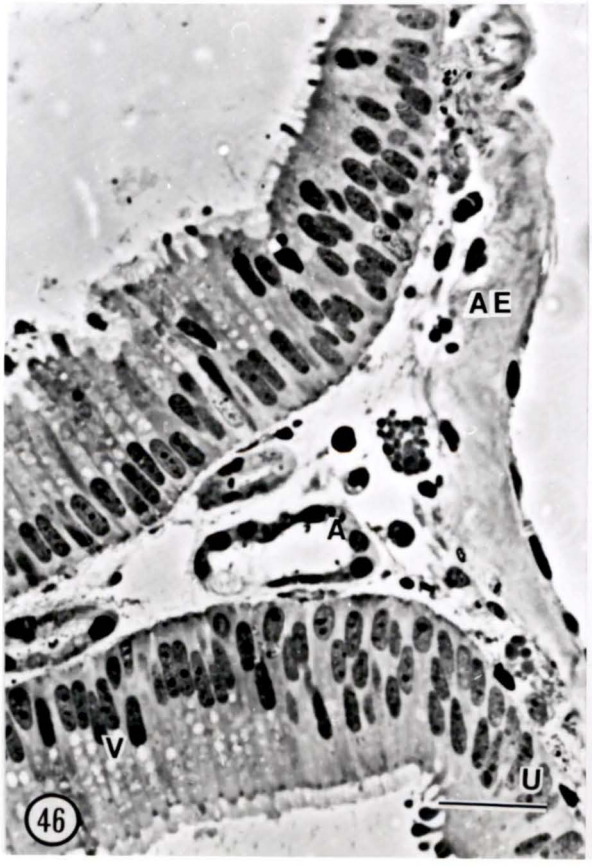
AE
A
V
U
46


PT
PI
A
IL
AE
48

Figures 49-52. PAS stained tissue sections of S. gibbsii which has been starved for 27 days (phase contrast light photomicrographs).

Figure 49. PAS positivity is not apparent in any of the cells of the stomach (scale = 30 μm).

Figure 50. Note the gradation from undifferentiated cells in the trough of the stomach ridge to vacuolated cells along the sides of the stomach ridge as well as the intimate contact between a pyloric ampulla and the atrial epithelium (scale = 20 μm).

Figure 51. PAS reactivity is absent within the pyloric tubules and pyloric ampullae which underlie the mid-intestinal epithelium (scale = 30 μm).

Figure 52. PAS reactivity is not apparent within pyloric ampullae, pyloric tubules and post-intestine (scale = 20 μm).

A: pyloric ampulla
AE: atrial epithelium
C: connective tissue
CM: ciliated mucous cell
IL: intestinal lumen
MI: mid-intestinal epithelium
PI: post-intestinal epithelium
PT: pyloric tubule
SI: side of stomach ridge
U: undifferentiated cell
V: vacuolated stomach cell


CM
A
SI
49


IL
MI
A
PT
AE
51

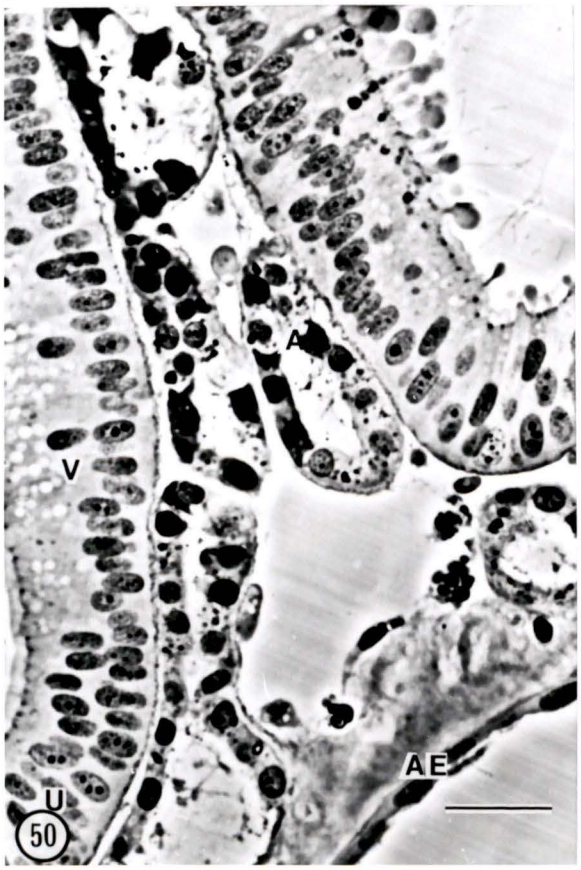
A
V
AE
U
50

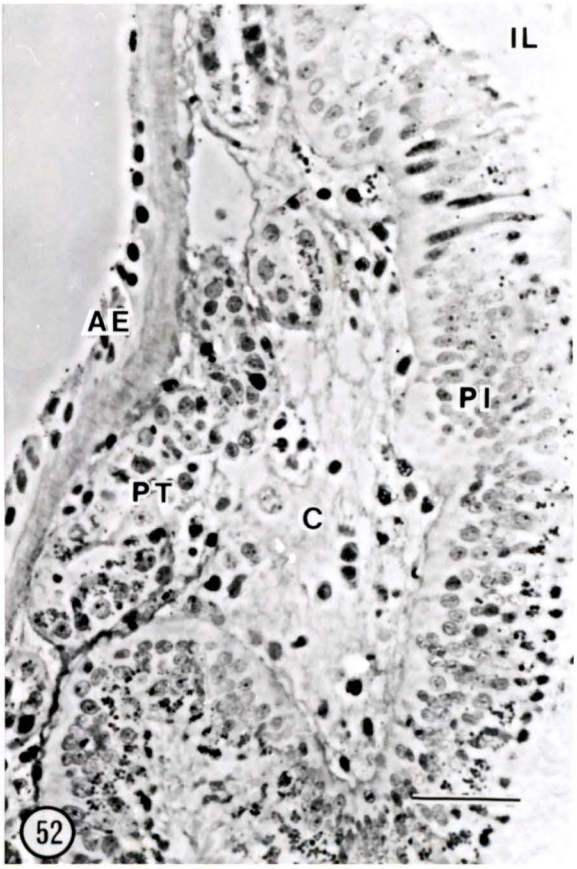
IL
AE
PI
PT
C
52

Figures 53–56. Tissue sections of C. huntsmani following PAS staining (phase contrast light photomicrographs).

Figure 53. PAS positive sites are not evident within the esophageal cells (scale = 20 μm).

Figure 54. PAS staining is noticeable within the cells of the ascending intestine and the cells of the pyloric ampullae and pyloric tubules (scale = 20 μm).

Figure 55. PAS positivity is almost negligible within the pyloric ampullae and the intestinal cells after 10 days of starvation (distal ascending intestine; scale = 30 μm).

Figure 56. In this area of contiguous pyloric ampullae, PAS positive reaction sites are still evident within the intestinal epithelial cells and within the pyloric ampullae after 10 days of starvation (scale = 20 μm).

A: pyloric ampulla
AE: atrial epithelium
BC: blood cell
CPA: contiguous pyloric ampulla
E: esophagus
I: ascending intestine
IL: intestinal lumen
PT: pyloric tubule

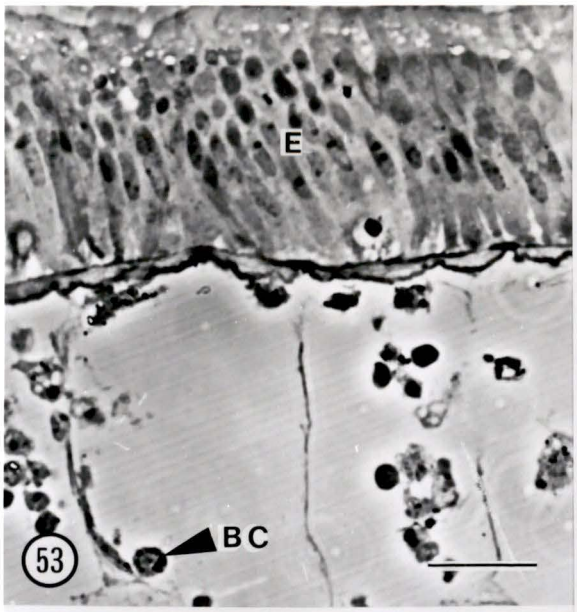
E
BC
53

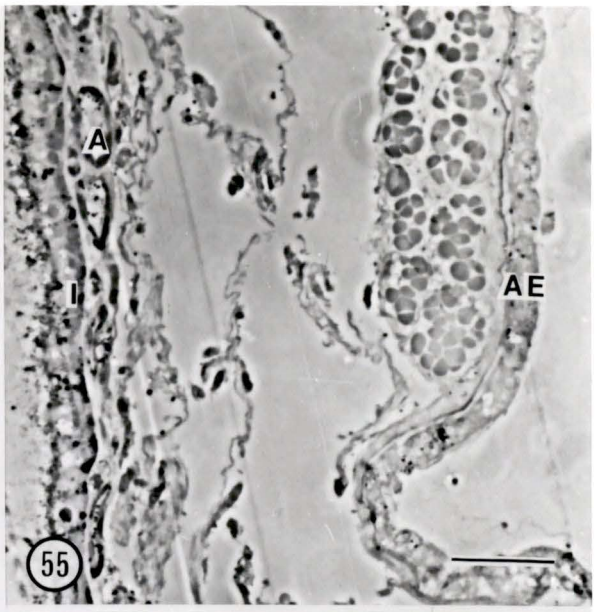
A
I
AE
55

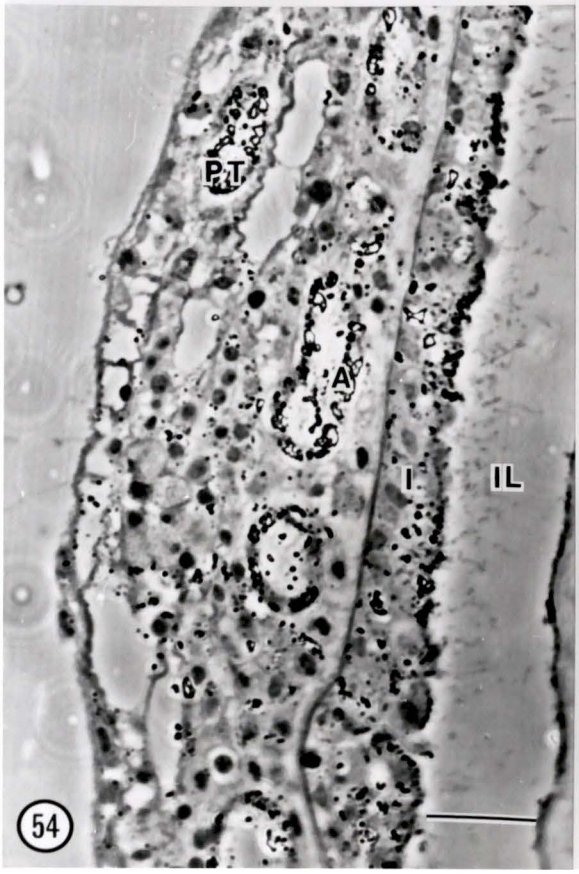
PT
A
I
IL
54

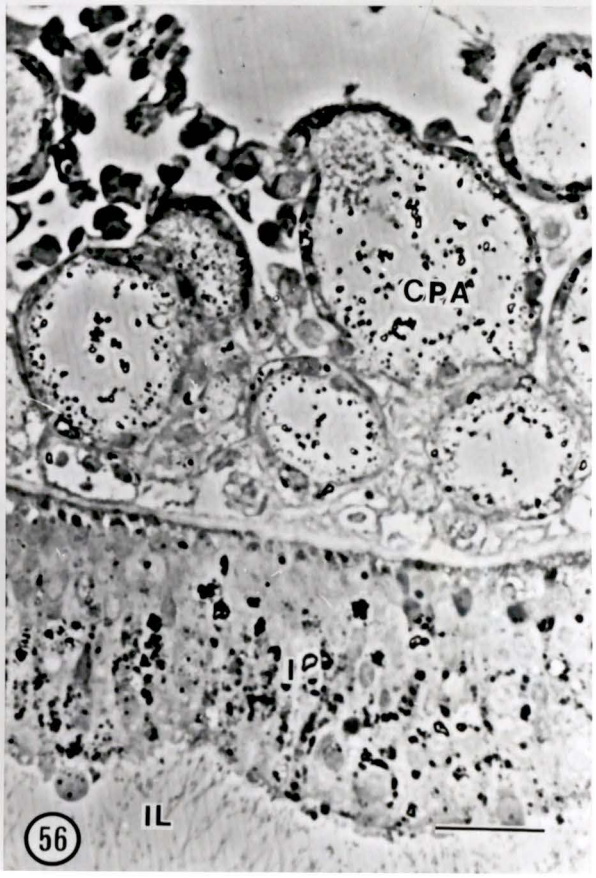
CPA
I
IL
56

ampullae and tubules which surround the ascending intestine (fig. 54).

Following 10 days of starvation, some PAS positivity is still noticeable within the pyloric ampullae and the cells of the ascending intestine. The extent of the PAS reaction is negligible in more distal ampullae and intestinal epithelia relative to the large dilated ampullae and underlying mid-intestinal epithelium (figs. 55,56).

The individual zooids of C. huntsmani were consistently unable to survive more than 10-14 days in nutrient depleted seawater.

J. Summary of Glycogen Storage and Depletion

In C. inflata, the mid-intestinal pyloric ampullae and the main pyloric gland collecting ducts are the only two tissues (other than the atrial epithelium and the vitellogenic oocytes) which contain glycogen after starvation (table 2). In S. gibbsii, all tissues which were PAS positive in control animals are devoid of glycogen following 18 and 27 days of starvation (table 2). Of the PAS positive sites found within the tissues of C. huntsmani, only the large dilated pyloric ampullae and the underlying mid-intestinal epithelium are appreciably PAS positive after 10 days of starvation (table 2).

Table 2. Summary of the extent of PAS reactivity in tissues of C. inflata, S. gibbsii and C. huntsmani starved for varying lengths of time. +++ = intense staining; ++ = moderate staining; + = light staining; 0 = no staining

TISSUE	STARVATION PERIOD			
	Control	10 days	18 days	27 days
		Corella inflata		
Esophagus	0	0	0	0
Stomach	++	0	0	0
Mid-intestinal epithelium	++	0	0	0
Mid-intestinal pyloric ampullae	++	++	0	0
Main pyloric gland duct	++	+	0	0
Post-intestinal epithelium	0	0	0	0
Post-intestinal pyloric tubules	+	0	0	0
Pre-vitellogenic oocytes	0	0	0	0
Vitellogenic oocytes	++	++	++	++
Atrial epithelium	+	+	+	+
		Styela gibbsii		
Stomach	++		0	0
Stomach pyloric tubules	+++		0	0
Mid-intestinal epithelium	++		0	0
Mid-intestinal pyloric ampullae	+++		0	0
Post-intestinal epithelium	++		0	0
Post-intestinal pyloric tubules	+++		0	0
Atrial epithelium	+		0	0
		Clavelina huntsmani		
Esophagus	0	0		
Ascending intestine	++	+		
Pyloric ampullae	++	0		
Dilated pyloric ampullae	++	+		
Atrial epithelium	0	0		

Chapter 10. Autoradiographical Results

A. Tissue Types

The ANOV results for the 7 tissue types examined indicate that the uptake of labelled glucose by Corella inflata, as reflected by the mean (N = 20) autoradiographic grain counts (table 3), varies significantly ($p < .005$; $p < .01$ for the esophagus) within a particular tissue over the post-pulse incubation periods examined. The only exception to this is the post-intestinal epithelium for which mean grain density does not vary significantly over the 5 incubation periods.

The following summaries of sources of variation arise from 7 separate Newman-Keuls multiple range tests (alpha = .05), performed on each ANOV dealing with a particular tissue type over the range of 5 incubation periods from 2 hours to 5 days. Average corrected mean grain densities are shown $\pm$ the standard error of the mean. Average grain counts for background areas in each tissue (n = 20) range from .3 - 1.3 / 25 μm^2 (figs. 57,58).

1. Esophagus

The trend of glucose uptake in the esophagus indicates uptake at a more or less steady rate although the mean grain densities for the 2 and 12 hour incubation periods (6.05

Table 3. Mean autoradiographic grain counts (n = 20) per 25 μm2 for various tissues of C. inflata which were exposed to 14-C-1-glucose and post-incubated in non-labelled seawater for the time periods indicated. Standard error of the mean values are indicated in parentheses. E = esophagus, S = Stomach, MI = Mid-intestinal Epithelium, PI = Post-intestinal Epithelium, PA = Mid-intestinal Pyloric Gland Ampullae, PT = Post-intestinal Pyloric Gland Tubules, V = Vitellogenic Oocytes

	POST-INCUBATION PERIOD				
TISSUE	2 HOUR	12 HOUR	36 HOUR	3 DAY	5 DAY
E	6.05(.61)	6.25(.77)	3.70(.68)	4.65(.73)	3.20(.57)
S	8.95(.95)	7.45(.48)	8.20(1.1)	6.00(.60)	14.55(1.0)
MI	1.75(.26)	4.85(.64)	13.4(1.3)	10.4(.88)	11.85(1.1)
PI	1.20(.27)	1.35(.23)	2.25(.38)	2.25(.42)	2.05(.42)
PA	1.10(.28)	1.65(.36)	3.10(.40)	1.95(.46)	5.70(.59)
PT	.05(.05)	.15(.11)	.05(.05)	.80(.29)	1.60(.21)
V	4.20(.67)	4.55(.57)	6.0(1.2)	11.0(1.2)	10.8(1.5)

Figures 57-58. Autoradiographs of tissue sections of *C. inflata*, not exposed to ^{14}C-1-glucose, illustrating background silver grain density (toluidine blue staining; phase contrast light photomicrographs; scale = 20 μm).

Figure 57. Typical background silver grain density shown over the post-intestinal epithelium.

Figure 58. Background grain counts are almost negligible for all tissues studied as illustrated by this autoradiograph of the stomach lining.

A: pyloric ampulla
C: connective tissue
CM: ciliated mucous cell
IL: intestinal lumen
PI: post-intestinal epithelium
S: silver grain
SI: side of stomach ridge
U: undifferentiated cell

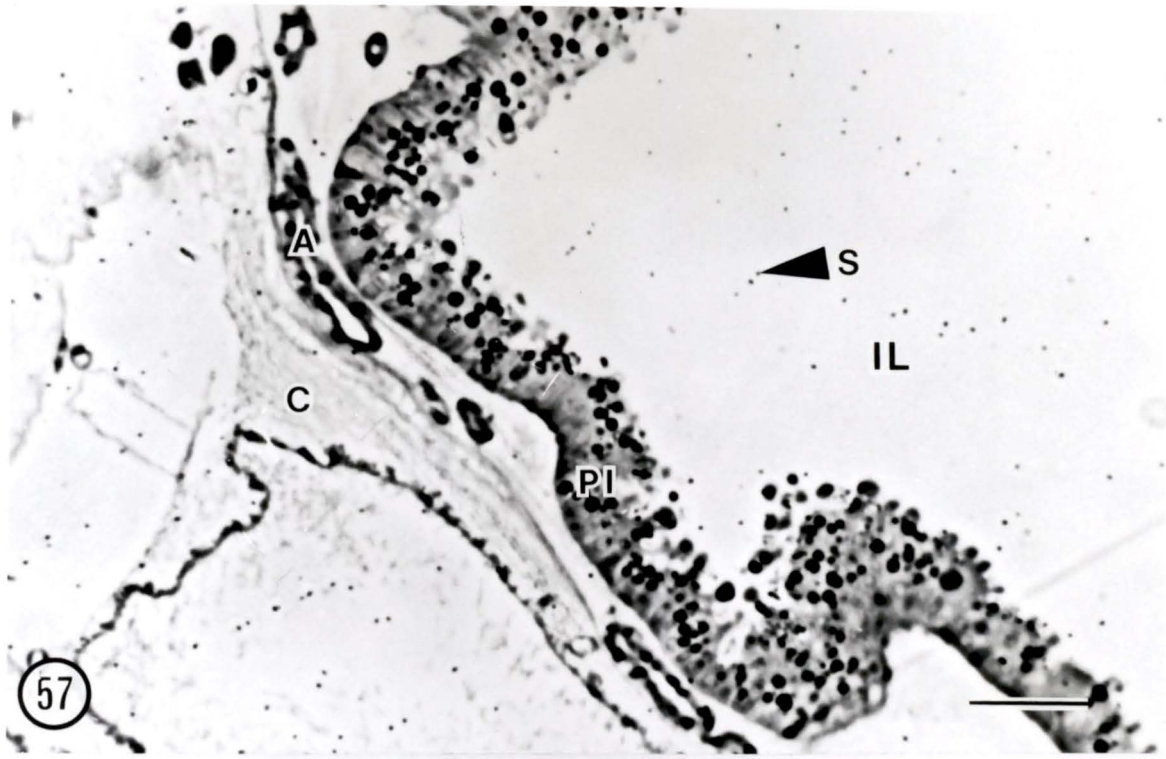
A
S
IL
C
PI
57


CM
C
SI
U
58

$\pm$.61 and 6.25 $\pm$ .77 respectively), which correspond to the presence of the labelled glucose pulse in the gut, are significantly higher than the counts recorded by the end of five days of incubation (3.2 $\pm$ .57).

2. Stomach

Substantial uptake of labelled glucose into the stomach tissue is noted 2 hours after the labelled glucose pulse (8.95 $\pm$ .95) and is maintained at much the same level until the 5 day incubation period (14.55 $\pm$ 1.0). However, there is a significant drop in mean grain density from the 12 hour to the 3 day incubation period (6.0 $\pm$ .60) although the significance is not evident if alpha is set at .025. The grain count in the stomach for the 5 day incubation period is significantly greater (14.55 $\pm$ 1.0) than the grain counts recorded for the stomach at all other incubation periods.

3. Mid-intestinal Epithelium

The mean grain count recorded for the 2 hour incubation period (1.75 $\pm$ .26) is significantly lower than the mean grain counts recorded for all other incubation periods. The mean grain count for the 12 hour incubation period (4.85 $\pm$ .64) is also significantly lower than the counts recorded for successive incubation periods. The level of uptake of labelled glucose into the mid-intestinal lining is constant after 12 hours with no significant difference between the

thirty-six hour counts (13.4 ± 1.3) and those observed at 3 days (10.4 ± .88) and at 5 days (11.85 ± 1.1).

4. Post-intestinal Epithelium

Within the post-intestinal epithelium mean grain density ranges from 1.20 ± .27 after 2 hours to 2.05 ± .42 after 5 days of incubation. No significant difference exists between the mean grain counts recorded for post-intestinal epithelia at all 5 incubation periods.

5. Mid-intestinal Pyloric Gland Ampullae

Mean grain counts recorded for 2 hour (1.10 ± .28) and 12 hour (1.65 ± .36) incubation periods do not differ significantly from each other. However, counts recorded for 36 hours (3.10 ± .40) and 12 hours do differ significantly from each other. There is no significant difference in mean grain counts recorded for this tissue at 36 hours and 3 days (1.95 ± .46). The grain count in the pyloric ampullae of the mid-intestinal area is significantly greater at 5 days (5.70 ± .59) than any of the grain counts recorded for previous incubation periods for this particular tissue.

6. Post-intestinal Pyloric Gland Tubules

Mean grain counts recorded for the 2 hour (.05 ± .05), 12 hour (.15 ± .11) and 36 hour incubation periods (.05 ± .05) do not differ significantly from each other but

differ significantly from counts recorded for 3 days (.80 $\pm$ .29) and 5 days (1.6 $\pm$ .21). The counts recorded for 3 and 5 days are also significantly different from each other.

7. Vitellogenic Oocytes

The grain counts for 2 hours (4.2 $\pm$ .67), 12 hours (4.55 $\pm$ .57) and 36 hours (6.0 $\pm$ 1.2) do not vary significantly from each other. However, there is a significant increase in the grain density from 36 hours to 3 days (11.0 $\pm$ 1.2) and between 36 hours and 5 days of incubation (10.85 $\pm$ 1.5). There is no significant discrepency between the counts recorded at 3 days and those recorded at 5 days.

B. Incubation Times

The ANOV results for each of the 5 incubation times examined indicate that the uptake of labelled glucose by C. inflata, as reflected by the mean (N = 20) autoradiographic silver grain counts, varies significantly ($p < .005$) between the 7 different tissues examined at each of the incubation times. The following summaries of sources of variation in grain density at a particular incubation period arise from 5 separate Newman-Keuls multiple range tests (alpha = .05) which were performed on each ANOV dealing with all tissues examined at a particular incubation period.

1. 2 Hours

The mean grain densities recorded for the stomach (8.95 ± .95), esophagus (6.05 ± .61) and vitellogenic oocytes (4.20 ± .67; figs. 59,60,63) are all significantly different from each other. The grain counts recorded for the mid-intestinal epithelium (1.75 ± .26; fig. 61), post-intestinal epithelium (1.20 ± .27; fig. 62), mid-intestinal pyloric gland ampullae (1.10 ± .28) and post-intestinal pyloric gland tubules (.05 ± .05) do not differ significantly from each other.

2. 12 Hours

At this incubation period the stomach and the esophagus tissues have the highest mean grain density levels (7.45 ± .48 and 6.25 ± .77 respectively; figs. 64,65) and no significant difference in mean grain density exists between the two tissues. Mean grain densities recorded for the stomach and esophagus tissues are significantly higher than the second highest level of grain density which was recorded for the mid-intestinal epithelium and the vitellogenic oocytes with mean counts of 4.85 ± .64 and 4.55 ± .57 respectively (figs. 66,67,69). No significant difference exists between the mid-intestinal epithelium and the vitellogenic oocyte counts. The mean grain densities recorded for the mid-intestinal epithelium and the vitellogenic oocytes are

Figures 59-63. Autoradiographs of tissue sections of *C. inflata* 2 hours after a 90 min exposure to ^{14}C-1-glucose (5.0 μCi/ml)(toluidine blue staining; phase contrast light photomicrographs; scale = 20 μm)

Figure 59. The mean silver grain density over the esophageal cells is 6.05 ± .61.

Figure 60. The mean silver grain count over the cells of the stomach (8.95 ± .95) is significantly greater than the 2 hour esophagus counts.

Figure 61. The grain densities for the mid-intestinal epithelium (1.75 ± .26) and the mid-intestinal pyloric gland ampullae (1.10 ± .28) do not differ significantly from each other.

Figure 62. The grain densities for the post-intestinal epithelium (1.20 ± .27) and the post-intestinal pyloric gland tubules (.05 ± .05) do not differ significantly from each other.

Figure 63. The grain density for the vitellogenic oocytes (4.20 ± .67) is significantly less than counts recorded for the 2 hour esophagus and the 2 hour stomach.

A: pyloric ampulla
C: connective tissue
CM: ciliated mucous cell
E: esophagus

IL: intestinal lumen
MI: mid-intestinal epithelium
PI: post-intestinal epithelium
PT: pyloric tubule
SI: side of stomach ridge
V: vitellogenic oocyte


C
E
59

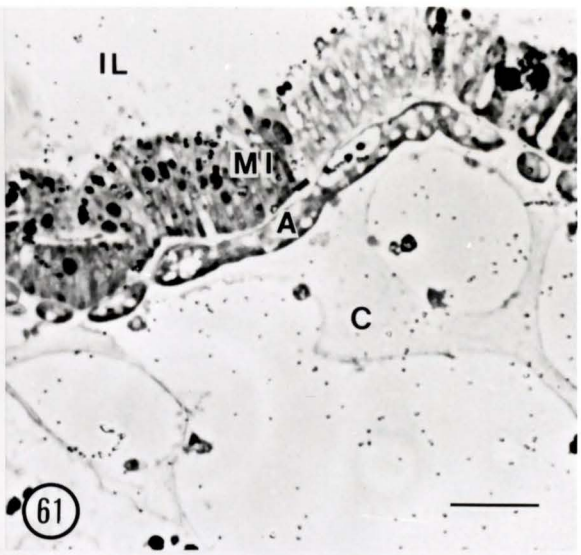
IL
MI
A
C
61

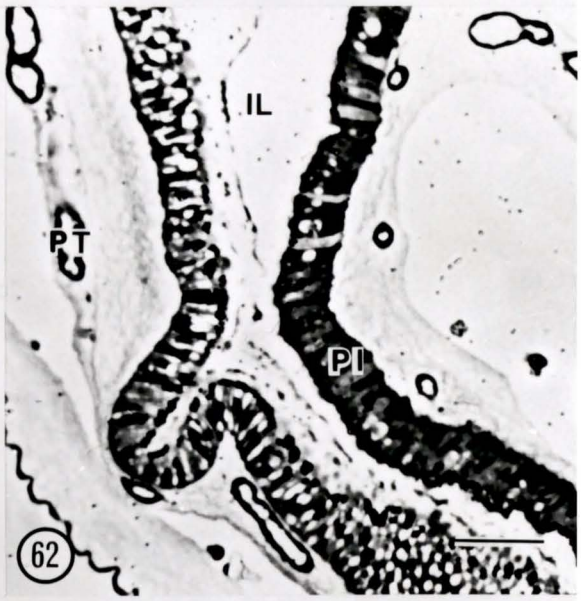
IL
PT
PI
62


CM
SI
C
60

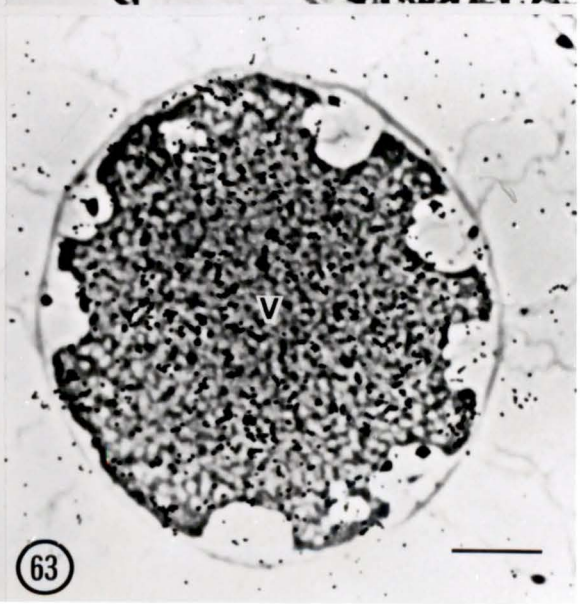
V
63

Figures 64–69. Autoradiographs of tissue sections of *C. inflata* 12 hours after a 90 min exposure to a ^{14}C-l-glucose pulse (5.0 μCi/ml)(toluidine blue staining; phase contrast light photomicrographs; scale = 20 μm).

Figure 64. The mean grain density over the esophageal cells is 6.25 ± .77.

Figure 65. The mean grain density over the stomach cells (7.45 ± .48) does not differ significantly from counts recorded over the 12 hour esophagus.

Figure 66. The mean grain density recorded for the mid-intestinal epithelium (4.85 ± .64) is significantly above the counts recorded for the mid-intestinal pyloric ampullae (1.65 ± .36).

Figure 67. Silver grains are not evident within the contiguous pyloric ampullae of the pyloric gland. Note the high grain density within the intestinal cells which underlie the contiguous pyloric ampullae.

Figure 68. The mean grain densities over the post-intestinal epithelium (1.35 ± .23) and the post-intestinal pyloric gland tubules (.15 ± .11) are not significantly different from each other.

Figure 69. The mean grain density recorded for vitellogenic oocytes (4.55 $\pm$ .57) does not differ significantly from the grain density recorded for the 12 hour mid-intestinal epithelium.

A: pyloric ampulla
C: connective tissue
CPA: contiguous pyloric ampulla
E: esophagus
IL: intestinal lumen
MI: mid-intestinal epithelium
PI: post-intestinal epithelium
PT: pyloric tubule
ST: stomach epithelium
V: vitellogenic oocyte

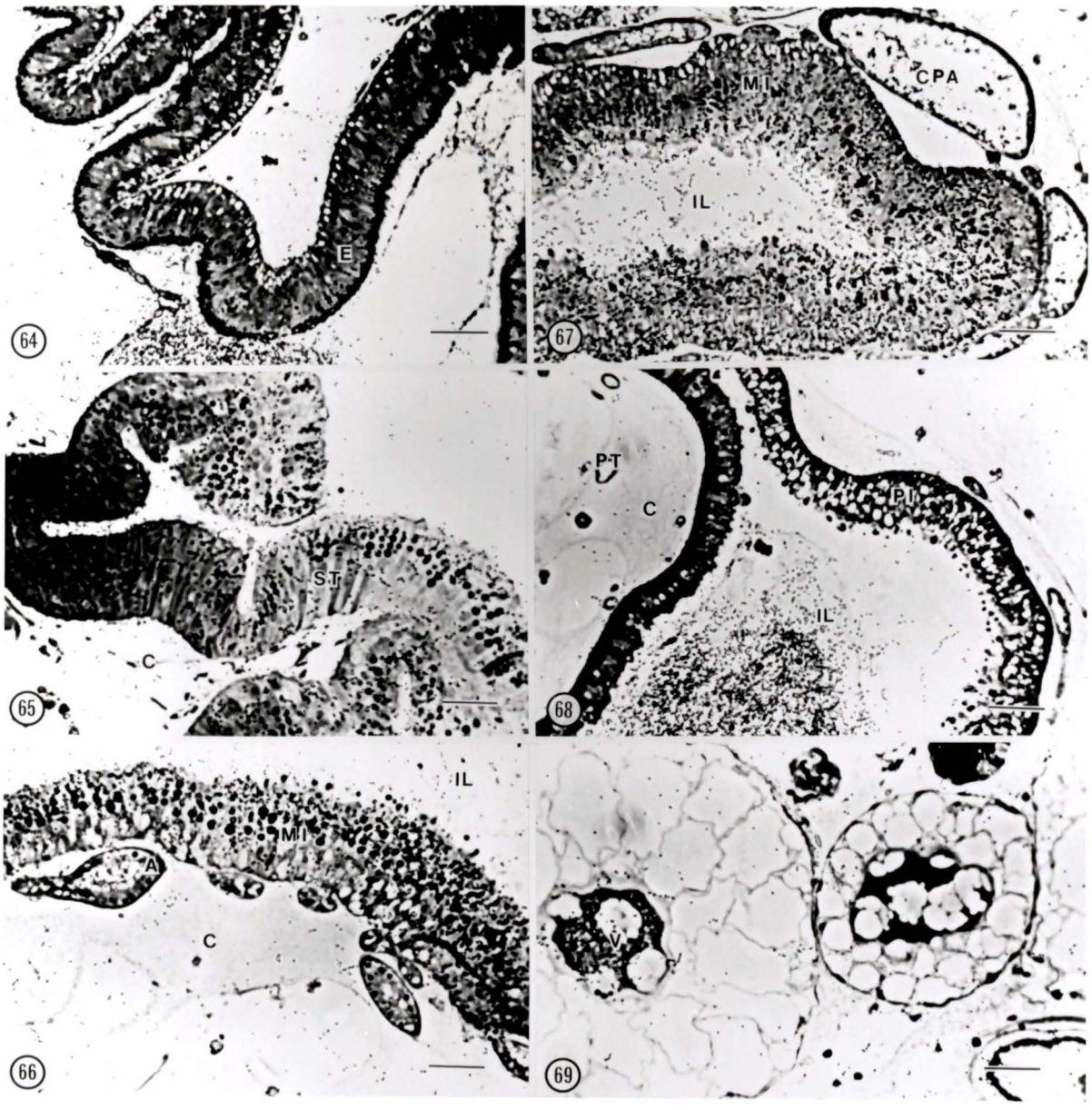
E
64
MI
CPA
IL
67
ST
C
65
PT
C
PI
IL
68
IL
MI
A
C
66
V
69

significantly higher than counts recorded for the mid-intestinal pyloric ampullae (1.65 ± .36), post-intestinal epithelium (1.35 ± .23; fig. 68) and post-intestinal tubules (.15 ± .11; fig. 68) which all have mean grain densities which are not significantly different from one another.

3. 36 Hours

After 36 hours of incubation the grain counts recorded for the mid-intestinal pyloric gland ampullae (3.10 ± .40), post- intestinal epithelium (2.25 ± .38) and esophagus (3.7 ± .68) do not differ significantly from one another (figs. 70-72). The esophagus and mid-intestinal pyloric gland ampullae have mean grain counts which are significantly higher than counts recorded for the post-intestinal pyloric gland tubules (.05 ± .05; fig. 72). The counts for the post-intestinal epithelium and the post-intestinal pyloric tubules are not significantly different from one another. The mean grain density for vitellogenic oocytes (6.0 ± 1.2; fig. 74) does not differ significantly from stomach counts (8.2 ± 1.1; fig. 70). The density of silver grains noted within the pre-vitellogenic oocytes is always minimal (fig. 73). The mean grain densities for all tissues are significantly lower than that recorded for the mid-intestinal epithelium (13.4 ± 1.3) which demonstrates the highest mean grain density after 36 hours (fig. 71).

Figures 70-74. Autoradiographs of tissue sections of C. inflata 36 hours after a 90 min exposure to a ^{14}C-1-glucose pulse (5.0 μCi/ml)(toluidine blue staining; phase contrast light photomicrographs; scale = 20 μm).

Figure 70. The mean grain counts recorded for the esophagus (3.7 ± .68) and the stomach epithelium (8.2 ± 1.1) are significantly different from each other.

Figure 71. The mean grain count recorded for the mid-intestinal pyloric gland ampullae (3.10 ± .40) is significantly lower than the mean grain count recorded for the mid-intestinal epithelium which has the highest mean grain density (13.4 ± 1.3) relative to all other tissues at 36 hours.

Figure 72. The counts recorded for the post-intestinal epithelium (2.25 ± .38) and post-intestinal pyloric tubules (.05 ± .05) do not differ significantly from each other.

Figure 73. Note the absence of silver grains over the pre-vitellogenic oocytes.

Figure 74. The mean grain count recorded for the vitellogenic oocytes (6.0 ± 1.2) is not significantly different from that recorded for the stomach but is

significantly lower than the counts recorded for the mid-intestinal epithelium.

A: pyloric ampulla
CO: ciliated oviduct
E: esophagus
IL: intestinal lumen
MI: mid-intestinal epithelium
PI: post-intestinal epithelium
PO: pre-vitellogenic oocyte
PT: pyloric tubule
ST: stomach epithelium
V: vitellogenic oocyte

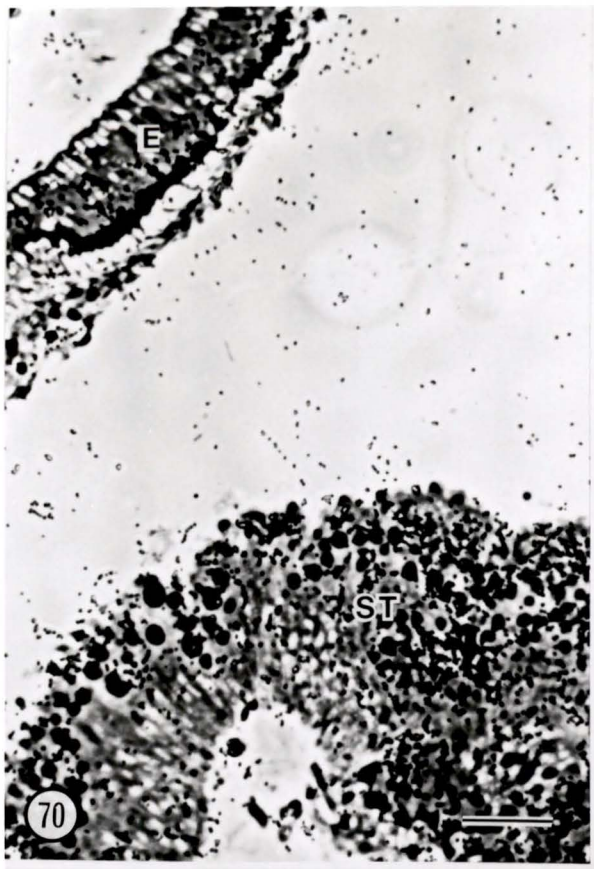
E
ST
70

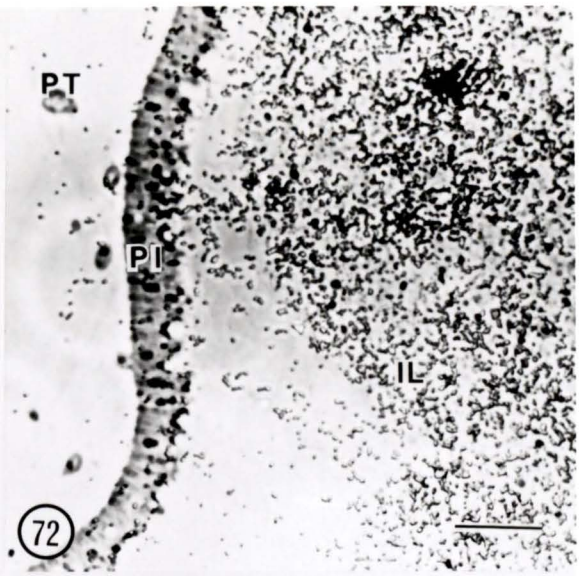
PT
PI
IL
72

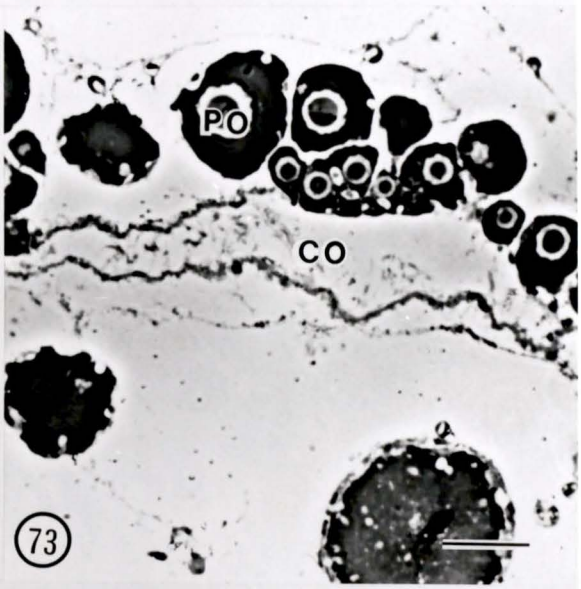
PO
CO
73

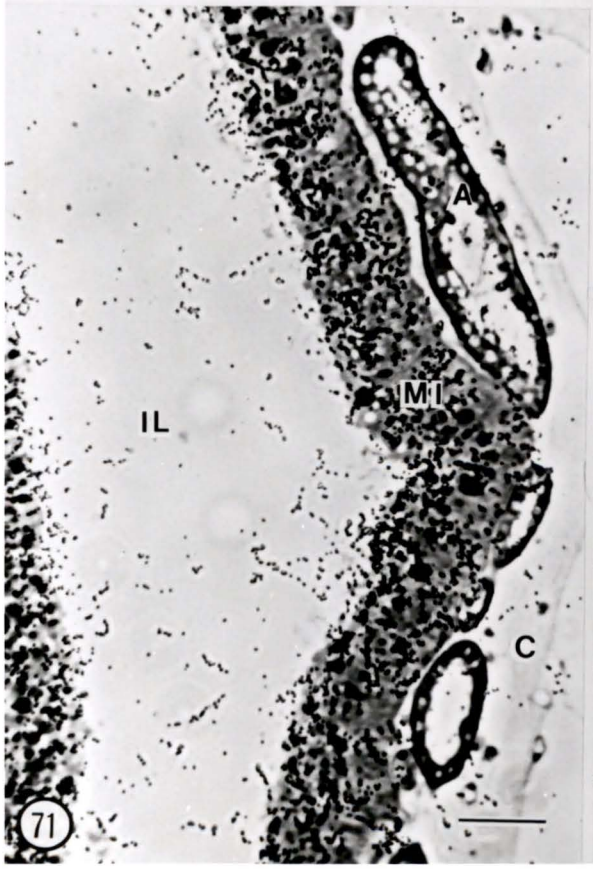
A
MI
IL
C
71

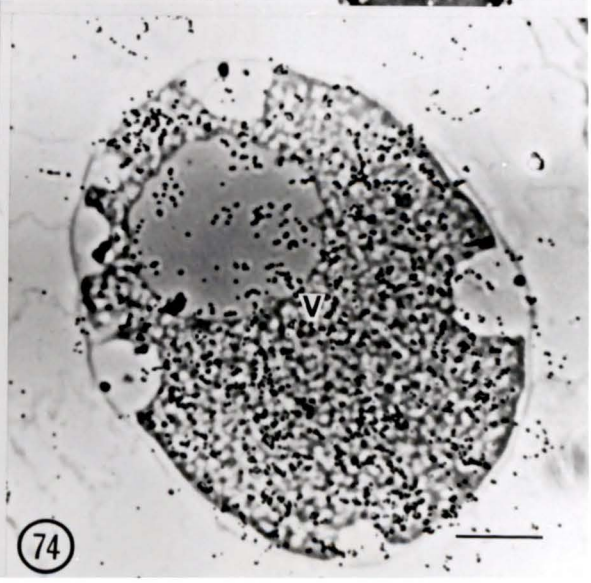
V
74

4. 3 Days

After 3 days of incubation the post-intestinal epithelium (2.25 ± .42), mid-intestinal pyloric gland ampullae (1.95 ± .46) and post-intestinal pyloric gland tubules (.80 ± .29) all have mean grain densities which are not significantly different from one another (figs. 76,77). The level in these tissues differs significantly from the next highest density level which was recorded for the stomach (6.0 ± .60) and the esophagus (4.65 ± .73; fig. 75). The mean grain densities recorded for the stomach and esophagus do not differ significantly from one another. The grain densities for these two tissues are significantly less than the grain densities for the vitellogenic oocytes (11.0 ± 1.2) and the mid-intestinal epithelium (10.40 ± .88; figs. 76,78). The vitellogenic oocytes and the mid-intestinal epithelium maintain the highest rate of grain labelling and do not differ significantly from each other.

5. 5 Days

After 5 days of incubation the stomach maintains the highest grain density (14.55 ± 1.0; fig. 80). The counts in the mid-intestinal epithelium (11.85 ± 1.1; figs. 81,82) and the vitellogenic oocytes (10.8 ± 1.5; figs. 85,86) are both significantly lower than the stomach counts but do not differ significantly from each other. The grain density

Figures 75–78. Autoradiographs of tissue sections of *C. inflata* 3 days after a 90 min exposure to a ^{14}C-l-glucose pulse (5.0 μCi/ml)(toluidine blue staining; phase contrast light photomicrographs; scale = 20 μm).

Figure 75. Mean grain densities recorded for the esophagus (4.65 ± .73) and the stomach (6.0 ± .60) do not differ significantly from each other but are both significantly less than grain counts recorded for the vitellogenic oocytes (11.0 ± 1.2) and the mid-intestinal epithelium (10.4 ± .88).

Figure 76. The mean grain count recorded for the mid-intestinal pyloric gland ampullae (1.95 ± .46) differs significantly from the mean grain density recorded for the mid-intestinal epithelium. Mean grain density recorded for the mid-intestinal epithelium (10.40 ± .88) is the highest grain count recorded for any of the tissues at 3 days other than the vitellogenic oocytes (11.0 ± 1.2) from which it does not differ significantly.

Figure 77. The post-intestinal epithelium (2.25 ± .42) and the post-intestinal pyloric tubules (.80 ± .29) have mean grain densities which are not significantly different from each other.

Figure 78. Mean grain density for the vitellogenic oocytes (11.0 ± 1.2) is the highest recorded for any tissue from 3

day post-pulse C. inflata. Note the absence of silver grains over the pre-vitellogenic oocytes.

A: pyloric ampulla
C: connective tissue
E: esophagus
IL: intestinal lumen
MI: mid-intestinal epithelium
PI: post-intestinal epithelium
PO: pre-vitellogenic oocyte
PT: pyloric tubule
ST: stomach epithelium
V: vitellogenic oocyte


ST
C
E
75

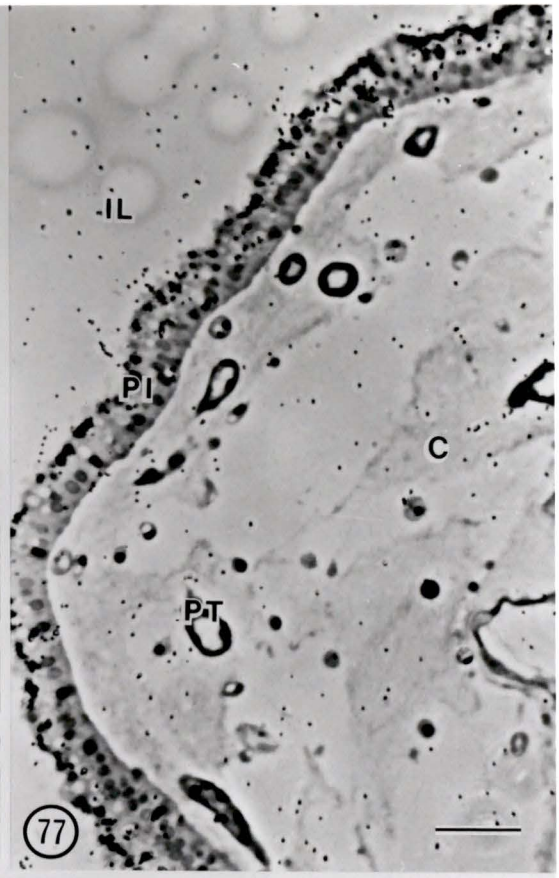
İL
PI
C
PT
77

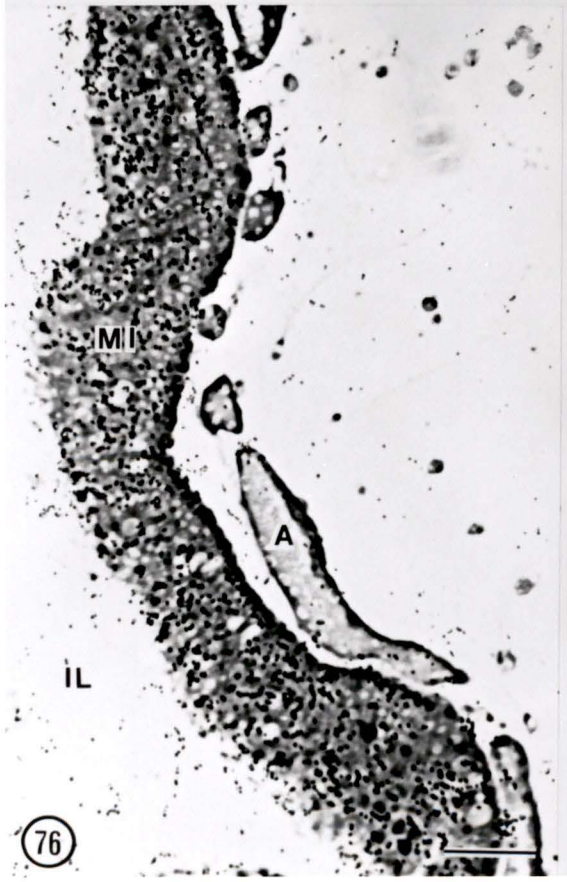
MI
A
İL
76


V
PO
78

Figures 79-86. Autoradiographs of tissue sections of *C. inflata* 5 days after exposure to a 90 min ^{14}C-1-glucose pulse (5.0 μCi.ml)(toluidine blue staining; phase contrast light photomicrographs; scale = 20 μm).

Figure 79. The mean grain density recorded for the esophagus is 3.2 ± .57.

Figure 80. The stomach has the highest mean grain density (14.55 ± 1.0) relative to all other tissue from *C. inflata* at 5 days post-pulse.

Figure 81. The grain density recorded for the mid-intestinal pyloric gland ampullae (5.70 ± .59) is significantly lower than the grain count recorded for the mid-intestinal epithelium.

Figure 82. The concentrations of grains which are seen in the mid-intestinal pyloric ampullae in fig. 81 are not evident within the contiguous pyloric gland ampullae even though both pyloric structures underlie a heavily labelled mid-intestinal epithelium.

Figure 83. The mean grain densities recorded for both the post-intestinal epithelium (2.05 ± .42) and the post-intestinal pyloric tubules (1.60 ± .21) do not differ significantly from each other.

Figure 84. Note the absence of silver grains in both the post-intestinal epithelium and the post-intestinal pyloric gland tubules.

Figure 85. The mean grain count recorded for the vitellogenic oocytes (10.8 $\pm$ 1.5) is significantly lower than the count determined for the stomach epithelium but does not deviate significantly from the mid-intestinal epithelium count.

Figure 86. Note the absence of silver grains over the pre-vitellogenic oocytes.

A: pyloric ampulla
C: connective tissue
CPA: contiguous pyloric ampulla
E: esophagus
IL: intestinal lumen
MI: mid-intestinal epithelium
PI: post-intestinal epithelium
PT: pyloric tubule
PO: pre-vitellogenic oocyte
ST: stomach epithelium
V: vitellogenic oocyte

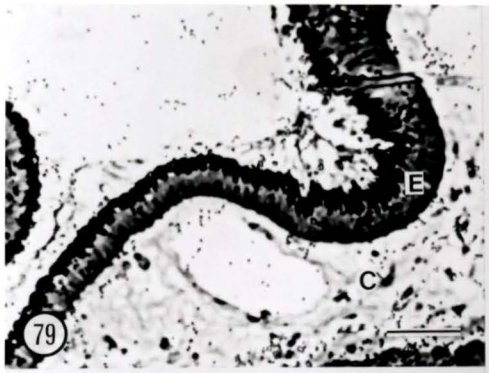
E
C
79

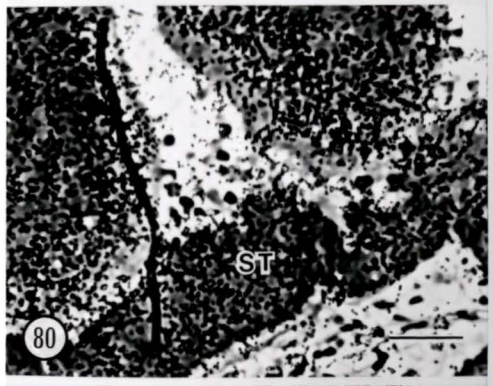
ST
80

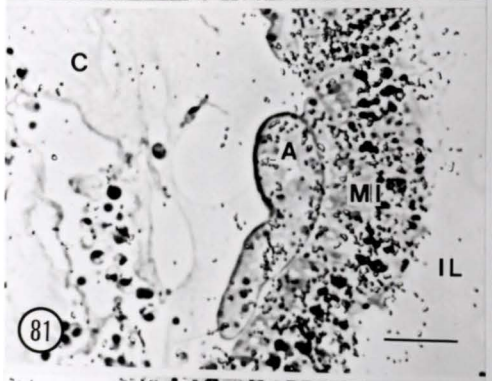
C
A
MI
IL
81

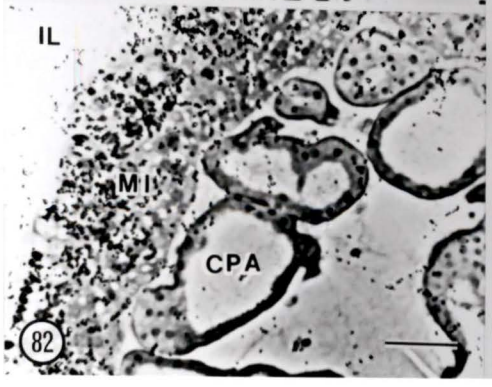
IL
MI
CPA
82


IL
PI
PT
83

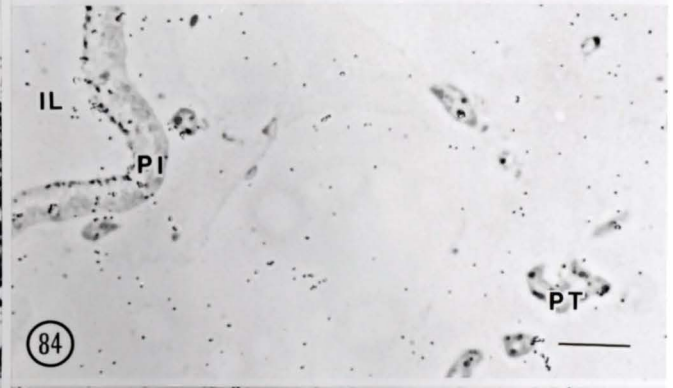
IL
PI
PT
84

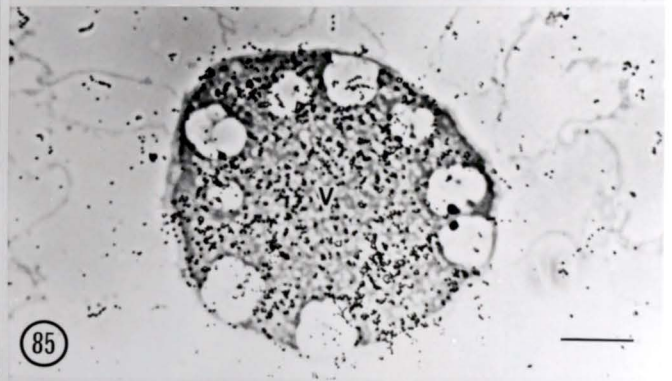
V
85

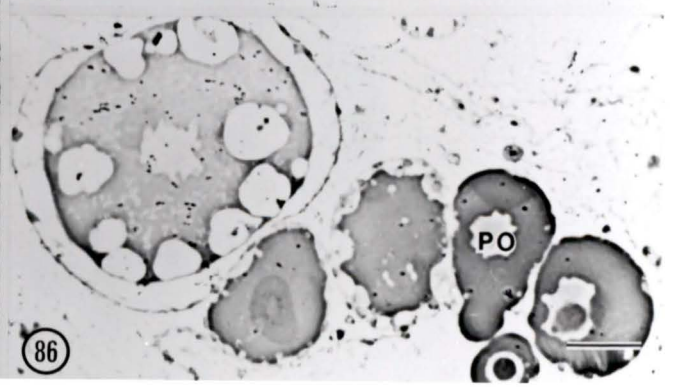
PO
86

recorded for the mid-intestinal pyloric ampullae (5.70 ± .59; fig. 81) is significantly lower than the counts for the stomach, mid-intestinal epithelium and vitellogenic oocytes. However the grain density for the mid-intestinal pyloric ampullae is significantly higher than the remaining tissues which do not deviate significantly from one other (esophagus = 3.2 ± .57; post-intestinal epithelium = 2.05 ± .42; post-intestinal pyloric tubules = 1.60 ± .21)(figs. 79,83,84).

A summary of the movement of a ^{14}C-labelled glucose pulse with time within the various tissues of C. inflata (fig. 87) reflects the affinities of each of the tissues for absorbing and storing glucose.

Chapter 11. Ultrastructure of the Pyloric Gland

A. PA-TSC-SP Staining of Glycogen

A Periodic Acid-Thiosemicarbazide-Silver Proteinate staining reaction (PA-TSC-SP) was used to stain glycogen in thin tissue sections.

Like the PAS staining reaction, if a non-specific oxidant (1% hydrogen peroxide) is used instead of the periodic acid, the glycogen is not stained (fig. 88).

Dimedone blocking was also used in this staining reaction, as it was in the PAS reaction, in order to ensure

Figure 87. The location of ^{14}C-labelled glucose in tissues of *C. inflata* over 5 different incubation periods. The grain density refers to the mean number of silver grains in a 25 μm^2 square (n = 20) for each tissue type at a given incubation time. ▲ = 2 hour; ○ = 12 hour; □ = 36 hour; ■ = 3 days; ◆ = 5 days

E: esophagus
MI: mid-intestinal epithelium
A: mid-intestinal pyloric ampullae
PI: post-intestinal epithelium
PT: post-intestinal pyloric tubules
S: stomach
VO: vitellogenic oocytes

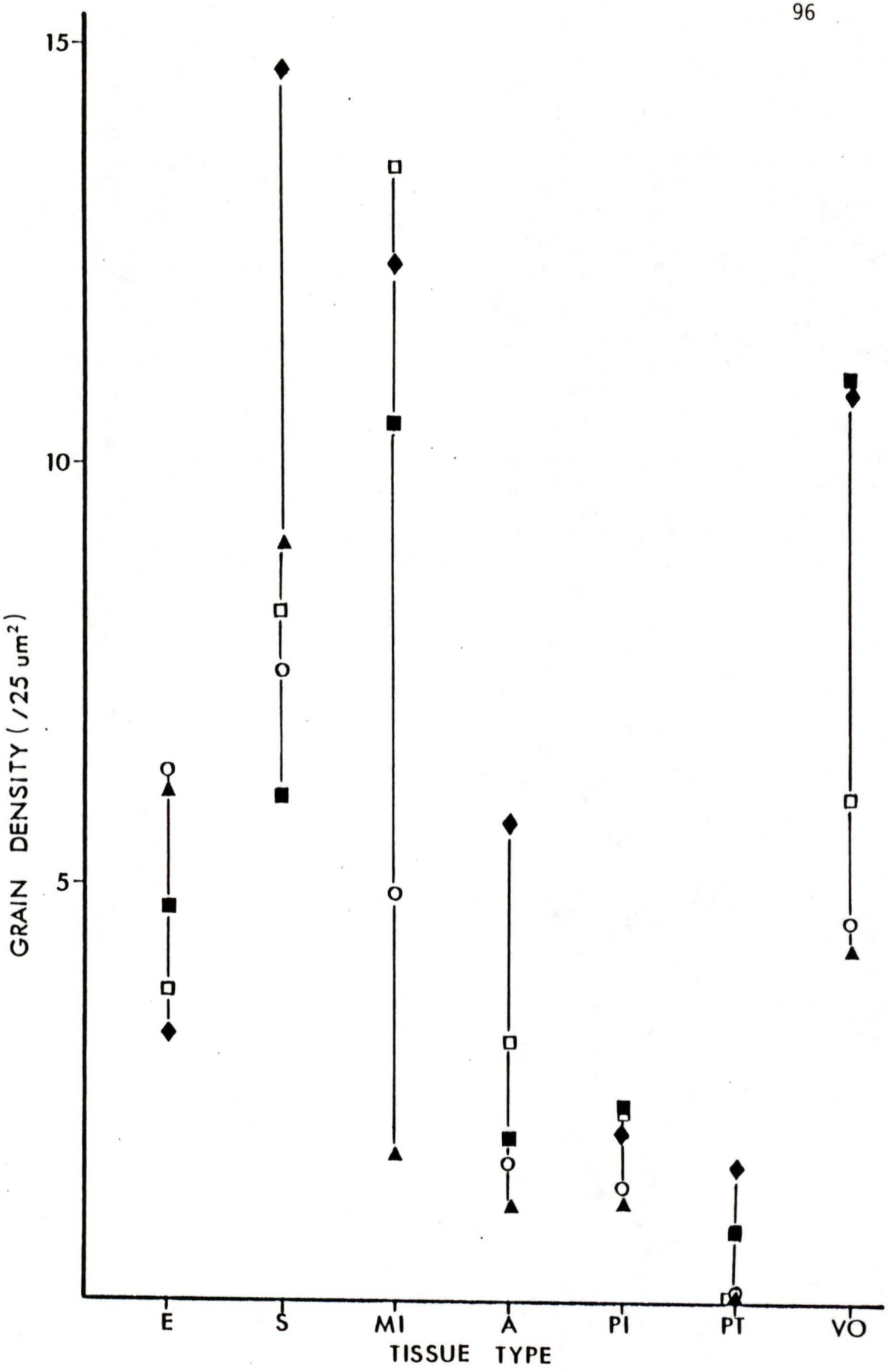
15
10
5
GRAIN DENSITY (/25 um²)
E
S
MI
A
PI
PT
VO
TISSUE TYPE

Figures 88-94. Thin sections of C. inflata (PA-TSC-SP staining; transmission electron photomicrographs (TEM's)).

Figure 88. In this section a non-specific oxidant (1% hydrogen peroxide) was used in the PA-TSC-SP staining procedure in lieu of periodic acid in order to control for the specific oxidation of glycogen by the periodic acid. The glycogen within the pyloric cells and the lumen of the pyloric ampulla is not stained (scale = 2 μm).

Figure 89. This section was placed in a saturated solution of Dimedone in 5% aqeous acetic acid for 3 hours at 60 °C prior to periodic acid oxidation in order to mask aldehyde groups. Note the PA-TSC-SP positive staining of glycogen particles (scale = 1 μm).

Figure 90. This section was masked with Dimedone after the periodic acid treatment and prior to the addition of the thiosemicarbazide and silver proteinate in order to ensure that the aldehyde detecting reagents are staining aldehyde groups introduced by the periodic acid oxidation (scale = 1 μm).

Figure 91. Note the staining of the glycogen within the cells of the pyloric ampulla following the PA-TSC-SP staining procedure (scale = 1.5 μm).

Figure 92. This thin section is the same as that shown in the previous figure except the section was treated with 10%

aqueous sodium thiosulphate following PA-TSC-SP staining. This was necessary in order to remove silver ions which are electron opaque and as such are indistinguishable from metallic silver. Note the staining of glycogen particles which is essentially the same as that shown in the previous figure (scale = 1 μm).

Figure 93. This section was reduced with benzyl mercaptan and alkylated with iodoacetate, following treatment with periodic acid, in order to mask catecholamines, free sulfhydryl groups and disulphide linkages. This step was necessary since these reducing groups are capable of reducing silver ions to metallic silver. Note the staining of the glycogen particles within the pyloric cells (scale = 1 μm).

Figure 94. The periodic acid step was omitted from the staining protocol used for this section. This was necessary in order to control for reducing groups existing in the tissue prior to periodic acid oxidation. Note that glycogen within the pyloric cell is not stained (scale = 0.5 μm).

Figure 95. Thin section (formvar coated) through a pyloric ampulla in S. gibbssi following PA-TSC-SP staining and treatment with alpha amylase. To ensure that PA-TSC-SP positivity was due to glycogen, alpha amylase was used to extract the PA-TSC-SP positive material from the section.

Note the holes in the tissue following the extraction of glycogen (arrow)(scale = 2 μm).

BL: basal lamina
CI: cilium
G: glycogen
LU: lumen of pyloric ampulla
M: microvilli
N: nucleus

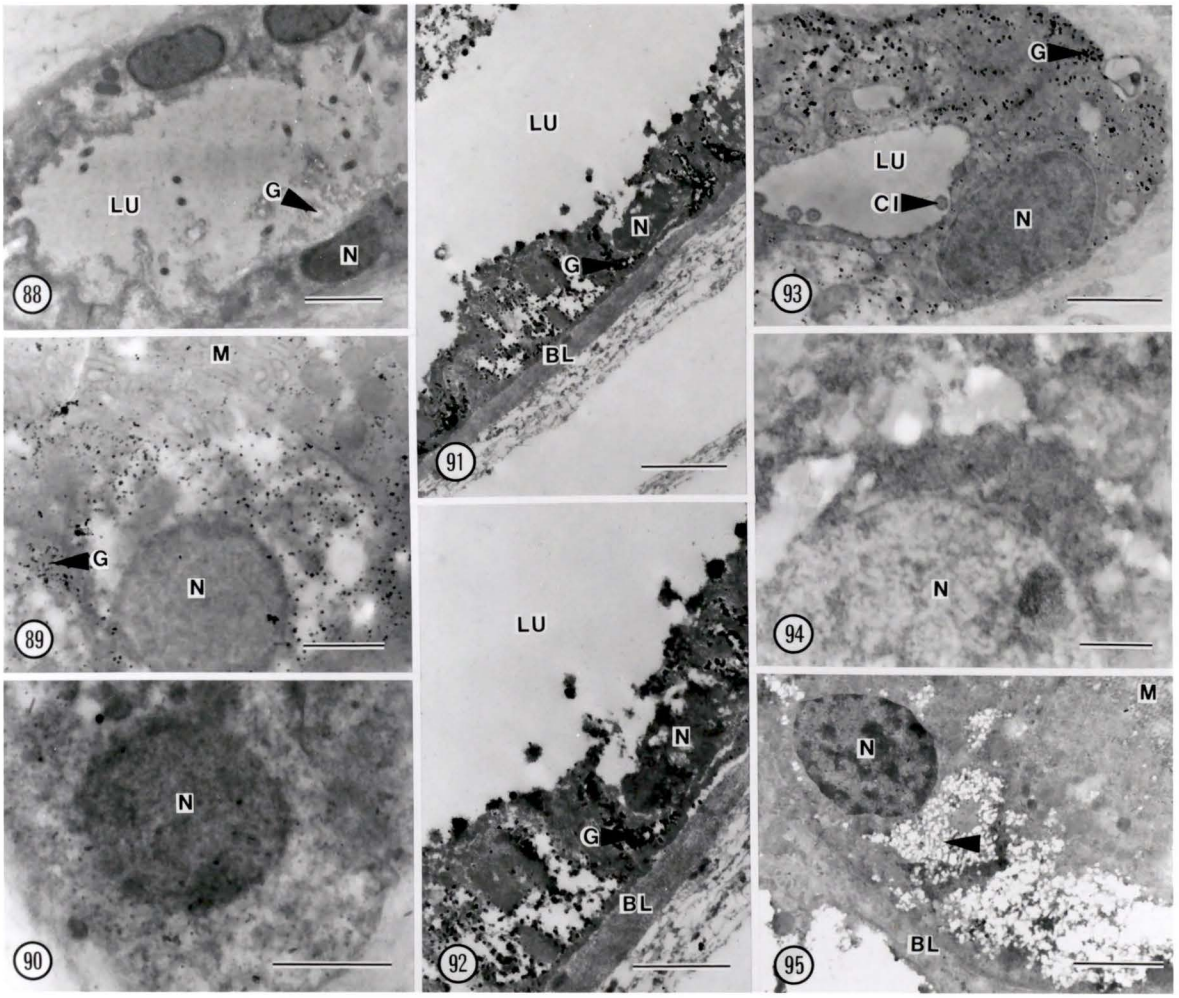
LU
G
N
88
M
G
N
89
N
90
LU
N
G
BL
91
LU
N
G
BL
92
G
LU
CI
N
93
N
94
M
N
BL
95

that PA-TSC-SP positivity is due to the specific action of periodic acid on the glycogen molecule (figs. 89,90).

The PA-TSC-SP positive staining reaction is seen as electron-opaque areas in discrete clumps within the tissue (fig. 91). The tissue section in fig. 92 was soaked for 18 hours in 10 % aqeous sodium thiosulphate, following PA-TSC-SP staining, in order to remove silver ions which are electron opaque and as such are indistinguishable from metallic silver.

Since reducing agents including catecholamines, free sulfhydryl groups and disulphide linkages may reduce silver ions to metallic silver, sections were reduced and alkylated with benzyl mercaptan and iodoacetate respectively, after periodic acid oxidation, in order to mask these groups (fig. 93).

Staining the tissue with the TSC-SP aldehyde detecting reagents, without periodic acid oxidation, was used as a control for pre-existing reducing groups (fig. 94). To ensure that the PA-TSC-SP positivity was due to the presence of glycogen, alpha amylase was used to extract the PA-TSC-SP positive material from the tissue section (fig. 95).

B. General Pyloric Cell Ultrastructure

All areas of the pyloric gland, within all three species studied, are lined by a single-layered epithelium. The base of each cell, and hence the entire gland, is bordered by a thick basal lamina of connective tissue (fig. 96).

The apical portion of each pyloric cell is lined with numerous microvilli and at least one cilium. Often there is more than one cilium per cell but they are always less numerous then the microvilli (fig. 96).

A tight junction (Mackie, et al., 1974) occurs at the apical cell borders between pyloric gland cells in each of the three species studied (fig. 96). Infoldings of the lateral plasma membranes are frequently observed (fig. 97) and infoldings of the basal membrane within pyloric cells of S. gibbsii are noted following starvation.

The nucleus within each cell contains dark chromatin masses within a lighter granular matrix (fig. 96). Each cell contains a number of mitochondria as well as masses of glycogen (figs. 91,95). The number of mitochondria within the cells of the mid-intestinal pyloric ampullae is greater than the number of mitochondria found within the post-intestinal pyloric tubules and ampullae (figs. 98,99).

Figure 96. Thin section of a stage I pyloric cell in S. gibbsii (TEM). The apex of the cell is bordered by numerous microvilli and the bottom of the cell is lined by a basal lamina of connective tissue. A tight junction separates the pyloric cell from an adjacent pyloric cell. Note the lysosome and numerous mitochondria within the cellular cytoplasm (scale = 1 μm).

Figure 97. Thin section of a pyloric cell in C. huntsmani (TEM). Note the interdigitations of the lateral cell membrane (scale = 1 μm).

Figure 98. Thin section of a pyloric ampulla in C. inflata (TEM). Numerous mitochondria can be seen as well as microvilli which fill the lumen of the ampulla (scale = 2 μm).

Figure 99. Thin section of a pyloric tubule in C. inflata (TEM). A large lysosome is located within one of the pyloric cells and cilia can be seen within the lumen of the tubule (scale = 1 μm).

BL: basal lamina
CI: cilium
G: glycogen
I: intestine
LI: lateral membrane infolding
LU: pyloric gland lumen
LY: lysosome
M: microvilli
MT: mitochondrion
N: nucleus
TJ: tight junction

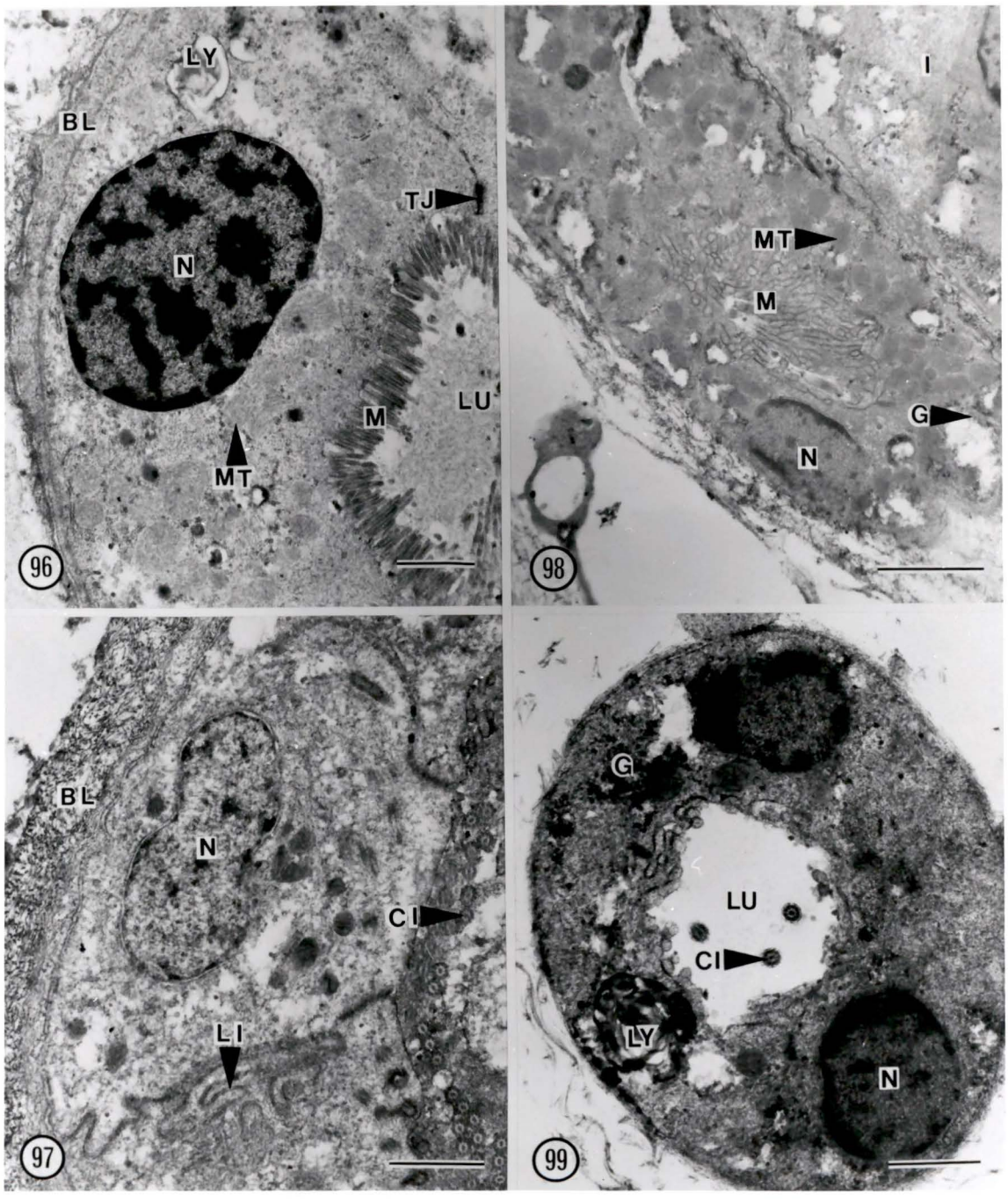
LY
BL
TJ
N
M
LU
MT
96
I
MT
M
G
N
98
BL
N
CI
LI
97
G
LU
CI
LY
N
99

Also, the cells of the pyloric ampullae generally contain greater amounts of glycogen than do cells within the more distal areas of the gland within the same animal. The glycogen is arranged in clumps, not in the typical beta or alpha subunit arrangement (figs. 91,92). The glycogen is found throughout the cell but the greatest concentration is usually found beneath or lateral to the nucleus sometimes bordering directly on the basal lamina. Treatment of the sections with alpha amylase eliminates the PA-TSC-SP reactive material leaving large unstained holes in the pyloric cells (fig. 95). Lysosomes, containing heterogenous inclusions, are also frequently found within pyloric cells (figs. 96,99).

C. Starvation Effects

With increasing starvation time, the basal lamina of connective tissue underlying the pyloric cells in S. gibbsii deteriorates and the base of the cell begins to interdigitate (fig. 100). Following 18-27 days of starvation in S. gibbsii the interdigitations pinch off as the cellular contents of the pyloric cell are released into the mesenchymal space surrounding the pyloric gland (fig. 101). Numerous lysosomal bodies with heterogenous inclusions are seen throughout the cytoplasm of the pyloric cells within animals which have been starved (figs. 102,103).

Figures 100-103. Thin sections of pyloric cells in *S. gibbsii* (TEM's).

Figure 100. Interdigitations of the basal lining of the pyloric cell can be seen following 18 days of starvation (scale = 1 μm).

Figure 101. Release of cellular contents from the base of the pyloric cell, into the surrounding mesenchymal haemocoel, is seen following 27 days of starvation (scale = 1.5 μm).

Figure 102. Extensive breakdown is evident in a pyloric cell which is adjacent to two intact pyloric cells. Note the lysosomes (arrow) within the pyloric cells (scale = 2 μm).

Figure 103. In this stage II pyloric cell (starved 27 days) microvilli have begun to break down and lysosomes are visible. Note the tight junction (arrow) which separates adjacent pyloric cells (scale = 1 μm).

LU: pyloric gland lumen
LY: lysosome
M: microvilli
N: nucleus

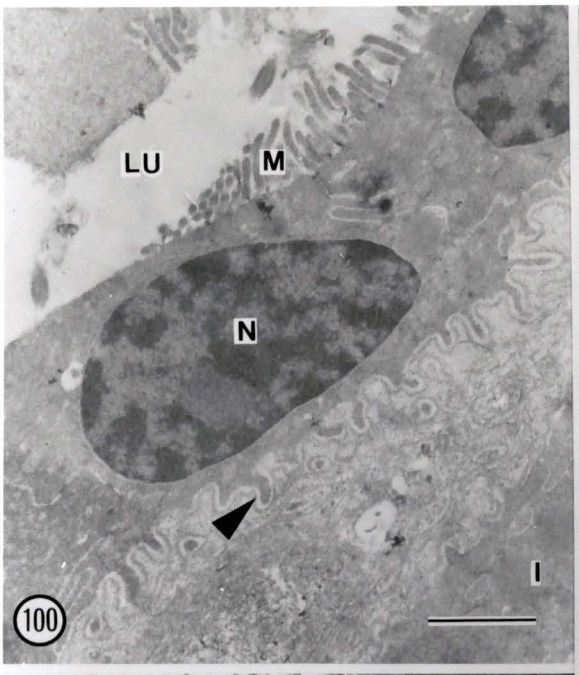
LU
M
N
I
100

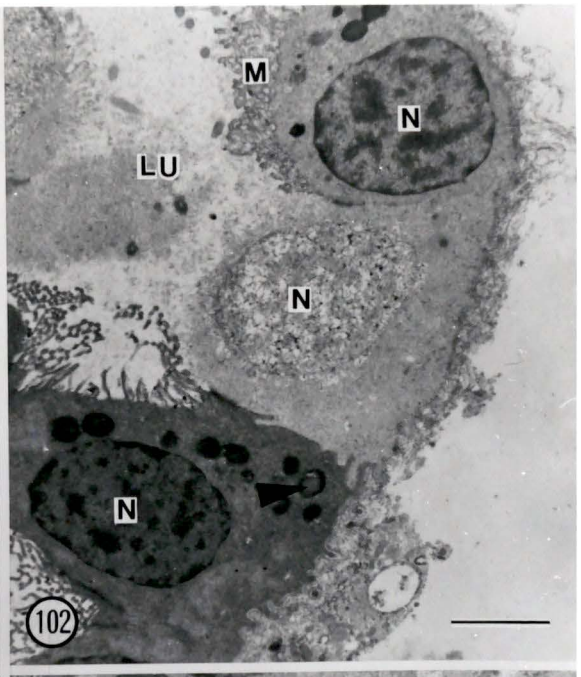
M
N
LU
N
N
102

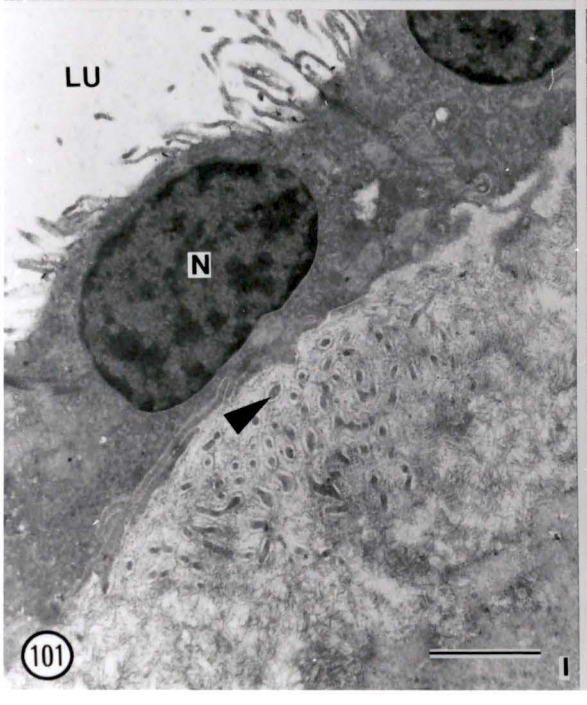
LU
N
I
101

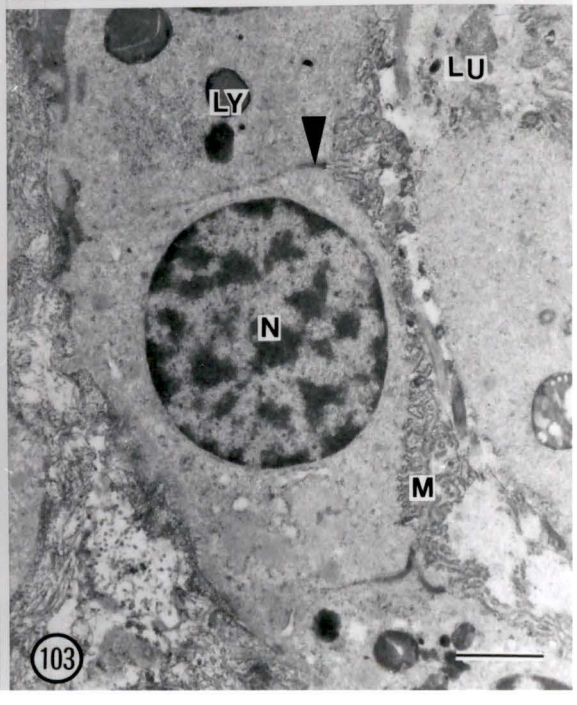
LU
LY
N
M
103

D. The Cytonuclear Cycle

Within the pyloric gland of all three species examined there is a cycle which results in the release of the cellular contents into the pyloric lumen. The advanced stages of the cytonuclear cycle are more evident in the area of the large dilated ampullae surrounding the mid-intestinal epithelium, relative to cells of the more distal pyloric tubules and ampullae where the initial stages of the cycle predominate. The advanced stages of the cycle are less evident within the pyloric ampullae around the stomach and mid-intestine of S. gibbsii which have been starved 18-27 days (figs. 47-51).

The first sign of the cycle is the modification of the apical microvilli of the pyloric cell. As the microvilli break down (figs. 102,103) the glycogen masses within the cytoplasm become vacuolated (figs. 98,104). As the cell continues to disintegrate, a reticulated structure becomes increasingly evident within the nucleus (fig. 105). Eventually all or most of the cellular contents are released into the lumen of the gland (figs. 105,106). In the final stage, all that remains of the cell is some amorphous cellular material clinging to the basal lamina (figs. 106,107).

Figure 104. Thin section of a stage II pyloric cell in S. gibbsii (TEM). Most of the glycogen is found at the base of the cell and lateral to the nucleus (scale = 2 μm).

Figure 105. Thin section of a stage III pyloric cell in C. inflata (TEM). A reticulated network can be seen within the nucleoplasm and extending away from the nucleus (scale = 2 μm).

Figure 106. Thin section of a stage IV pyloric cell in C. huntsmani (TEM). The contents of the cell, including the nucleus, are being voided into the pyloric lumen (scale = 2 μm).

Figure 107. Thin section of a late stage IV pyloric cell in C. inflata (TEM). Almost all of the contents of the pyloric cell have been released into the lumen of the gland. Some material remains attached to the basal lamina (scale = 1 μm).

BL: basal lamina
CI: cilium
G: glycogen
LU: pyloric gland lumen
N: nucleus

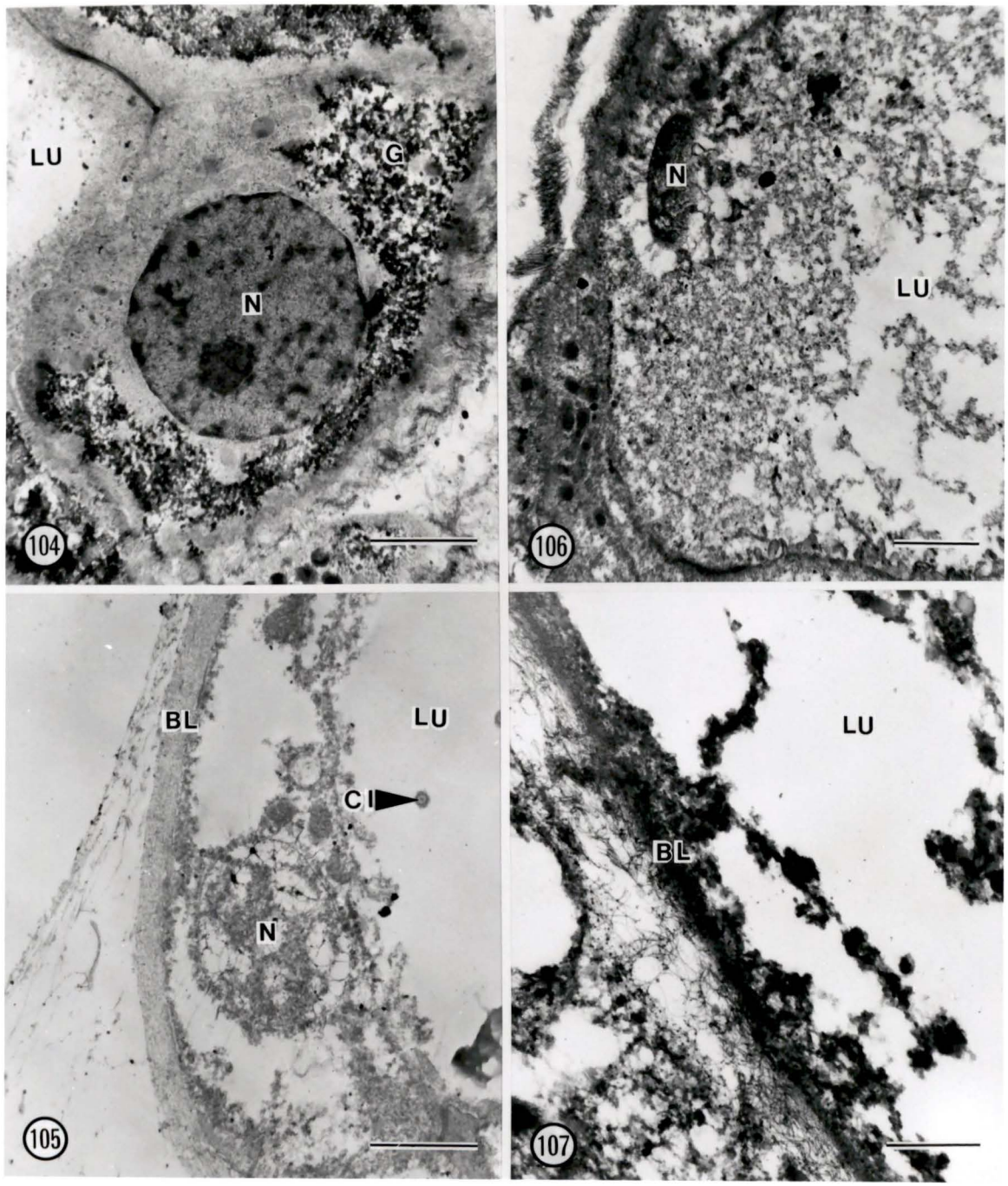
LU
G
N
104
N
LU
106
BL
LU
CI
N
105
LU
BL
107

The cytonuclear cycle does not occur in synchrony throughout any particular part of the pyloric gland. A particular cell may be in the last stages of destruction while the cell immediately adjacent to it shows no signs of breakdown (fig. 102).

E. Intestinal Epithelia and the Pyloric Gland

Mucus-secreting and vacuolated cells are found along the gastrointestinal tract of all three species studied. The esophagus contains ciliated mucus-secreting cells (fig. 108).

The intestine in all three species contains mucus-secreting and vacuolated cells (fig. 109). The vacuoles within the vacuolated cells are larger and more numerous in the post-intestinal area relative to the midgut. The vacuolated cells in the post-intestinal area often release all or most of their contents into the intestinal lumen (fig. 110). In the area of the mid-intestine, surrounded by large dilated pyloric ampullae, the intestinal cells are shorter and less vacuolated relative to other mid-intestinal cells not surrounded by large dilated pyloric ampullae (fig. 111).

Figure 108. Thin section of esophagus cells in C. inflata (TEM). Long cilia line the apex of each cell and numerous mucous granules can be seen within the apical cytoplasm (scale = 2 μm).

Figure 109. Thin section of intestinal cells in C. inflata (TEM). Vacuolated cells and ciliated mucous cells are evident as well as tight junctions (arrow) which separate adjacent intestinal cells (scale = 2 μm).

Figure 110. Thin section of the apex of post-intestinal cells in C. inflata (TEM). An intestinal cell can be seen releasing most or all of its contents into the intestinal lumen (scale = 1 μm).

Figure 111. Thin section of mid-intestinal cells of S. gibbsii in the area of large dilated pyloric ampullae (TEM). The height of each intestinal cell is approximately half the height of mid-intestinal cells which are not in the area of contiguous pyloric ampullae. Ciliary rootlets (arrow) are evident at the cell apex (scale = 2 μm).

BL: basal lamina
CI: cilium
CM: ciliated mucous cell
IL: intestinal lumen
MU: mucous granules
N: nucleus
V: vacuolated cell

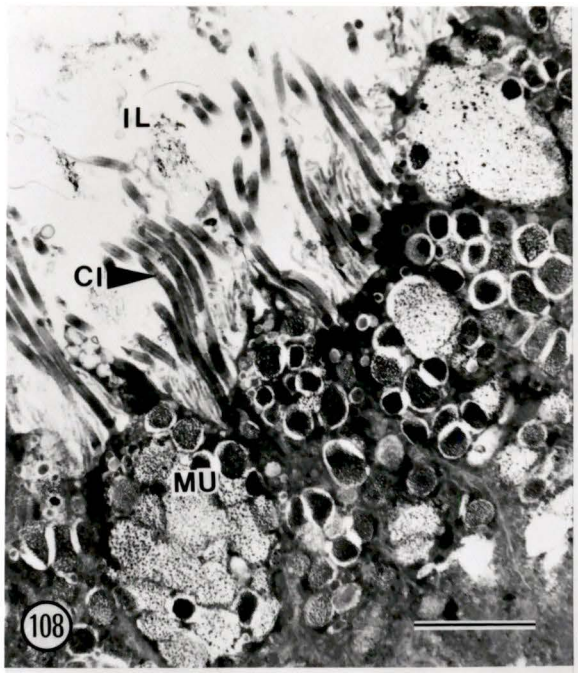
IL
CI
MU
108

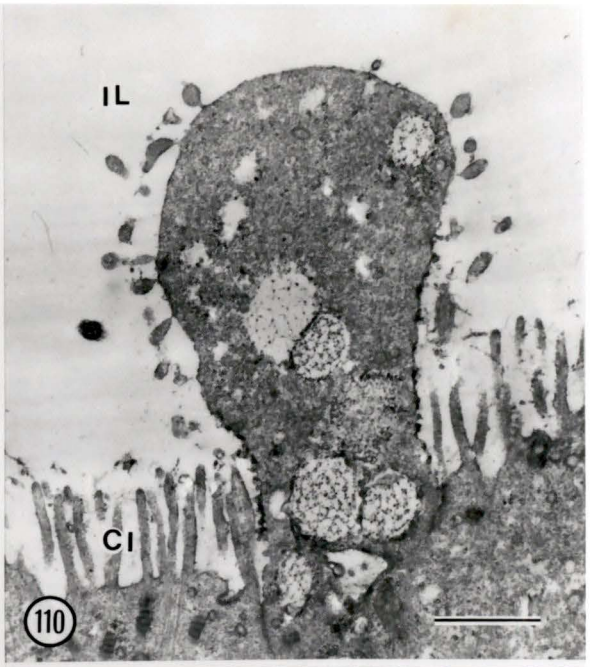
IL
CI
110

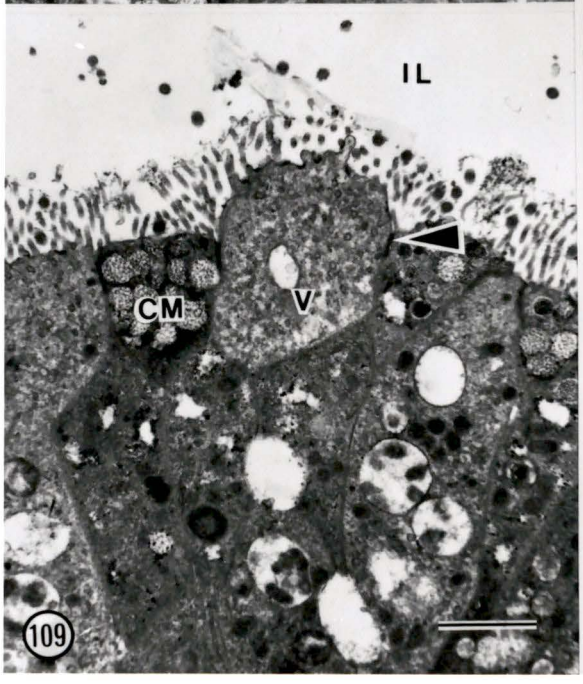
IL
CM
V
109

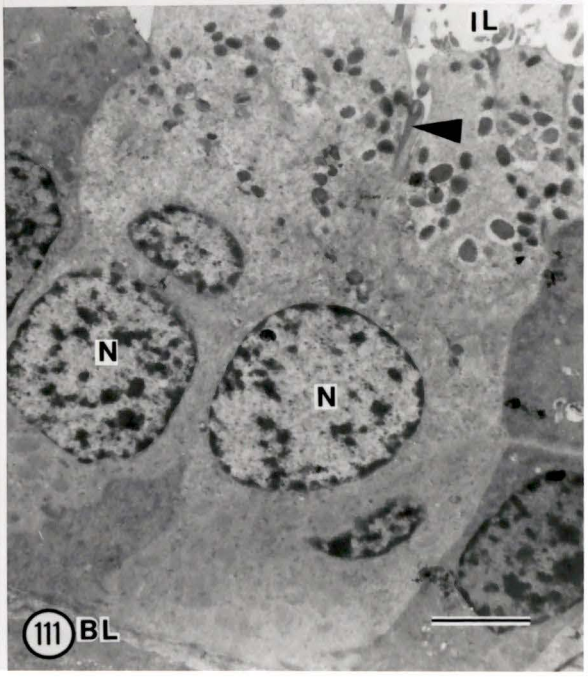
IL
N
N
111
BL

DISCUSSION

The results of this study suggest a number of possibilities concerning the role(s) of the ascidian pyloric gland. The fact that a substantial amount of PAS positive material, presumed to be glycogen, is found within the glands of all species examined, suggests a role common to all species involving this substance.

Chapter 12. Uptake of ^{14}C-l-glucose by C. inflata

The uptake of ^{14}C-l-glucose into the digestive tract and associated tissues of C. inflata is summarized in fig. 87. The results suggest an absorptive function for the stomach and intestine of C. inflata which demonstrate heavy glucose uptake from the ^{14}C-l-glucose-labelled mucous cord. Previous studies have also suggested an absorptive role for the ascidian stomach and intestine (Yonge, 1925; Van Weel, 1940; Burighel and Milanesi, 1977; Gaill, 1981).

The stomach of C. inflata demonstrates heavy uptake of labelled glucose at all post-incubation times examined (Table 3). This is in contrast to the observations noted for D. grossularia and S. argus in which labelling in the stomach and mid-intestine decreases after the portion of the mucous food cord containing labelled glucose passes the tissue (Gaill, 1981).

In C. inflata the labelled glucose has travelled the length of the gastrointestinal tract after 12 hours of post-incubation which is comparable to the time noted for the label to pass through the gastrointestinal tracts of D. grossularia and S. argus (Gaill, 1981).

In this study, appreciable amounts of labelled glucose are still present in the food cord of C. inflata when it reaches the post-intestine. As a result, substantial amounts of the labelled glucose are voided into the surrounding seawater with the feces. Since a self-contained tank of recirculating seawater was used for post-incubation in this study, it seems probable that the seawater became contaminated with labelled glucose contained within the feces. As a result, the animals fixed after 12 hours, which might be expected to show a decrease in labelled glucose within the food cord following the initial labelled glucose pulse, continued to filter labelled glucose from the seawater after the initial pulse. I feel that this is a more plausible explanation for the continued labelling of the stomach and mid-intestine after 36 hours, 3 and 5 days, rather than interpreting the results as suggesting that the stomach and mid-intestine are primary sites of glycogen storage.

The pattern of labelling within the esophagus also supports this conclusion. The degree of labelling in the

esophagus is maintained at a level only slightly less than that recorded with the passing of the labelled pulse. If C. inflata did not continue to ingest labelled glucose the counts in the esophagus would decrease to background levels with the passing of the initial labelled glucose pulse, since labelling in the ciliated mucous cells of the esophagus is due to diffusion (Gaill, 1981).

Since the D. grossularia and S. argus used by Gaill (1981) were placed in running seawater, any labelled glucose which may have passed through the gastrointestinal tract was not maintained within a recirculating seawater system. As a result, Gaill (1981) did not observe labelling in the mucous cord, and hence the stomach and mid-intestine, after 12 hours of post-incubation.

The labelling seen within the vitellogenic oocytes of C. inflata (figs. 63,69,74,78,85) could be from a number of sources. The labelled glucose within the oocytes, presumed to be glycogen accumulated during vitellogenesis (Karp and Berrill, 1981), could have diffused through the esophagus, or through the branchial basket, and into the haemocoel. The initial concentration of labelled glucose noted in the vitellogenic oocytes is comparable to that initially seen in the esophagus. Although the branchial basket itself did not accumulate labelled glucose in this study, glucose could have passed through the basket and into the haemocoel. The

branchial basket and esophagus may both be routes for initially providing glucose to vitellogenic oocytes.

Grain densities recorded for the post-intestinal epithelium are not markedly above background counts as is expected for a non-absorptive epithelium (Table 1). The pyloric tubules, which are found in the post-intestinal area, do not appear to accumulate label although they are exposed to the same concentrations of labelled glucose within the haemocoel as the vitellogenic oocytes.The pyloric gland ampullae, which surround the mid-intestine, accumulate labelled glucose after 5 days of post-incubation but the accumulation is noticeably less than that noted for D. grossularia (Gaill, 1981; 5.7/25 μm^2 vs. 21/25 μm^2).

As a result, it seems the ^{14}C-1-glucose uptake results suggest that the pyloric gland, particularly the ampullae, may be responsible for limited glycogen storage in C. inflata. If the pyloric ampullae do store glucose as glycogen, it is present in much lower concentrations than that observed in D. grossularia by Gaill (1981). The other possibility is that glucose accumulation within the pyloric gland of C. inflata may take longer than it does in D. grossularia.

If a glycogen storage hepatic role is being played by the pyloric gland of Phlebobranchs, in this case C. inflata,

it is a substantially reduced role relative to the hepatic role played by the pyloric ampullae in stolidobranchs (D. grossularia; Gaill, 1981). It seems that as one examines the pyloric gland in ascidians, an hepatic role is either non-existent (aplousobranchs; S. argus, Gaill, 1981), marginal (phlebobranchs; C. inflata, this study) or pronounced (stolidobranchs; D. grossularia, Gaill, 1981).

The homogeneous glucose labelling noted by Gaill (1981) within the ampullae of D. grossularia was not noted within the pyloric ampullae of C. inflata. I do not feel it is valid to compare silver grain densities within different regions of an ampulla because of limitations in the autoradiographical technique, particularly in the case of C. inflata where the ampullae are considerably smaller than those found in D. grossularia. To do so would necessitate the assumption that the source of an emitted beta particle is directly below the resulting silver grain which is not necessarily the case.

The beta particles are released from the labelled glucose in all directions and as such the radius of uncertainty surrounding the resultant silver grain restricts how precisely one can pinpoint the actual location of the ^{14}C source. Specifically, for a carbon-14 source surrounded by emulsion on all sides, 29 % of the individual silver grains produced by beta particles originating from the

carbon-14 will be within a radius of 5 μm, 50 % within 9 μm, 75 % within 17 μm and 90 % within 25 μm (Rogers, 1979).

As Gaill (1981) points out, using glucose labelled at the first carbon increases the possibility of obtaining glycogen as the final labelled product. The fact that the silver grains are accumulated within the pyloric gland ampullae, which contain high concentrations of PAS positive material presumed to be glycogen, indicates that the radioactive glucose is being stored within the ampullae as glycogen.

Chapter 13. Nutrient Depletion Experiments

The reaction of the pyloric gland to nutrient depletion suggests some interesting possibilities relating to the function of the organ.

In *C. inflata*, and to a lesser extent in *C. huntsmani*, glycogen staining is not apparent within the distal pyloric tubules around the post-intestine following 10 days of starvation (figs. 28,55). In *C. inflata*, glycogen is still evident within the mid-intestinal pyloric ampullae and main pyloric gland collecting ducts after 10 days of starvation (figs. 26,27,29). The same phenomenon is noted for *C. huntsmani* except the mid-intestinal epithelium still has glycogen deposits after 10 days of starvation unlike the mid-intestinal epithelium of *C. inflata* which is devoid of

glycogen following the same starvation period (figs. 27,29,56). All gastrointestinal and pyloric tissues in S. gibbsii, which were intensely PAS positive in freshly-collected animals, do not demonstrate PAS positivity following 18 days of starvation (figs. 45-48).

The zooids of C. huntsmani were unable to survive more than 10-14 days of starvation. Survival in C. inflata was variable after 27 days with some animals surviving up to 5 weeks. C. inflata also suffered due to infection from a parasitic flatworm, Euryleptra leoparda Freeman, which enters the animal via the branchial siphon and ingests the entire body contents leaving only the tunic (Lambert, 1968). S. gibbsii are very hardy and were seen to survive up to 7 weeks of nutrient deprivation.

However, with increasing starvation the basal lamina surrounding the pyloric gland in S. gibbsii breaks down and the contents of the pyloric cells are released into the surrounding haemocoel (figs. 100-103). The basal disintegration of the pyloric ampullae is never seen in fed animals but can be seen only after starvation and as such seems to be associated with nutrient deprivation. PAS positivity is never seen in any of the pyloric cells in which this process occurs.

I suggest that under starvation conditions, this basal disintegration is the mode of release of nutrients from the pyloric ampullae of S. gibbsii into the surrounding haemocoel. When one considers the extensive network of glycogen-rich pyloric ampullae found in S. gibbsii, it is not surprising that the animal can survive long periods of starvation. I have seen S. gibbsii live in a recirculating seawater system, under varying conditions of nutrient availability, for over 2 years. One individual of Styela montereyensis is reported still alive after 3 years (Morris et al, 1980).

The short lifespan of C. inflata and C. huntsmani is in marked contrast to the longevity of the Styelids. C. inflata lives 6-8 months (Lambert et al, 1981; Morris et al, 1980) and is noticeably less hardy in laboratory conditions than S. gibbsii. C. huntsmani must be collected from the sea along with the substrate to which the colony is attached if they are to survive even 10 days of starvation. Zooid regression in C. huntsmani is noticeable as early as 7 days into the nutrient depleted conditions. The basal removal of material from the pyloric ampullae of starved animals, as seen in S. gibbsii, is never noted in C. huntsmani or C. inflata under starvation conditions.

It seems that the long life span of the solitary S. gibbsii could be associated with the accumulation of

nutrients within the pyloric gland which are subsequently released by basal disintegration during starvation, not by the pyloric cytonuclear cycle which releases material into the lumen of the gland. This hypothesis is supported by the presence of increasing numbers of intact pyloric cells in the ampullae of S. gibbsii with increasing starvation. If the cytonuclear cycle, and subsequent release of PAS positive material into the pyloric gland lumen, is the means of nutrient release during starvation one would expect to find mass cellular release in the ampullae of starved animals.

I suggest that under starvation conditions the glycogen-rich cytonuclear cycle in the ampullae of S. gibbsii is observed to be much less prevalent due to the need for basal removal of pyloric cell nutrients to maintain the animal. It seems likely that the nutrient released may be glucose derived from the PAS positive glycogen product associated with the cytonuclear cycle.

Although the cycle is still evident to some degree in the pyloric ampullae of starved S. gibbsii, the large concentrations of PAS positive material found in fed animals are no longer present. If the basal removal of nutrients is the means of maintenance of the animal during starvation, this implies that the cytonuclear cycle and its associated PAS positive material serves some other role.

Indeed, the fact that PAS positive material is found in 10 day starved zooids of C. huntsmani supports this contention. If nutrient depletion is prolonged, the C. huntsmani zooid regresses and nutrients are stored in trophocytes within the stolonic system and are the eventual sites for budding of new zooids. Up to this point the individual zooid, under starvation conditions, still has PAS positive material within the pyloric ampullae and the underlying mid-intestinal epithelium. In C. huntsmani, the strategy is not to stop this glycogen-rich cycle in favour of releasing nutrients into the haemocoel via basal pyloric disintegration (as in S. gibbsii). If starvation is prolonged the entire zooid regresses. Up to this point the glycogen rich pyloric cell cycle is maintained. Although an individual zooid of C. huntsmani is short-lived (6 months), the entire collection of zooids, along with the stolonic system, provides a strategy for a lifespan of many years, as is the case for S. gibbsii.

C. inflata presents another situation. The individual animal lives about 6-8 months (Lambert et al, 1981; Morris et al, 1980) With starvation, the basal disintegration of the pyloric ampullae as noted in S. gibbsii, is not seen in C. inflata although the glycogen-rich cytonuclear cycle is less evident. The shut down of the cycle with starvation seems to be associated with the solitary life-style.

C. huntsmani can maintain the cytonuclear cycle within the pyloric gland up to the point of zooid regression because the whole animal includes the perennial stolonic system as well as the transient zooids.

A long-lived solitary ascidian must have a mechanism for maintaining the zooid during periods of minimal nutrient availability because a stolonic "over-wintering" option is not available. Basal disintegration of the pyloric ampullae is not apparent in the solitary C. inflata and I feel this is related to the short 6-8 month lifespan of the animal. S. gibbsii, a solitary perennial, has developed a means of releasing nutrients basally from the pyloric ampullae into the haemocoel and hence a means of surviving periods of low nutrient availability and starvation. C. inflata is a short-lived solitary species which does not have this ability. However, like S. gibbsii the pyloric cytonuclear cycle, which results in the release of large amounts of glycogen-rich material into the stomach lumen, is rare in starved C. inflata.

The questions remains, what is the role of the PAS positive material and the associated cytonuclear cycle found in ascidians? The most likely explanation is that the PAS positive material released from the pyloric cells, as the end result of cytonuclear disintegration, is released into

the stomach via the main pyloric gland collecting duct(s) and is involved with somehow altering the mucous cord.

Chapter 14. Cellular Ultrastructure and the Pyloric Cytonuclear Cycle

The ultrastructure of the pyloric cells in S. gibbsii, C. inflata and C. huntsmani share many similarities with the pyloric cells found in other species (Table 1).

The apical portion of each intact pyloric cell is lined with a prominent brush border and cilia. Although some studies suggest that the cilia beat toward the pyloric gland junction with the stomach, this is difficult to determine unless the cilia are observed in live animals.

Tight junctions at the apex of each cell separate adjacent pyloric cells. The infoldings of the lateral membranes are observed in cells of all species as was noted for S. clava by Ermak (1977). Interdigitations of the basal membrane, noted in S. argus by Gaill (1974), are only present within the pyloric cells of starved S. gibbsii. The differences in the basal membranes of pyloric cells of starved and fed S. gibbsii may explain the apparently conflicting observations of Gaill (1974) and Ermak (1977).

Mitochondria and PAS positive glycogen compounds seem to be more numerous within the pyloric ampullae than within

the pyloric tubules. The glycogen deposits are often vacuolated particularly as the cell begins to disintegrate. It is difficult to determine if this vacuolization is a fixation artefact. The vacuoles could be the result of extraction, by fixation, of the material which associates with the glycogen just prior to its release into the pyloric lumen via cell degeneration.

The secondary structure and possible binding of glycogen to proteins or other materials within living cells are speculative matters since all methods used in its isolation or visualization necessarily change its natural state (Stetten and Stetten, 1960). Like other organic metabolites, glycogen must form associations with enzymes catalyzing its various reactions. In addition, glycogen associates with a variety of enzymatically indifferent proteins (serum globulin, Mystkowski, 1937; concanavaline A, Cifonelli, 1956) and may associate with a host of other cellular constituents. When one adds to this the polydispersity of glycogen itself, as well as its heterogenous distribution within cells, it is clear that there may exist a host of different forms of glycogen, not merely the typical alpha and beta types (Stetten and Stetten, 1960).

As a result, it is entirely possible that the glycogen, which stains PAS positive, is a molecular complex which

contains glycogen. This complex, upon entering the stomach, may be responsible for lowering the viscosity of the mucous cord (Yonge, 1935; Morton, 1960; Goodbody, 1974) in order to permit mixing with digestive enzymes. Removal of the non-glycogen portion of this material may explain why the remaining glycogen is not arranged into alpha or beta subunits, but instead is formed into large clumps.

The fact that a cytonuclear cycle occurs in all species within which the pyloric gland has been examined suggests its importance in a function common to all ascidians, such as the modification of ingested nutrient-containing mucus in order to aid digestion. If the pyloric gland does serve a function that is universal in all ascidians this function may be the modification of the stomach contents with the PAS positive glycogen product of the pyloric cytonuclear cycle.

Within long-lived solitary ascidians, such as Styelids, the gland can function as a reserve organ during times of nutrient deprivation. This is accomplished by conversion of the glycogen to glucose, breakdown of the pyloric basal lamina, and release of the glucose from the base of the pyloric cell directly into the surrounding haemocoel. Since the animal is necessarily not ingesting nutrients during starvation, this glucose release is of no consequence to the other function of the organ. That is, the PAS positive glycogen-rich material is not required for conditioning

stomach contents since during starvation the ingested material would be minimal.

LITERATURE CITED

Azéma, M. 1937. Rechèrches sur le sang et l'excretion chez les Ascidies. Annls. Inst. Oceanogr. Paris 17: 1-150

Berrill, N.J. 1929. Digestion in ascidians and the influence of temperature. J. Exp. Biol. 6: 275-291

Biava, C. 1963. The identification and structural forms of human particulate glycogen. Lab. Invest. 12: 1179-1197

Brevis, P.J.R. and M.C. Thorndyke. 1978. Endocrine cells in the esophagus of the ascidian Styela clava. A cytochemical and immunoflorescence study. Cell Tiss. Res. 187: 153-158

Brown, A.C. and A. B. Davies. 1971. The fate of thorium dioxide introduced into the body cavity of Ciona intestinalis. J. Invert. Path. 18: 276-279

Bulmer, D. 1959. Dimedone as an aldehyde blocking reagent to facilitate the histochemical demonstration of glycogen. Stain Technol. 34: 95-98

Burighel, P. 1973. Osservazioni morfologiche ed istochimiche sull'apparato digerente dell'ascidia coloniale Botrylloides leachii(Savigny). Acc. Pat. SC.LL.AA. 85: 117-132

Burighel, P. and C. Milanesi. 1973. Fine structure of the gastric epithelium of the ascidian Botryllus schlosseri. Vacuolated and zymogenic cells. Z. Zellforsch 145: 541-555

----- 1975a. Fine structure of the gastric epithelium of the ascidian Botryllus schlosseri. Mucous, endocrine and plicated cells. Cell Tiss. Res. 158: 481-496

----- 1975b. The cytology of the gut epithelium in the colonial ascidian Botryllus schlosseri. Bull. Zool. 42: 439

----- 1977. Fine structure of the intestinal epithelium of the colonial ascidian Botryllus schlosseri. Cell Tiss. Res. 182: 357-369

Chambost, M. D. and C. Thomassin-Steck. 1972. Histochemie et ultrastructure du tube digestif de Ciona intestinalis. L. Tethys. 4: 493-504

Chandelon, T. 1875. Rechèrche sur une annexe du tube digestif des Tuniciers. Bulletin de l'Academie royale de Belgique, Classe des Sciences, 39: 911-949

Chatterjee, B. and K.C. Ghose. 1974. Seasonal variation in stored glycogen and lipid in the digestive gland and genital organs of two freshwater prosobranchs. Proc. Mal. Soc. Lond. 400: 407-412

Chayen, J., Bitensky, L. and R. Butcher. 1973. Practical Histochemistry. John Wiley and Sons, Toronto

Cifonelli, J.A., Montgomery, R. and F. Smith. 1956. The reaction between Concanavalin-A and glycogen. J. Am. Chem. Soc. 78: 2485-2488

Coimbra, A. 1967. Evaluation of the glycogenolytic effect of alpha amylase using radioautography and electron microscopy. J. Histochem. Cytochem. 14: 898-905

Colton, H. S. 1910. The "Pyloric Gland" of the ascidian Botryllus-an organ of excretion? Biol. Bull. Mar. Biol. Lab Woods Hole 19: 35-51

Croxall, J.P. 1971. "The Digestive System, Feeding and Ecology of some New Zealand Ascidians". Ph.D. Thesis, Auckland

Das, S.M. 1944. On the alimentary canal and gonads in Microcosmus mangarensis, a monascidian of Madras. Proc. Indian Sci. Congr. 3: 31-92

Degail, L. and C. Levi. 1964. Etude au microscope electronique de la glande digestive des Pyuridae (Ascidies). Cah. Biol. Mar. 5: 411-422

Doezema, P. and J.H. Philips Jr. 1970. Glycogen storage and synthesis in the gut of the purple sea urchin, Strongylocentrotus purpuratus. Comp. Biochem. Phys. 34: 691-697

Eakin, R.M. and A. Kuda. 1972. Glycogen in lens of tunicate tadpole (Chordata: Ascidiacea). J. Exp. Zool. 180: 267-270

Ermak, T.H. 1975. Cell proliferation in the digestive tract of Styela clava(Urochordata: Ascidiacea) as revealed by autoradiography with triated thymidine. J. Exp. Zool. 194: 449-466

----- 1977. Glycogen deposits in the pyloric gland of the Ascidian Styela clava (Urochordata). Cell Tissue Res. 176: 47-55

----- 1981. A comparison of cell proliferation patterns in the digestive tract of ascidians. J. Exp. Zool. 217: 325-339

Fiala-Medioni, A. and E. Pequignat. 1980. Direct absorption of amino acids and glucose by the branchial sac and the digestive tract of benthic filter-feeders (Ascidians). J. Zool. Lond. 192: 403-419

Fouque, G. 1949. Relations entre la structure de l'intestin et la structure de la glande pylorique chez Botryllus schlosseri(Pallas). Bull. Inst. Ocean. Monaco 959: 1-9

----- 1954. Contribution à l'étude de la glande pylorique des ascidiaces. Ann. Inst. Océanogr. Paris 28: 189-317

----- 1959. Observations sur le "foie" de quelques des Ascidiaces. Rec. Trav. Stat. Mar. d'Endoume. 29: 181-191

Fritsch, H.A.R. 1976. The occurrence of argyrophilic and argentaffin cells in the gut of Ciona intestinalis L. Cell Tiss. Res. 175: 131-135

Fritsch, H.A.R. and R. Sprang. 1977. On the ultrastructure of polypeptide hormone-producing cells in the gut of the ascidian Ciona intestinalis L. and the bivalve, Mytilus edulis L. Cell Tiss. Res. 177: 407-413

Gaill, F. 1973. Etude histologique de la glande pylorique de Synocium argus (Polyclinidae.Tuniciers). Arch. Zool. Exp. Gen. 114: 97-110

----- 1974. Aspect ultrastructual de la glande pylorique et de l'intestine postérieur de Sydnyum argus (Polyclinidae.Tuniciers). Cah. Biol. Mar. 15: 337-341

----- 1976. La glande pylorique de Boltenia hirta (Pyuridae, Ascidiacea), ses relations avec le manteau. C. R. Acad. Sci., Paris, sér.D, 282: 817-820

----- 1977. Morphologie et histologie de la glande pylorique des Styelidae (Ascidies). Bull. Mus. Natn. Hist. Nat. Paris. 491: 1041-1055

----- 1980. Glycogen and degeneration in the pyloric gland of Dendrodoa grossularia (Ascidiacea. Tunicata). Cell Tiss. Res. 208: 197-206

----- 1981. Functions of digestive diverticula in marine invertebrates I. Ascidians fed with labelled glucose; its absorption and storage in the pyloric gland. Cell Tissue Res. 219: 185-195

Goodbody, I. 1974. The physiology of ascidians. Adv. Mar. Biol. 12: 1-150

Godeaux, J. 1954. Observations sur la glande pylorique des Thaliacés. Annales de la Societé royale zoologique de Belgique. 85: 103-118

Hanker, J.S., Seaman, A.R., Weiss, L.P., Ven, O.H., Bergman, R.A. and A.M. Seligman. 1964. Osmiophilic reagents. A new cytchemical aprinciple for light and electron microscopy. Science,N.Y. 146: 1039-1043

Humason, G.L. Animal Tissue Techniques. 569 pp. 2ed. San Francisco: W.H. Freeman and Co. 1967

Isert, A. 1903. Untersuchungen über den Bau der Drüsengange des Darms bei den Monascidien. Archs. Naturg. 69: 257-296

Jamieson, J.D. and G.E. Palade. 1966. Role of the golgi complex in the intracellular transport of secretory proteins. Proc. nat. Acad. Sci. (Wash.) 55: 424

Karp, G. and N.J. Berrill. Development. 692 pp. 2 ed. New York: McGraw Hill Co. 1981

Koch, G.L.E. and C. Marsh. 1972. Glucosidase activity of the hepatopancreas of the ascidian Pyura stolonifera. Comp. Biochem. Physiol. 42: 577-590

Lambert, G. 1968. The general ecology and growth of a solitary ascidian, Corella willmeriana. Biol. Bull. 135: 296-307

Lambert, G., Lambert, C.C. and D.P. Abbott. 1981. Corella species in the american pacific northwest: distinction of C. inflata Huntsman,1912 from C. willmeriana Herdman, 1898 (Ascidiacea, Phlebobranchia). Can. J. Zool. 59: 1493-1503

Leeson, C.R. and T. Leeson. 1970. Staining methods for sections of epon-embedded tissue for light microscopy. Can. J. Zool. 48: 189-191

Lewis, P.R. and D.P. Knight. Staining Methods for Sectioned Material. in Practical Methods in Electron Microscopy. edited by Audrey M. Glauert. North Holland Co., New York 1977

Lillie, R.D. 1954. Argentaffin and schiff reactions after periodic acid oxidation and aldehyde blocking reactions. J. Histochem. Cytochem. 2: 127-136

Mackie, G.O., Paul, D.H., Singla, C.M., Sleigh, M.A. and D.E. Williams. Branchial innervation and ciliary control in the ascidian Corella. Proc. roy. Soc. B187: 1-35

Millar, R.H. 1949. Concretions in the pyloric gland of Ciona intestinalis Nature(Lond.) 164: 717f-718

----- 1953. Ciona. LMBC Mem. Typ. British Mar. Plants and Animals 35: 1-123

Mirre, C. and Y. Thouveny. 1977. Etude ultrastructurale de la glande pylorique de l'ascidie Botryllus schlosseri. P. Bull. Soc. Zool. France. 102: 439-444

Morris, R.H., Abbott, D.P. and E.C. Haderlie. Intertidal invertebrates of California. 690 pp. Stanford: Stanford University Press 1980

Morton, J.E. 1960. The functions of the gut in ciliary feeders. Biol. Rev. 35: 92-140

Movat, H.Z. 1961. Silver impregnation methods for electron microscopy. Am. J. Clin. Path. 35: 528

Mystkowski, E.M. 1937. Ultracentrifugal studies of compounds of proteins with polysaccharides. Compounds between proteins and glycogen. Biochem. J. 31: 716-720

Palade, G.E. 1966. Structure and function at the cellular level. J. Amer. med. Ass. 198: 815-825

Parson, D.S. and C.A.R. Boyd. 1972. Transport across the intestinal mucosa cell: hierarchies of function. Int. Rev. Cytol. 32: 209-253

Pearse, A.G.E. Histochemistry-Theoretical and Applied-Vol.I (3rd ed.) J.A. Churchill Ltd., London 1968

Pestarino, M. 1982. Occurrence of different secretin-like cells in the digestive tract of the ascidian Styela plicata (Urochordata, Ascidiacea). Cell Tiss. Res. 226: 231-235

Pickett-Heaps, J.D. 1967. Preliminary attempts at ultrastructural polysaccharide localization in root tip cells. J. Histochem. Cytochem. 15: 442

Relini-Orsi, L. 1968. Prime osservazioni morfoogiche ed istochimiche sull´apparato digerente di Styela plicata. Les. Boll. Musei Ist. Biol. Univ. Genova. 36: 157-184

----- 1969. L´apparato digerente nei Tunicati: Aspetti istochimici e funzionali in Ciona intestinalis. Les. Boll. Musei Ist. Biol. Univ. Genova. 37: 103-116

Richardson, G.S., Weliky, I., Balchelder, W., Griffith, M. and L.L. Engel. 1963. Radioautography of 14C- and 3H-labeled steroids on thin-layer chromatograms. J. Chromatog. 12: 115

Rogers, A.W. Techniques of Autoradiography. 3 ed. New York: North Holland Biomedical Press 1979

Roule, M.L. 1884. Rechèrches sur les Ascidies simples des Cotes de Provence. Phallusiadees. Monographic de la Ciona intestinalis. Ann. Mus. Hist. Nat. Marseilles 2: 1-270

Rybicka, K. 1979. Glycosomes(protein-glycogen comples) in the canine heart. Ultrastructure, histochemistry and changes induced by acidic treatment. Virchow´s Arch. B. Cell Pathol. 30: 335

----- 1981. Simultaneous demonstration of glycogen and protein in glycosomes of cardiac tissue. J. Histochem. Cytochem. 29(1): 4-8

Seligman, A.M., Hanker, J.S., Wasserkrieg, K., Dmochowski, H. and L. Katzoff. 1965. Histochemical demonstration of some oxidized macromolecules with thiocarbohydrazide (TCH) or thiosemicarbazide(TSC) and osmium tetroxide. J. Histochem. Cytochem. 13: 629-639

Stephens, R.J. and R.F. Bils. 1967. The ultrastructural changes in the developing chick liver.I.General cytology. J. Ultrastruct. Res. 18: 456-474

Stetten, D.Jr. and M.R. Stetten. 1960. Glycogen Metabolism. Physiol. Rev. 40: 505-537

Swiff, J.A. 1969. The electron histochemical demonstration of cystine-containing proteins in the guinea pig hair follicle. Histochemie 19: 88

Thiery, J.P. 1967. Mise en evidence des polysaccharides sur coupes fines in microscopie electronique. J. Microscopie 6: 987-1018

Thomas, N.W. 1970a. Mucus secreting cells from the alimentary canal of Ciona intestinalis. J. mar. biol. Ass. U.K. 50: 429-438

----- 1970b. Morphology of cell types from the gastric epithelium of Ciona intestinalis. J. mar. biol. Ass. U.K. 50: 746-757

Thorndyke, M. C. 1977. Observations on the gastric epithelium of ascidians with special reference to Styela clava. Cell Tiss. Res. 184: 539-550

Thorndyke, M.C. and P.J.R. Brevis. 1978. Endocrine cells in the gut of the ascidian Styela clava. Cell Tiss. Res. 187: 159-165

Toner, T.G. 1968. Cytology of intestinal epithelial cells. Int. Rev. Cytol. 24: 233-324

Torrence, S.A. and R.A. Cloney. 1981. Rhythmic contractions of the ampullar epidermis during metamorphosis of the ascidian Molgula occidentalis. Cell Tissue Res. 216: 293-312

Tsuk, R.G., Castro, Th., Laufer, L. and D.R. Schwarz, in J. Sirchis(Ed.), Proceedings of the Conference on Methods of Preparing and Storing Marked Molecules, Euratom, (EUR 1625e), Brussels, 1964

Vonk, H.J. 1960. Digestion and metabolism. In: Physiology of crustacea(T.H. Waterman, ed.), Vol. 1, New York: Academic Press

Vye, M.V. and D.A. Fischman. 1971. A comparative study of three methods for the ultrastructural demonstration of glycogen in thin sections. J. Cell Sci. 9: 727-749

Weel, P.B. van. 1940.Beitrage zur Ernahrungsbiologie der Ascidien. Pubbl. St. Zool. Napoli. 18: 50-79

Yonge, C. M. 1925. Studies on the comparative physiology of digestion. III. Secretion, digestion and assimilation in the gut of Ciona intestinalis. J. Exp. Biol. 2: 373-388

----- 1935. On some aspects of digestion in ciliary feeding animals. J. Mar. Biol. Assoc. U.K. 20: 341-346

Zhuravlijova (=Naumkina), L. 1985. SIF-cells in the oesophagus of ascidians. Proc. of the Koshtojants-Conference, Moscow

VITA

Surname: Gowan Given Names: Richard Frederick

Place of Birth: St. Stephen, N.B. Date of Birth: 31 July, 1960

Educational Institutions Attended:

Mount Allison University	1978	to 1983
University of Victoria	1983	to 1986

Degrees, Diplomas, Etc., Awarded:

Honours B.Sc.	1982	Mount Allison University
B.Ed.	1983	Mount Allison University

Honours and Awards:

1978	Sharpe Scholarship; Mount Allison University
1981	Dean's Scholarship; Mount Allison University

PARTIAL COPYRIGHT LICENSE

I hereby grant the right to lend my thesis or dissertation (the title of which is shown below) to users of the University of Victoria Library, and to make **single copies only** for such users or in response to a request from the library of any other university, or similar institution, on its behalf or for one of its users. I further agree that permission for extensive copying of this thesis for scholarly purposes may be granted by me or a member of the University designated by me. It is understood that copying or publication of this thesis for financial gain shall not be allowed without my written permission.

Title of Thesis/Dissertation

The Ascidian Pyloric Gland: Aspects of its Form and Function in Clavelina huntsmani Van Name,1931, Corella inflata Huntsman,1912 and Styela gibbsii(Stimpson,1864).

Author [redacted]
Signature

Richard Frederick Gowan
Name

August 15, 1986
Date